CRCLEME
Cooperative Research Centre for
Landscape Evolution & Mineral Exploration

CSIRO
EXPLORATION AND MINING

AMIRA
Australian Mineral Industries Research Association Limited ACN 004 448 266

OPEN FILE REPORT SERIES

# THE REGOLITH GEOLOGY AND GEOCHEMISTRY OF THE AREA AROUND THE HARMONY GOLD DEPOSIT, (BAXTER MINING CENTRE), PEAK HILL, WESTERN AUSTRALIA

## Volume 1

*I.D.M. Robertson, C. Phang and T.J. Munday*

**CRC LEME OPEN FILE REPORT 94**

**March 2001**

(CRC LEME Restricted Report 5R/
CSIRO Division of Exploration and Mining Report 194R, 1996.
2nd Impression 2001.)

CRC LEME is an unincorporated joint venture between The Australian National University, University of Canberra, Australian Geological Survey Organisation and CSIRO Exploration and Mining, established and supported under the Australian Government's Cooperative Research Centres Program.

AMIRA
Australian Mineral Industries Research Association Limited ACN 004 448 266

CRCLEME
Cooperative Research Centre for Landscape Evolution & Mineral Exploration

CSIRO
EXPLORATION AND MINING

# THE REGOLITH GEOLOGY AND GEOCHEMISTRY OF THE AREA AROUND THE HARMINY GOLD DEPOSIT, (BAXTER MINING CENTRE), PEAK HILL, WESTERN AUSTRALIA

## Volume 1

*I.D.M. Robertson, C. Phang and T.J. Munday*

**CRC LEME OPEN FILE REPORT 94**

March 2001

(CRC LEME Restricted Report 5R/
CSIRO Division of Exploration and Mining Report 194R, 1996.
2nd Impression 2001.)



CRC LEME is an unincorporated joint venture between The Australian National University, University of Canberra, Australian Geological Survey Organisation and CSIRO Exploration and Mining
*Headquarters:* CRC LEME c/o CSIRO Exploration and Mining, Private Bag No 5, PO Wembley, Western Australia, 6913.

## RESEARCH ARISING FROM CSIRO/AMIRA YILGARN REGOLITH GEOCHEMISTRY PROJECTS 1987-1996

In 1987, CSIRO commenced a series of multi-client research projects in regolith geology and geochemistry which were sponsored by companies in the Australian mining industry, through the Australian Mineral Industries Research Association Limited (AMIRA). The initial research program, "Exploration for concealed gold deposits, Yilgarn Block, Western Australia" had the aim of developing improved geological, geochemical and geophysical methods for mineral exploration that would facilitate the location of blind, buried or deeply weathered gold deposits. The program commenced with the following projects:

**P240: Laterite geochemistry for detecting concealed mineral deposits (1987-1991).** Leader: Dr R.E. Smith.
Its scope was development of methods for sampling and interpretation of multi-element laterite geochemistry data and application of multi-element techniques to gold and polymetallic mineral exploration in weathered terrain. The project emphasised viewing laterite geochemical dispersion patterns in their regolith-landform context at local and district scales. It was supported by 30 companies.

**P241: Gold and associated elements in the regolith - dispersion processes and implications for exploration (1987-1991).** Leader: Dr C.R.M. Butt.
The project investigated the distribution of ore and indicator elements in the regolith. It included studies of the mineralogical and geochemical characteristics of weathered ore deposits and wall rocks, and the chemical controls on element dispersion and concentration during regolith evolution. This was to increase the effectiveness of geochemical exploration in weathered terrain through improved understanding of weathering processes. It was supported by 26 companies.

These projects represented 'an opportunity for the mineral industry to participate in a multi-disciplinary program of geoscience research aimed at developing new geological, geochemical and geophysical methods for exploration in deeply weathered Archaean terrains'. This initiative recognised the unique opportunities, created by exploration and open-cut mining, to conduct detailed studies of the weathered zone, with particular emphasis on the near-surface expression of gold mineralisation. The skills of existing and specially recruited research staff from the Floreat Park and North Ryde laboratories (of the then Divisions of Minerals and Geochemistry, and Mineral Physics and Mineralogy, subsequently Exploration Geoscience and later Exploration and Mining) were integrated to form a task force with expertise in geology, mineralogy, geochemistry and geophysics. Several staff participated in more than one project. Following completion of the original projects, two continuation projects were developed.

**P240A: Geochemical exploration in complex lateritic environments of the Yilgarn Craton, Western Australia (1991-1993).** Leaders: Drs R.E. Smith and R.R. Anand.
The approach of viewing geochemical dispersion within a well-controlled and well-understood regolith-landform and bedrock framework at detailed and district scales continued. In this extension, focus was particularly on areas of transported cover and on more complex lateritic environments typified by the Kalgoorlie regional study. This was supported by 17 companies.

**P241A: Gold and associated elements in the regolith - dispersion processes and implications for exploration (1991-1993).** Leader: Dr. C.R.M. Butt.
The significance of gold mobilisation under present-day conditions, particularly the important relationship with pedogenic carbonate, was investigated further. In addition, attention was focussed on the recognition of primary lithologies from their weathered equivalents. This project was supported by 14 companies.

Most reports related to the above research projects were published as CRC LEME Open File Reports Series (Nos 1-74), with an index (Report 75), by June 1999. Publication now continues with release of reports from further projects.

**P252: Geochemical exploration for platinum group elements in weathered terrain.** Leader: Dr C.R.M. Butt.
This project was designed to gather information on the geochemical behaviour of the platinum group elements under weathering conditions using both laboratory and field studies, to determine their dispersion in the regolith and to apply this to concepts for use in exploration. The research was commenced in 1988 by CSIRO Exploration Geoscience and the University of Wales (Cardiff). The Final Report was completed in December 1992. It was supported by 9 companies.

**P409: Geochemical exploration in areas of transported overburden, Yilgarn Craton and environs, WA.**
Leaders: Drs C.R.M. Butt and R.E. Smith.
About 50% or more of prospective terrain in the Yilgarn is obscured by substantial thicknesses of transported overburden that varies in age from Permian to Recent. Some of this cover has undergone substantial weathering. Exploration problems in these covered areas were the focus of Project 409. The research was commenced in June 1993 by CSIRO Exploration and Mining but was subsequently incorporated into the activities of CRC LEME in July 1995 and was concluded in July 1996. It was supported by 22 companies.

Although the confidentiality periods of Projects P252 and P409 expired in 1994 and 1998, respectively, the reports have not been released previously. CRC LEME acknowledges the Australian Mineral Industries Research Association and CSIRO Division of Exploration and Mining for authority to publish these reports. It is intended that publication of the reports will be a substantial additional factor in transferring technology to aid the Australian mineral industry.

This report (CRC LEME Open File Report 94) is a second impression (second printing) of CSIRO, Division of Exploration and Mining Restricted Report 194R, first issued in 1996, which formed part of the CSIRO/AMIRA Project P409.

**Copies of this publication can be obtained from:**
The Publication Officer, c/- CRC LEME, CSIRO Exploration and Mining, Private Bag 5, Wembley, WA 6913, Australia. Information on other publications in this series may be obtained from the above or from http://leme.anu.edu.au/
**Cataloguing-in-Publication:**
Robertson, I.D.M.
The regolith geology and geochemistry of the area around the Harmony Gold Deposit, (Baxter Mining Centre), Peak Hill, Western Australia.
ISBN v1: 0 643 06689 6 v2: 0 643 06690 X Set: 0643 06691 8
1. Regolith - Western Australia - Yilgarn Block 2. Gold ores - Western Australia - Yilgarn Block 3. Geochemistry - Western Australia - Yilgarn Block 4. Geology - Western Australia - Yilgarn Block
I. Phang, C. II. Munday, T.J. III. Title
CRC LEME Open File Report 94.
ISSN 1329-4768

## PREFACE AND EXECUTIVE SUMMARY

The CRC LEME-AMIRA Project 409 *Exploration in Areas of Transported Overburden, Yilgarn Craton and Environs* has, as its principal objective, the development of geochemical exploration methods for areas having substantial cover of surficial sediments, through investigation of the processes of geochemical dispersion from concealed mineralisation.

The Harmony Deposit, and the Baxter Mining Centre which surrounds it, are set within the Proterozoic Glengarry Basin on the periphery of the Yilgarn Craton. The Baxter Mining Centre was chosen for substantial study in the project because it is an example of some of the important problems of exploring areas of extensive colluvial-alluvial deposition plains. These plains have very little surface relief, yet drilling reveals considerable buried relief to the weathered Proterozoic basement. Also revealed are varied valley-fill sediments and partly lateritised basement. Extensive rotary air-blast and reverse circulation drilling through and around the deposit provided an ideal opportunity for a three dimensional inventory of regolith materials and a study of dispersion processes.

The study commenced prior to mining. Logging and sampling of a large number of drill holes and soils was carried out over the essentially undisturbed land surface, including over the location of the present Harmony pit. Regolith relationships over the 240 $km^2$ of the surrounding district is provided by a 1:25 000 scale map. This was based on interpretation of colour air-photography, image enhanced Landsat TM images and field traverses. The treatment of Landsat TM imagery using "CSIROREG" parameters is again shown to be particularly effective in this arid region. During the course of the study, mining exposed details of the stratigraphy, thickness and facies variations of the sedimentary cover. Also exposed were units of the residual weathered profile.

Various sample media have been assessed to establish their usefulness in exploration, including ferruginous saprolite, lateritic residuum, ferruginous mottles from the weathered basement, valley-fill clays of palaeochannels, the base of the colluviun and the soil developed on this colluvium. Groundwaters were also studied (separate report). The study shows that sampling the top of the residual weathered profile and the immediately overlying colluvial gravels allows the gold deposit to be recognised and outlined.

**C.R.M. Butt and R.E. Smith**
*Project Leaders*

30th June, 1996

# CONTENTS

## APPENDICES

Appendix

# ABSTRACT

Primary Au mineralisation at Harmony is associated with quartz veins but is low in sulphides. Gold and W (scheelite) are the most significant indicators in mineralised fresh rock at Harmony, supplemented by Ta and Nb. Elements associated with a phyllic alteration halo are K, Rb and Ba. Some REE, namely Eu, Lu and Yb, increase in abundance and range near mineralisation for reasons that are not clear yet. Although As and Sb are elevated, their abundances are not as great as for other, sulphide-rich mineralisation styles.

The Harmony Au deposit was completely covered by a blanket of soil and colluvium. Drilling beneath this revealed a complex regolith of weathered and partly lateritised Proterozoic basement, clay-rich valley fill sediments and colluvium. Logging the main regolith units produced a 3D regolith model which provided a valuable guide to sampling and later interpretation. The basement has been eroded and weathered and consists of mafic and ultramafic metavolcanics and fine-grained metasediments. The higher parts of this basement are of ferruginous saprolite, the axes of the palaeovalleys are largely of saprolite and mottled zone and are deeply weathered. Lateritic residuum occupies the flanks of the palaeorelief.

The colluvium varies from 0.5 m over parts of Harmony deposit to 20 m over the palaeovalleys and probably contained some alluvium where the cover was at its deepest. It presents a significant hindrance to exploration. The base of the colluvium is complex in places, being a mixture of saprolite blocks included in what appears to have been a palaeosol.

The palaeovalleys have been infilled with smectite-kaolinite sediments, probably derived from the surrounding saprolites. Hematitic, manganiferous and dolomitic mega-mottles have developed in these sediments and the tops of some valley-fill sediments contain pisolitic structures. All this indicates intense post-depositional weathering both at the surface and at oxidation fronts within the sedimentary pile. Parts of the valley-fill sediments were eroded prior to deposition of the colluvium.

Sampling of the top of the basement (ferruginous saprolite, lateritic residuum and mottles washed from the mottled zone) on a 250 m sample spacing showed significant Au and W anomalies in the vicinity of the Harmony mineralisation. Au dispersion in the ferruginous saprolite is restricted and requires close-spaced sampling (50 m). Some elements (Si, Fe, Cr, Zr, Hf, V, Rb, Ba, As and Sb) are influenced to some extent by the distribution of regolith types. Data normalisation to the modes of background populations removed most of this dependency. Gold and W anomalies were unchanged.

The unconformity between the stripped basement and the colluvium was tested, using a 150 m sample spacing as an alternate to ferruginous saprolite sampling in the vicinity of mineralisation. This capitalised on any mechanical dispersion, soil dispersion or hydromorphic permeation along the unconformity that may have developed during or since deposition of the colluvium. Dispersions of Au, W, Ta and Nb along this interface, indicating mechanical down-slope migration, produced better anomalies than the basement sampling in this stripped environment.

The geochemistry of the valley fill sediments indicated probable leaching of Au, even where a small clay-filled palaeovalley had drained the Harmony Au deposit; however W was mechanically dispersed here. The soil fine fraction (<75 μm) may not be relied upon to locate mineralisation, even though some very weak Au anomalies appeared where the colluvial cover over the Harmony mineralisation was extremely thin (~0.5 m).

# 1 INTRODUCTION

The Harmony deposit (previously known as the Contact deposit) is located approximately 9 km west of Peak Hill and some 90 km north-northeast of Meekatharra (Figures 1 and 2) at 25° 39' 10"S, 118° 37' 50"E in the Baxter Mining Centre. The deposit is hosted by early Proterozoic rocks which form part of the Glengarry Basin.

The deposit was discovered in 1991 by RAB drilling the contact between the Ravelstone and Narracoota Formations, and sampling buried lateritic residuum. Subsequent orientation studies of surficial materials (lag and soil as BLEG) gave rather equivocal results. Mining commenced on 3rd July 1995. The Harmony deposit has a reserve of 2.148 Mt at 3.6 g/t Au. Prospecting is still very active in the area.

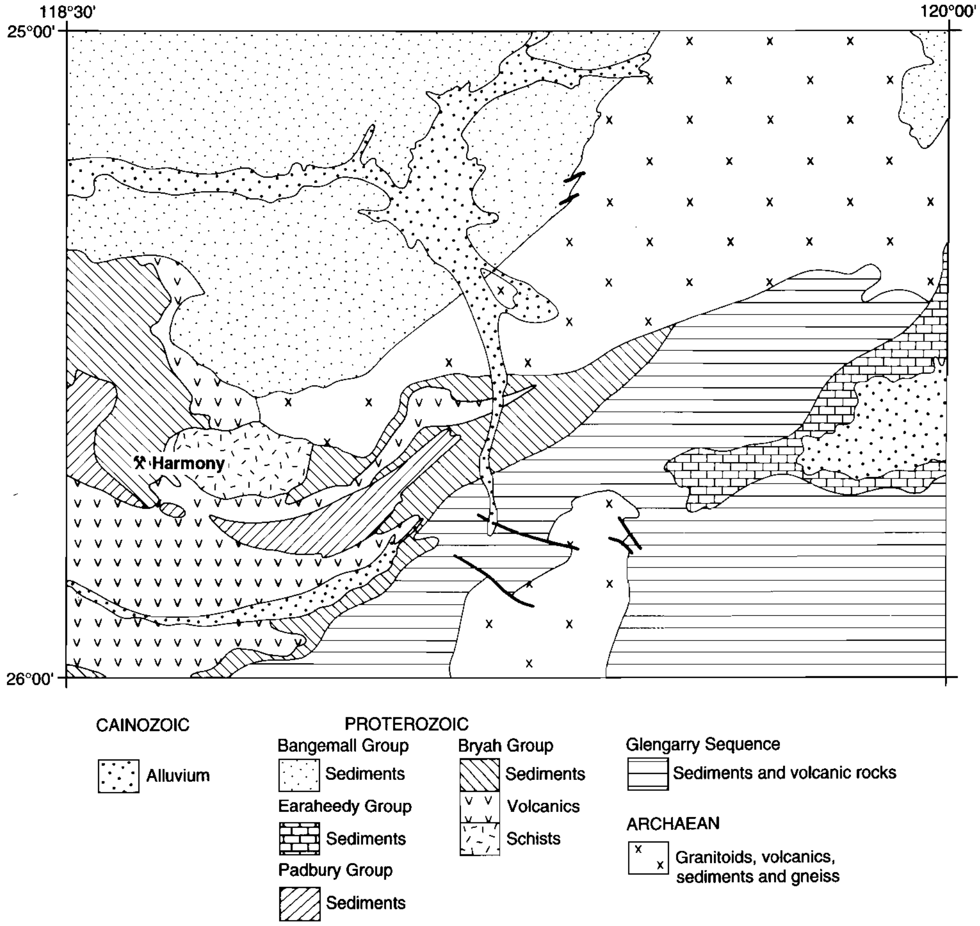


**Figure 1. Regional geology of the Peak Hill area after Pirajno *et al.*, (1995) showing the major lithologies.**

The Harmony deposit is concealed by a thin cover of colluvium over a basement of deeply weathered Proterozoic rocks, now represented partly by lateritic duricrust and by an eroded regolith of mottled zone, saprolite and ferruginous saprolite as a number of buried low ridges and valleys. The valleys were subsequently partly filled with clay-rich sediments prior to deposition of the colluvium. The objective of the study has been to investigate the nature and stratigraphy of the regolith and to evaluate the residual and cover materials as geochemical sample media. Extensive RAB and RC drilling around the deposit provided an ideal opportunity for a 3D inventory of regolith materials and a study of dispersion processes.

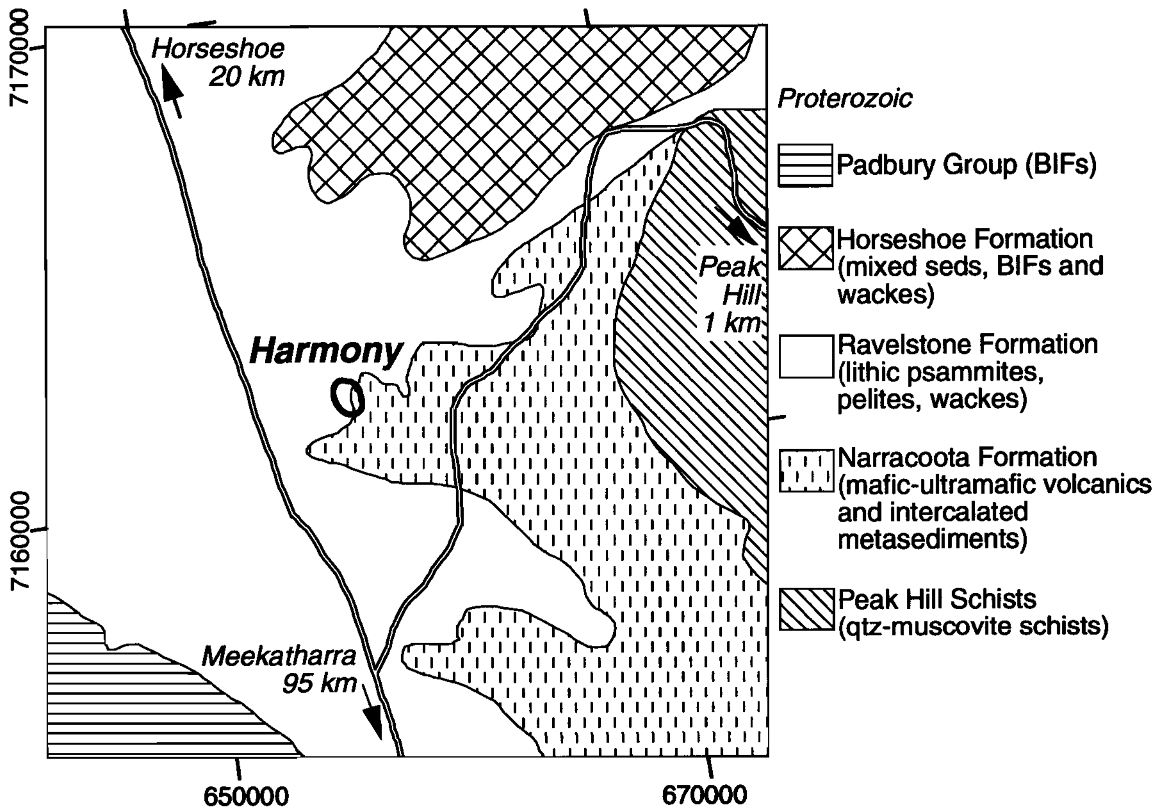


Figure 2. District bedrock geology of the area around the Harmony Au deposit adapted from Robinson (1992) and Pirajno and Occhipinti (1995). The Harmony deposit lies on the contact between the metavolcanics of the Narracoota Formation and metasediments of the Ravelstone Formation.

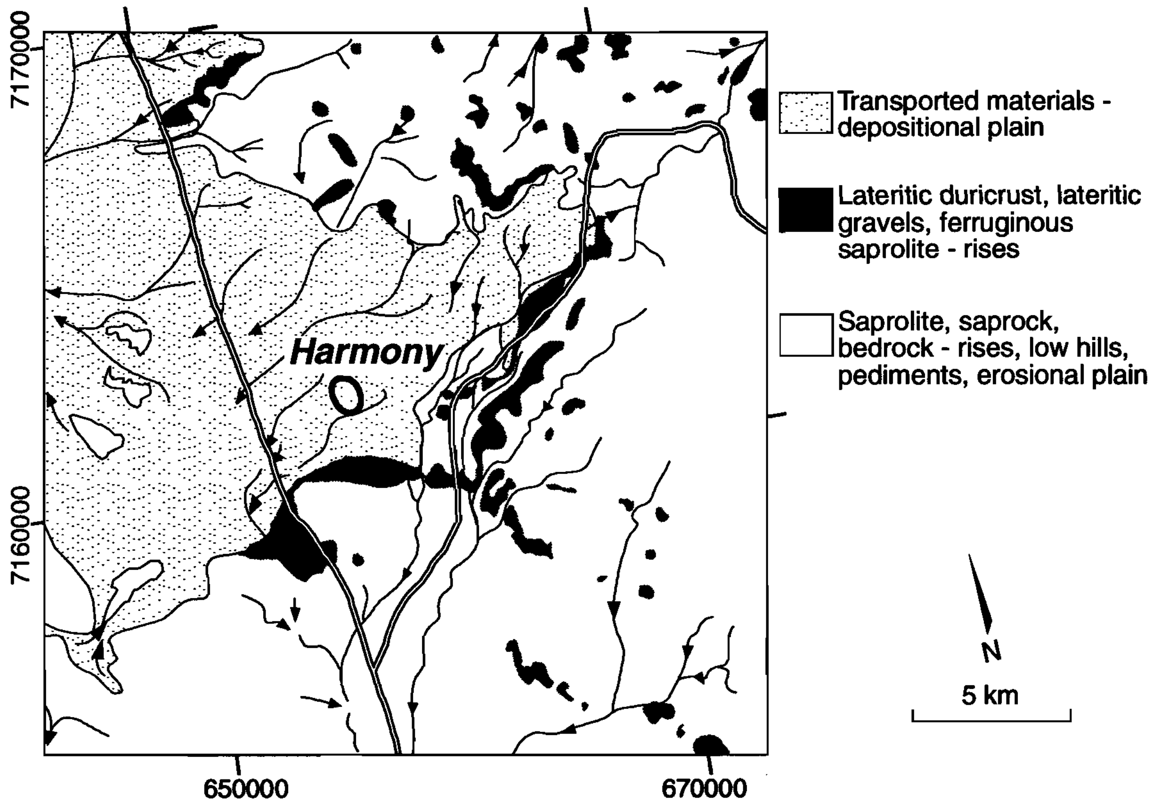


Figure 3. District regolith geology of the area around the Harmony Au deposit showing the distributions of the residual terrain (relict and erosional landforms) and the depositional plain covering the Harmony mineralisation.

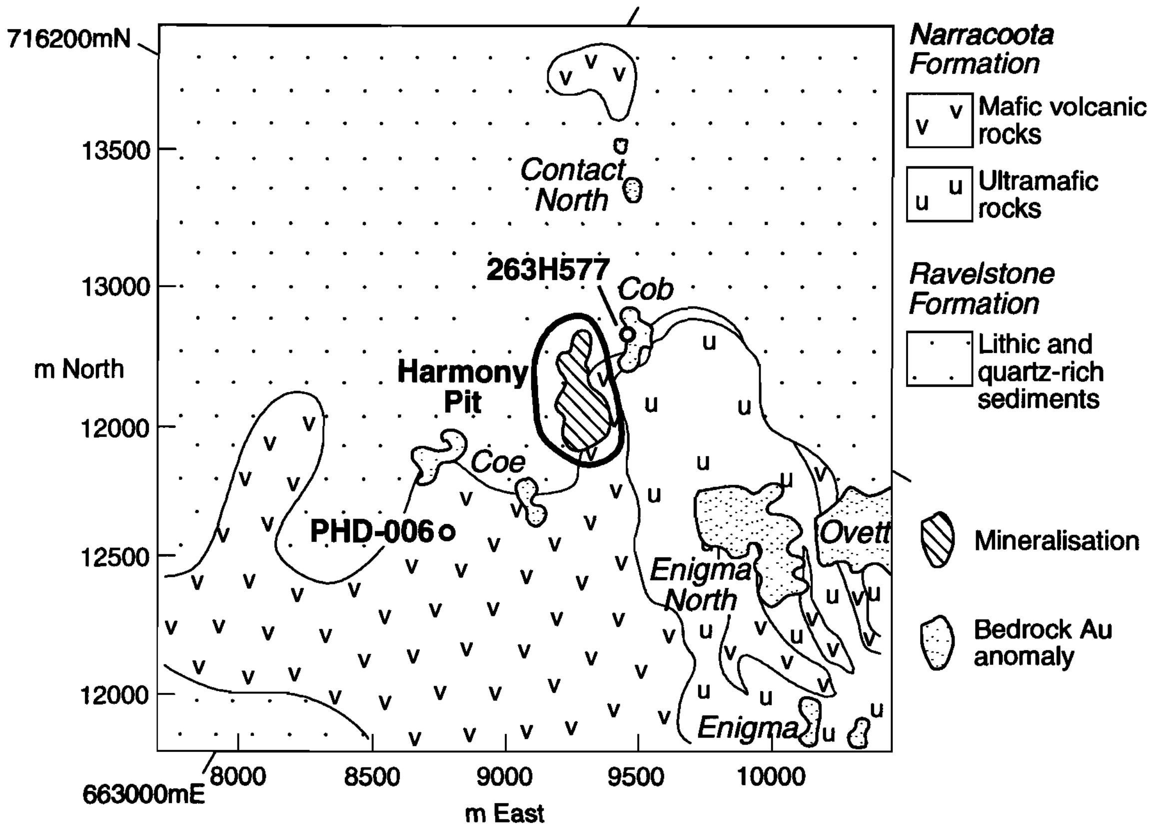


Figure 4A. Local geology of the area surrounding the Harmony pit, as determined by Plutonic Operations Ltd from intensive RAB drilling. The known bedrock geochemical anomalies, the locations of drillholes PHD-006 and 263H577 and the outline of the Harmony mineralisation have been added.

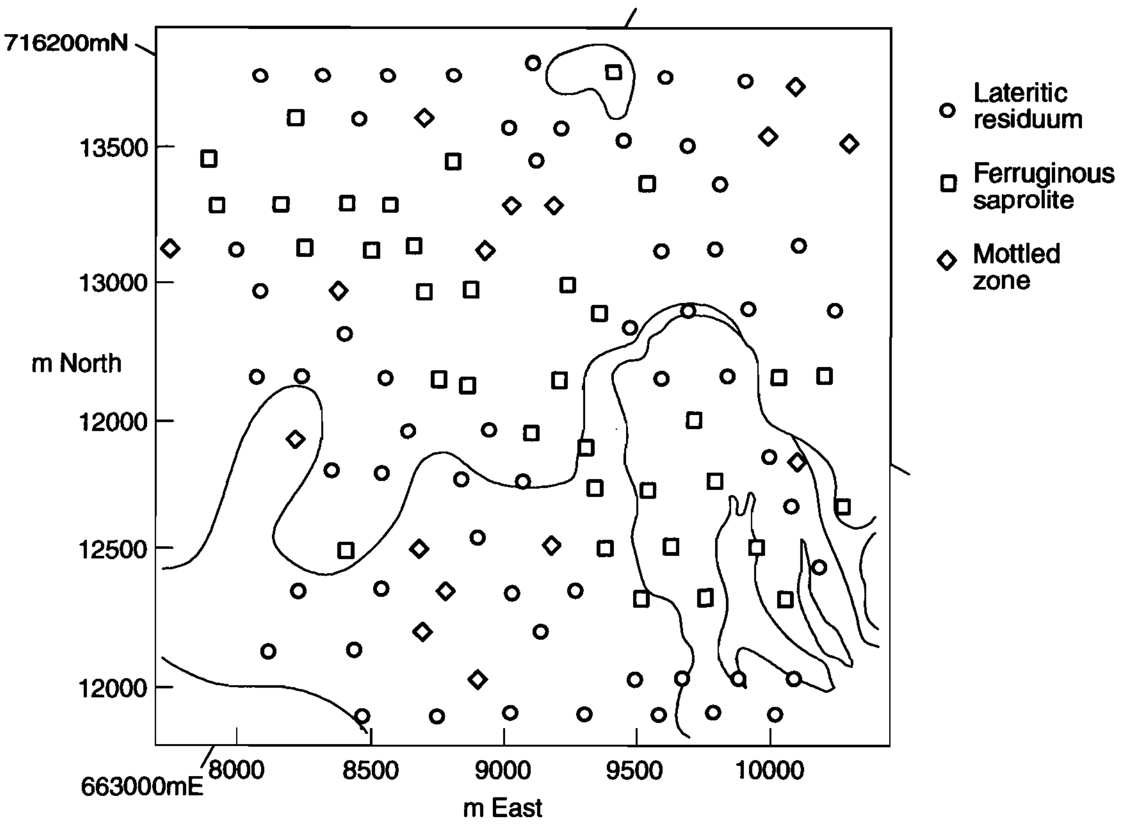


**Figure 4B Outline of the bedrock geology with sampled drillholes and the nature of the top of the residual regolith.**

The work program was as follows:-

i) To establish a framework for the geochemical orientation study of the Harmony Au deposit by mapping regolith-landform relationships on a district scale.
ii) To map the sub-surface regolith stratigraphy, using the existing drilling and compile 3D models.
iii) To characterise regolith materials to assist in their recognition in drillspoil.
iv) To determine the extent of the dispersion halo in the basement materials which could contribute to dispersion in the overburden.
v) By using type sections, to investigate the stratigraphy, mineralogy and geochemistry of the transported overburden, including the colluvium and the sediments infilling the palaeovalleys. There was also an opportunity to compare the geochemistry of the sediments in a palaeovalley draining the Au deposit with that of another draining unmineralised rocks.
vi) To investigate the geochemistry of the interface between the basement and the colluvium close to the Harmony deposit.
vii) To investigate the composition, mineralogy and geochemistry of the soil developed from the colluvium covering the deposit and its immediate surroundings.
viii) To investigate the geochemistry of groundwaters around the Harmony deposit.

Groundwaters around the Harmony deposit were investigated by sampling numerous drillholes (Gray, 1995) to study the interaction of these groundwaters with the mineralised rocks. The groundwaters are neutral, with a similar Eh range to neutral groundwaters throughout the Yilgarn Craton, but they have very low salinities and diverge markedly from seawater ionic ratios. This suggests a strong lithological or hydrological control to the water chemistry.

Elements and anions controlled by mineral equilibration are Ba (barite), Ca, Mg and $HCO_3$ (carbonate), Pb and V (chervetite). Gold occurs in low abundances in the groundwaters and is not thought to be mobile under present conditions. A small group of elements, namely Sc, Mo, W and Rb, have greater groundwater concentrations near mineralisation. Chromium concentrations in groundwater correlate with the occurrence of ultramafic rocks. Concentrations of Ni and As in groundwaters correspond to an As-rich trend southeast of the Harmony deposit.

Co-ordinates used in this report are local exploration grid co-ordinates; this grid being inclined at 28.89° west of AMG north (see Appendix 9 for conversion information). The two grids are shown together in Figures 4A and B. Detailed study methods are given in Appendix 9.

## 2 REGIONAL SETTING AND LOCAL GEOLOGY

The region is arid and is characterised by low, irregular rainfall averaging 200 mm per annum. Vegetation cover is thin and consists largely of mulga and other drought-resistant shrubs and some grasses. The deposit is located within a broad colluvial-alluvial depositional plain (Figure 3), bounded to the west by the westerly extent of the Robinson Ranges, to the north by the southerly extension of the Horseshoe Range and to the east and south by rises and low hills.

The Peak Hill district, within which the Harmony Au deposit is located, forms part of a major, Early Proterozoic basin known as the Glengarry Basin. The geology and tectonic evolution of the basin was recently summarised by Pirajno and Occhipinti, 1995. The inception and evolution of the Glengarry Basin was due to pull-apart openings that developed from oblique collision of the Yilgarn and Pilbara Cratons. Basin history is represented by a series of sag- and rift-basin successions, including shelf and turbiditic facies sediments and volcano-sedimentary rocks (shale, clastic rocks, mafic volcanics and subvolcanic rocks).

The Harmony deposit is located within the tectonostratigraphic domain known as the Bryah Rift Succession, in the western part of the basin. Rocks of the area have been grouped into a succession referred to as the Bryah Group (Pirajno and Occhipinti, 1995). They comprise mafic and ultramafic volcanic rocks (Narracoota Formation), turbiditic sedimentary rocks, banded iron formation (BIF) and associated clastic sediments (Horseshoe and Ravelstone formations), all of which are intensely deformed and metamorphosed to the low to mid greenschist facies. Deformation and metamorphism are linked to collision, compression and eastward indentation by a rigid Archaean block in the west and the Marymia Inlier in the north (Pirajno *et al.,* 1995). The origin of Au deposits of the Bryah domain, including the Harmony deposit, may be related to this tectonism and associated prograde and retrograde metamorphism.

Known Au deposits within the Bryah domain of the Glengarry Basin are epigenetic mesothermal lode-Au types, which occur in greenschist-facies metamorphic rocks and are hosted within high-strain zones in metasedimentary and/or metavolcanic rocks or along their contacts (Pirajno *et al.,* 1995).

The local geology of the Harmony deposit is summarised in Figure 2. It lies at the contact between metavolcanic rocks of the Narracoota Formation and the Ravelstone Formation metasediments, which form part of the Bryah Group. The metavolcanic rocks of the Narracoota Formation comprise a folded sequence of mafic and ultramafic rocks. The Ravelstone Formation is a thick, metamorphosed, turbidite sequence of fine-grained lithic, feldspathic and mafic wacke with subordinate interbedded slaty mudstone (Gee, 1987). To the northwest of the deposit, calcareous, manganiferous shales and subgreywackes of the Horseshoe Formation outcrop. BIF's of the Padbury Group form prominent ridges southwest of the area.

Primary gold mineralisation, associated with quartz veining, is stratabound and is hosted within dolerite and quench-textured basalt. Albitisation, silicification and almost complete destruction of Fe-Mg minerals are common. Most of the primary Au is associated with deformation marked by muscovite development. The deposit is low in sulphides with pyrite >> pyrrhotite and chalcopyrite. Minor scheelite was introduced at an early stage and carbonates (calcite, ankerite and dolomite) at a late stage. The primary orientation of the mineralisation appears to be sub-parallel to the hanging wall contact of the sediments and volcanic rocks associated with sub-vertical structures trending north-south (Figure 4A). The detailed structural setting of the deposit is under investigation. Mineralisation also occurs as a relatively flat-lying supergene deposit close to the surface in lateritic residuum and saprolite. The depth of oxidation over the deposit is variable, averaging approximately 80 m and the watertable is at 30 m.

The deposit was found by shallow RAB and RC drilling that sampled buried lateritic residuum. Anomalous Au abundances were detected in the vicinity of what is now known as the Harmony deposit and a follow-up drill program located mineralisation in what is now the southern part of the Harmony pit.

# 3 REGOLITH GEOLOGY

## 3.1 Regional regolith geology

A regional regolith map, including this study area, has been prepared as part of the Regional Geochemical Mapping Initiative of the Geological Survey of Western Australia. Regolith materials and geochemical maps of the Peak Hill 1:250 000 map sheet have been published as part of that program (Subramanya *et al.,* 1995).

The distribution of regolith materials and landforms in the district, centred on the Harmony deposit, have been mapped at 1:25 000 scale as part of this study (Appendix 11). The map covers some 240 $km^2$ and was based on interpretation of colour air photographs (1:25 000 scale) and Landsat TM imagery, combined with field traverses. Geocoded colour composite images at scales of 1:50 000 and 1:25 000 were used to aid the delineation of regolith units. A composite of Landsat TM band ratios (referred to as a CSIROREG image) comprising Band 5/Band 7 (red), Band 4/Band 7 (green) and Band 4/Band 2 (blue) (Figure 5), along with a colour composite of Bands 7 (red), 4 (green) and 2 (blue) were particularly valuable in mapping the regolith materials. Both of these image combinations have been used for regolith mapping in other parts of the Yilgarn Craton (*e.g.*, Gozzard *et al.*, 1992; Tapley and Gozzard, 1992; Anand *et al.*, 1993; Bradley *et al.*, 1995). A simplified version of the resultant map is given in Figure 3.

Two major geomorphic provinces were identified. These are i) an area of transported regolith, which includes the depositional plain on which the Harmony deposit is located, and ii) an area of subcropping and outcropping *in-situ* regolith (Figure 3 and Appendix 11).

### *3.1.1 Transported regolith*

The Harmony deposit is located beneath a broad colluvial-alluvial depositional plain comprising coalescing sheet-flood fans which have been aggraded by infrequent, active, sheet flow and channelled stream flow, with subordinate wind erosion (map units D1 and D2; Appendix 11). The plain comprises about 30% of the mapped area and extends towards the west and northwest. Heavy rainfall, channelled in the low hills to the north and north-east of the Harmony deposit, has dispersed sheet wash from gently inclined fans that make up the depositional plain. Drainage channels over these landforms are generally very shallow, ill-defined and seldom active. Their extent is commonly marked by lines of dense vegetation (white lines in the Landsat image). Wanderrie banks (sandy banks aligned along the contours, perpendicular to the sheet flow direction; see Mabbutt, 1963) are common over the plain.

Dark blues on the satellite image are areas where sands and clays, mantled by a fine to medium polymictic lag, accumulate (map unit D1; Figure 6A). Other parts of these sheet-flood fans are characterised by a medium to coarse lag of ferruginous and manganiferous lithic fragments, lithic clasts, brown to black nodules, pisoliths and some ferruginous saprolite fragments, with abundant quartz. This is set in a red-brown sandy-clay loam (map unit D2; Figures 6B and C). Areas with a coarser lag appear blue-brown on the Landsat image.

The sheet-flood deposits are underlain by extensive tracts of coarse colluvium-alluvium (map unit D3) which were deposited on weathered Proterozoic basement. This has been hardpanised since (Figure 6D). The colluvium-alluvium consists of poorly sorted granules and clasts, in a silty-clay matrix. Ferruginous fragments, including nodules, pisoliths and lithic clasts, dominate. The several facies in the colluvium-alluvium indicate varying conditions of deposition. Their varying chemistry and mineralogy are illustrated by Tables 1 and 2. The low hills of the Horseshoe Formation and, to a lesser extent, of the Narracoota Formation are interpreted as the sources of much of this detritus. A more detailed description of these transported materials follows.

The sheetwash deposits in the vicinity of the Harmony deposit (Figure 6G) are similar to those described above, namely medium to coarse, ferruginous, polymictic clasts set in a fine sandy-clay loam (Figure 6D). To the southwest of the Harmony deposit, these deposits give way to a hardpanised colluvium which is being eroded by the present drainage system (Figure 6E). These drainages trend southwest from the Harmony deposit and turn south (Figure 3; Appendix 11). Probable fossil termite mounds and burrow structures are found here (Figure 6F) which penetrate the upper metre of colluvium. Bioturbation in the upper part of the colluvium is important (see Section 8) where it has served to disperse some of the geochemical signal from the basement to the surface at Harmony, but only where the colluvium is extremely thin.

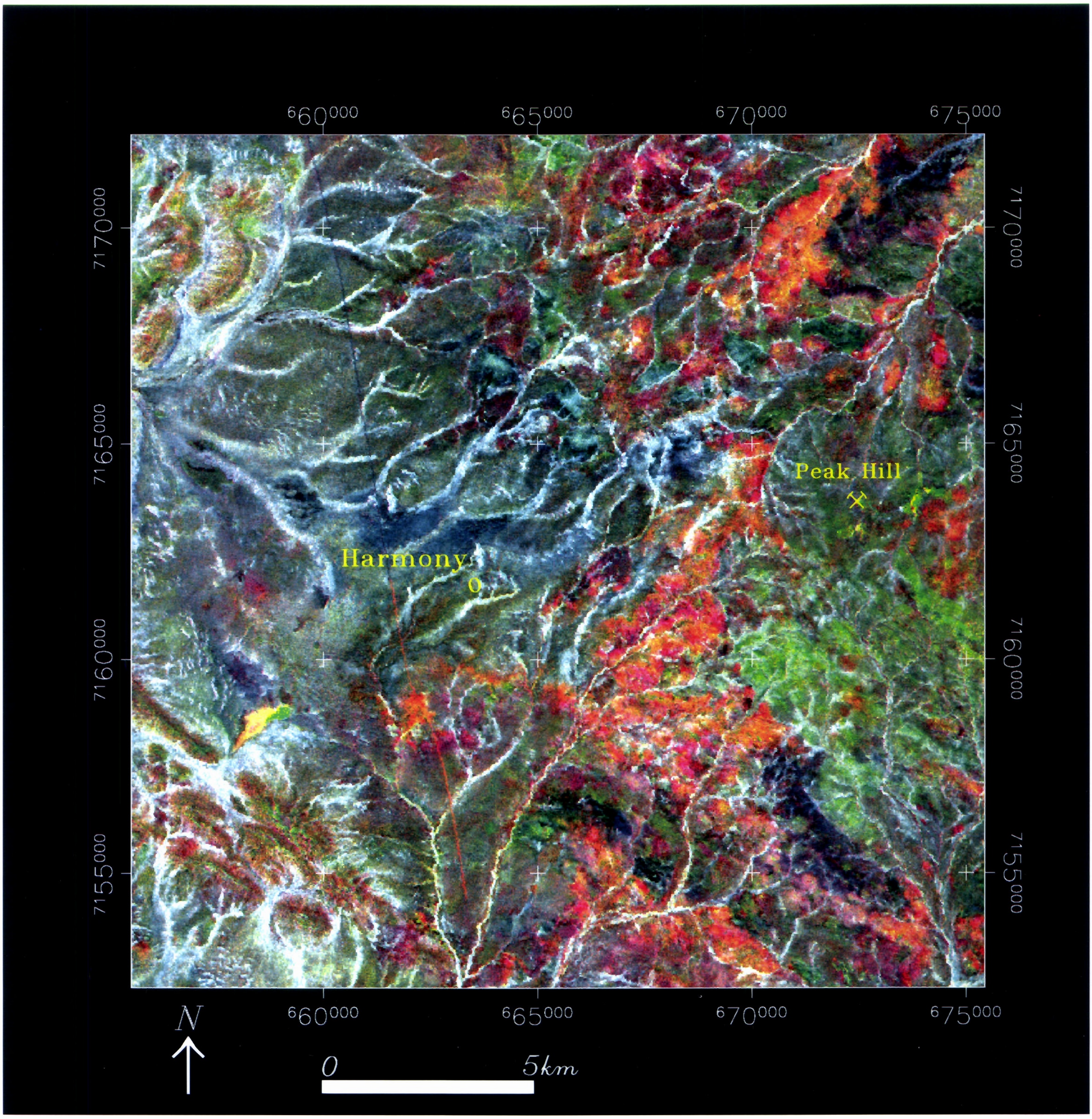


Figure 5. Landsat TM colour ratio composite for the region around the Harmony deposit. The image data have been spectrally processed to enhance differences between regolith materials. Orange and red - lateritic gravels and ferruginous saprolite. Green and purple - saprolite subcrop and outcrop. Blue and brown - colluvial blanket.

## FIGURE 6

## REGOLITH-LANDFORMS

**A.** Sheet-wash sands and gravels located on a depositional plain west of the Harmony Au Deposit. The lag comprises a coarse polymictic gravel set in a fine sandy-clay. AMG co-ordinates 660945E, 7163685N.

**B.** Sheet-wash gravels located on the depositional plain west of the Harmony Au Deposit. The material comprises a medium to coarse polymict lag of lithic clasts, ferruginous lithic fragments, ferruginous noduels, pisoliths and quartz set in a sandy-clay loam. These coarser materials are commonly found in areas where sheet-wash flow may have been deeper and have had a higher velocity. AMG co-ordinates 661755E, 7161645N.

**C.** Oblique view across the depositional plain beneath which the Harmony Au Deposit is located. The plain is covered with sheet-wash gravels which overlie medium to coarse hardpanised colluvium. The view is northeast towards the Horseshoe Range from AMG co-ordinates 661755E, 7161645N.

**D.** Hardpanised colluvium exposed in stream section to the south-west of the Harmony Pit. AMG co-ordinates 662385E, 7160925N.

**E.** Hardpanised colluvium being eroded by the modern drainage system. This site is located south-west of Harmony pit. AMG co-ordinates 662385E, 7160925N.

**F.** Probable fossil termite mound developed within the hardpanised colluvium south-west of the Harmony pit. AMG co-ordinates 662385E 7160925N

**G.** Oblique view looking north-east towards the location of the Harmony deposit prior to mining which is sited in the middle-ground. AMG co-ordinates 663285E 7161525N.

**H.** Coarse to medium blocky polymictic colluvium developed over a pediment of ferruginous saprolite. Here the colluvium comprises ferruginous lithic clasts and quartz over mafic meta-volcanics of the Narracoota Formation. AMG co-ordinates 669855E 7159005N

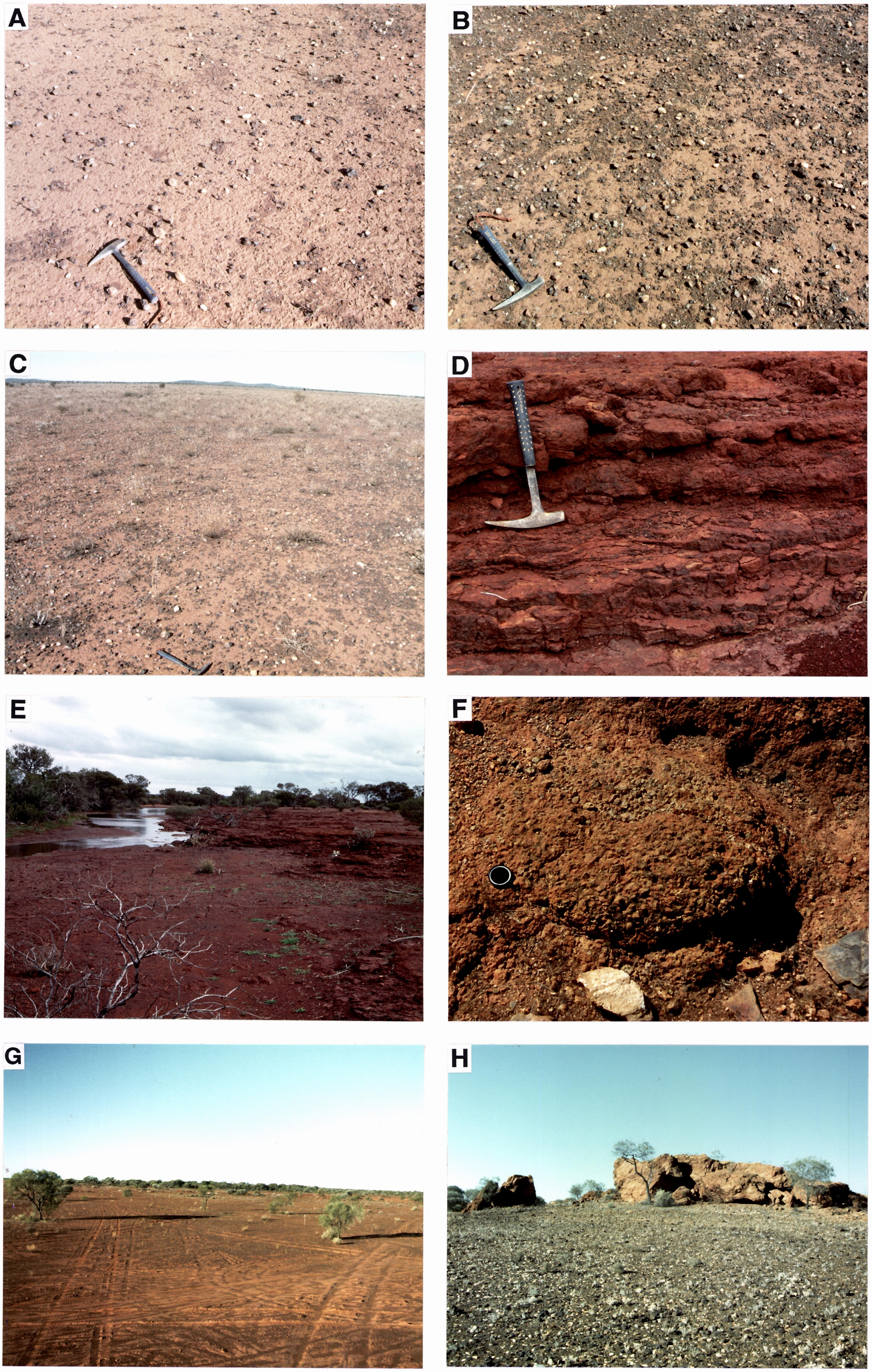
A
B
C
D
E
F
G
H

**FIGURE 6 (Contd)**

**REGOLITH-LANDFORMS**

**I.** Circular structure developed in ferruginous saprolite derived from metasediments of the Ravelstone Formation. The material of the circular structure consists of ferruginous nodules and pisoliths in a clay matrix. AMG co-ordinates 663315E 7159755N.

**J.** Coarse quartz-rich blocky lag on ferruginous saprolite developed over metasediments. A quartz blow crops out in the middleground. AMG co-ordinates 664965E 7158165N

**K.** Oblique view of remnants of Fe-rich duricrust developed on metasediments. AMG co-ordinates 662895E 7158165N.

**L.** Oblique view south over a series of low rises developed in the Narracoota volcanics. Ferruginous saprolite with remnant patches of Fe-rich occur in the foreground. AMG Co-ordinates 666885E 7160355N.

**M.** Remnants of Fe-rich diuricrust at the crest of a breakaway in the Narracoota volcanics. AMG co-ordinates 666885E 7156000N.

**N.** Hardpanised metasediments of the Ravelstone formation. Bedding in the section is near vertical. AMG co-ordinates 662715E 7156005N.

**O.** Oblique view of a sub-cropping metabasalt. AMG co-ordinates 666255E 7156695N.

**P.** Capping of manganiferous duricrust developed on metasediments of the Horseshoe Formation. AMG co-ordinates 669705E 7166385N

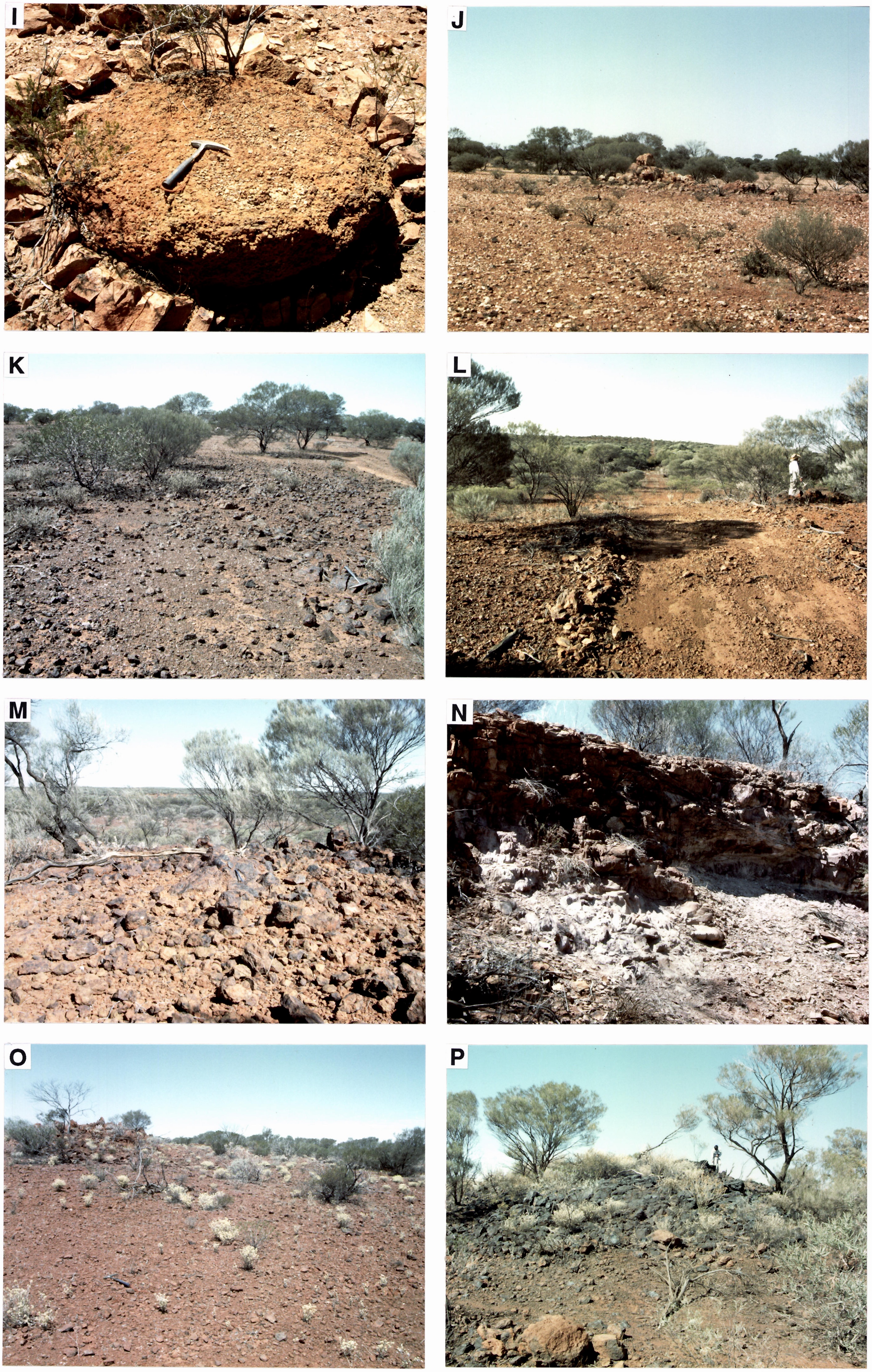
I
J
K
L
M
N
O
P

## FIGURE 7

## REGOLITH MATERIALS

**A.** Loose pisoliths with cutans from a hardpanised pisolitic duricrust. Most are a conglomeration of tiny hematitic subangular granules and clay balls of kaolinite (pale yellow spots) cemented in a matrix of goethite-rich clay. One dark brown elongate nodule (BN) is a hematitic ferruginous saprolite with a goethitic skin. Specimen 09-1178 : AMG co-ordinates 662205E 7158795N.

**B.** Pisolitic-nodular duricrust. The pisoliths (PL) and nodules (ND) are hematitic and are set in goethite-rich clay containing gibbsite, some kaolinite and quartz (QZ). Specimen 09-1200/2 : AMG co-ordinates 665325E 7165035N.

**C.** Dark, brownish red, vermiform duricrust. The ferruginous nodules (ND) are set in a matrix of goethite and clay (CL) which has been partly dissolved, leaving numerous vesicles (VO). Specimen 09-1204 : AMG co-ordinates 665805E 7166775N.

**D.** Matrix of vermiform duricrust. Tiny fragments of clay (CL) containing gibbsite surrounded by goethite (GO). The matrix and fragments have been partly dissolved leaving interlinked vesicles (VO). Specimen 09-1204 : co-ordinates 665805E 77166775N. Photomicrograph in normally reflected light. Compare Figure 7C.

**E.** Fragmental duricrust. Subangular hematite-rich fragments (HM) and pisoliths (PL) in a matrix of goethite- and quartz-rich gibbsitic clay (CL). Duricrust on iron formation member of Horseshoe Formation. Specimen 09-1199. AMG co-ordinates 665535E 7164555N.

**F.** Hematite-rich fragments and pisoliths of Figure 7E. Grains of magnetite, are now pseudomorphed by hematite (HM) with a characteristic trellis fabric (martite). The cementing matrix is goethite- and quartz-rich gibbsitic clay (CL), with voids (VO). Specimen 09-1199 : co-ordinates 665535E 716455N. Photomicrograph in normally reflected light.

**G.** Manganiferous vermiform duricrust showing a layer with colloform fabric of Mn oxides and goethite. The matrix is mainly Mn oxides with yellowish brown goethite (GO) patches. Generally underlying pisolitic manganiferous duricrust. Specimen 09-1202 : AMG co-ordinates 665265E 7165575N.

**H.** Colloform fabric of Mn oxides and goethite in a pisolite from a manganiferous pisolitic duricrust. Specimen 09-1207/1 : AMG co-ordinates 669735E 7166385N Photomicrograph in normally reflected light.

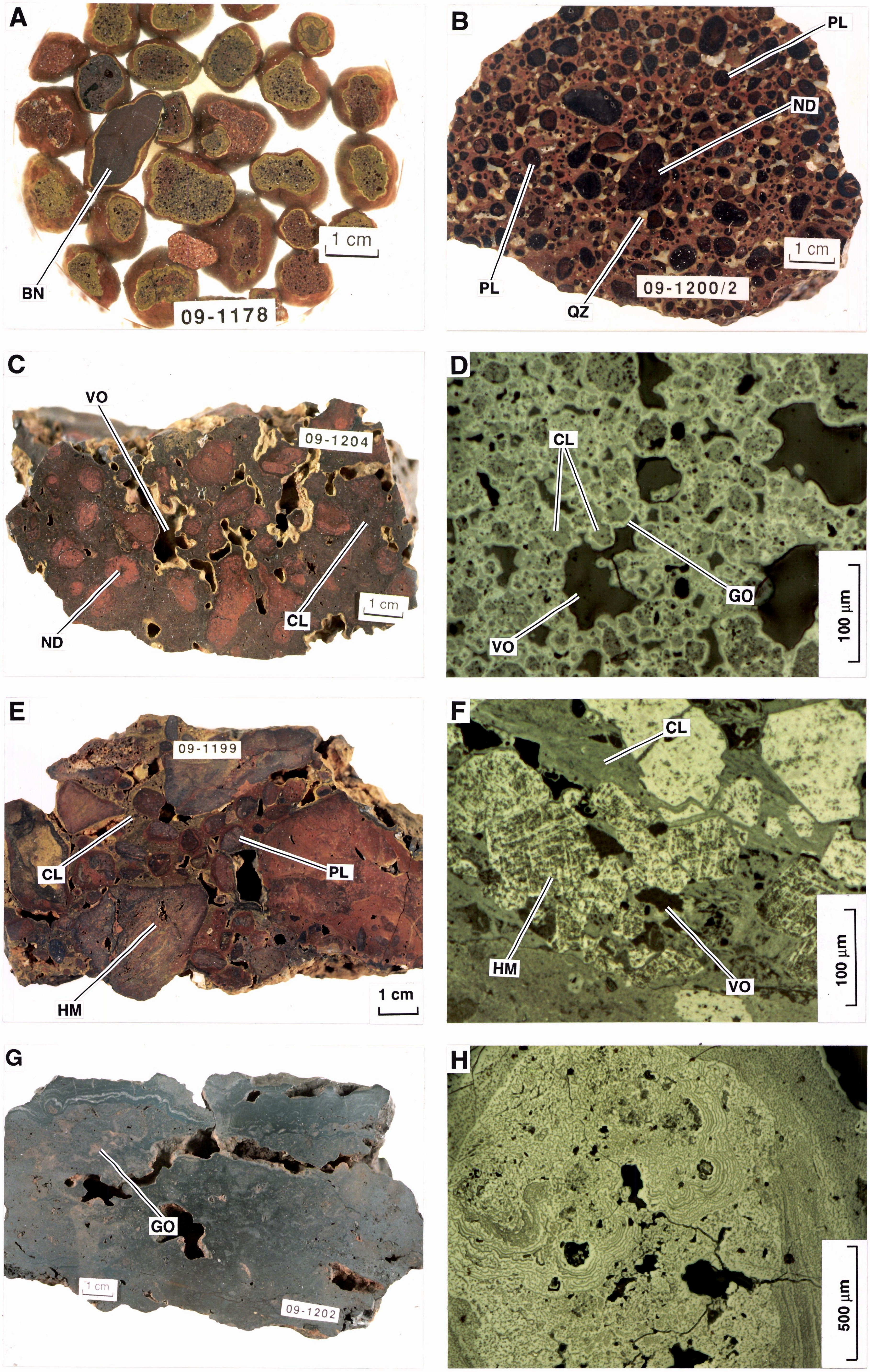
A
BN
1 cm
09-1178
B
PL
ND
PL
QZ
1 cm
09-1200/2
C
VO
09-1204
CL
1 cm
ND
D
CL
GO
VO
100 µm
E
09-1199
CL
PL
HM
1 cm
F
CL
HM
VO
100 µm
G
GO
1 cm
09-1202
H
500 µm

## TABLE 1

## RELATIVE MINERALOGICAL COMPOSITION OF REGOLITH MATERIALS

| | | Å | 3.34 | 3.04 | 7.15 | 4.85 | 2.69 | 4.18 | 3.45 | 2.39 | 3.26 |
|---|---|---|---|---|---|---|---|---|---|---|---|
| Sample | Regolith Type | Code | Quartz | Calcite | Kaolinite | Gibbsite | Hematite | Goethite | Barite | Cryptomelane | Anatase |
| 09-1157 | Fe-rich duricrust | LT229 | 5 | 0 | 0.5 | 0 | 7 | 7 | 0 | 0 | 0 |
| 09-1168 | Ferruginous saprolite | SP000 | 31.5 | 0 | 2 | 0 | 4 | 5.5 | 0 | 0 | 0 |
| 09-1177 | Hardpanised colluvial gravelly clay | CV104HP | 17.5 | 0 | 5 | 0 | 2 | 6 | 1 | 0 | 0 |
| 09-1199 | Hardpanised pisolitic duricrust | LT202HP | 6 | 0 | 0 | 6.5 | 7.5 | 5.5 | 0 | 0 | 0 |
| 09-1162 | Fragmental duricrust | LT205 | 1.5 | 0 | 4.5 | 0 | 4.5 | 11.5 | 0 | 0 | 1 |
| 09-1200/1 | Nodular duricrust | LT204 | 1 | 0 | 1 | 10 | 7.5 | 5.5 | 0 | 0 | 0 |
| 09-1200/2 | Pisolitic nodular duricrust | LT203 | 2.5 | 0 | 0.5 | 10 | 5 | 1 | 0 | 0 | 0 |
| 09-1202 | Manganiferous vermiform duricrust | LT231 | 0.5 | 0 | 0 | 0 | 1 | 1.5 | 0 | 5.5 | 0 |
| 09-1204 | Vermiform duricrust | LT231 | 1 | 0.5 | 0 | 4 | 4.5 | 6.5 | 0 | 0 | 0 |
| 09-1207/1 | Manganiferous pisolitic duricrust | LT203 | 0 | 0 | 0.5 | 0 | 2 | 3 | 0 | 2 | 0 |
| 09-1207/2 | Manganiferous vermiform duricrust | LT231 | 0 | 0 | 0 | 0 | 0 | 2.5 | 0 | 5.5 | 0 |
| 09-1221 | Colluvial gravelly clay | CV104 | 22.7 | 0 | 1 | 0 | 3.5 | 3.5 | 0 | 0 | 0 |
| 09-1222 | Colluvial silty clay | CV102 | 50.7 | 0 | 6 | 0 | 3 | 2.5 | 0 | 0 | 0 |
| 09-1223 | Colluvial gravelly clay | CV104 | 49.2 | 0 | 2 | 0 | 3.5 | 2 | 0 | 0 | 0 |
| 09-1232 | Ferruginous saprolite | SP000 | 1 | 0 | 5 | 0 | 3 | 6.5 | 0 | 0 | 0 |

Note : Numbers represent the XRD peak heights in cm; they represent approximate differences between samples and should not be used to compare abundances between different minerals

# TABLE 2
## GEOCHEMISTRY OF REGOLITH MATERIALS

| | | | | Method | XRF | XRF | XRF | XRF | XRF | XRF | XRF | XRF | XRF | XRF | Grav | NAA | INAA | XRF | INAA | NAA | XRF | INAA |
|---|---|---|---|---|---|---|---|---|---|---|---|---|---|---|---|---|---|---|---|---|---|---|
| | | | | | SiO2 | Al2O3 | Fe2O3 | MnO | MgO | CaO | Na2O | K2O | TiO2 | P2O5 | LOI | As | Au | Ba | Br | Ce | Cl | Co |
| | | | | Detn | 0.01 | 0.01 | 0.01 | 0.002 | 0.01 | 0.010 | 0.01 | 0.001 | 0.003 | 0.002 | - | 1 | 5 | 30 | 2 | 2 | 20 | 1 |
| Sample No | Regolith Type | Code | East | North | % | % | % | % | % | % | % | % | % | % | % | ppm | ppb | ppm | ppm | ppm | ppm | ppm |
| 09-1157 | Fe-rich duricrust | LT229 | 667245 | 7160745 | 10.73 | 3.86 | 76.24 | 0.043 | 0.08 | 0.10 | 0.02 | 0.03 | 0.29 | 0.218 | 7.74 | <1 | <5 | 241 | 2.91 | 20.90 | 270 | 22.90 |
| 09-1162 | Ferruginous saprolite | SP000 | 669195 | 7163115 | 19.04 | 17.45 | 49.87 | 0.017 | 0.06 | 0.00 | 0.00 | <0.01 | 2.66 | 0.036 | 11.64 | 4.11 | <5 | 89 | <2 | 12.60 | <20 | 11.20 |
| 09-1168 | Hardpanised colluvial gravelly clay | CV104HP | 663315 | 7159755 | 38.77 | 12.03 | 39.64 | 0.025 | 0.15 | 0.02 | 0.02 | 0.36 | 0.68 | 0.096 | 8.21 | 41.30 | <5 | 1005 | <2 | 12.50 | <20 | 4.64 |
| 09-1177 | Hardpanised pisolitic duricrust | LT202HP | 662205 | 7158795 | 43.53 | 22.78 | 18.78 | 0.032 | 0.14 | 0.03 | 0.03 | 0.12 | 0.84 | 0.029 | 11.33 | 23.80 | <5 | 8362 | <2 | 31.10 | <20 | 5.47 |
| 09-1199 | Fragmental duricrust | LT205 | 665535 | 7164555 | 3.43 | 19.94 | 61.42 | 0.402 | 0.07 | <0.01 | <0.01 | 0.01 | 1.20 | 0.087 | 13.98 | 34.30 | <5 | 138 | <2 | 21.10 | 40 | 29.80 |
| 09-1200/1 | Nodular duricrust | LT204 | 665325 | 7165035 | 4.39 | 29.59 | 46.80 | 0.160 | 0.08 | 0.00 | 0.02 | 0.04 | 1.42 | 0.127 | 17.69 | 51.20 | <5 | 116 | 2.17 | 9.20 | 30 | 9.25 |
| 09-1200/2 | Pisolitic nodular duricrust | LT203 | 665325 | 7165035 | 7.38 | 25.10 | 51.52 | 0.162 | 0.07 | <0.01 | 0.03 | 0.02 | 2.52 | 0.030 | 13.10 | 29.00 | <5 | 20 | <2 | 9.15 | <20 | 58.20 |
| 09-1202 | Manganiferous vermiform duricrust | LT231 | 665265 | 7165575 | 6.46 | 8.28 | 15.48 | 56.278 | 0.13 | 0.06 | 0.17 | 2.31 | 0.70 | 0.236 | 13.17 | 6.90 | <5 | 5445 | <2 | 122.00 | <20 | 700.00 |
| 09-1204 | Vermiform duricrust | LT231 | 665805 | 7166775 | 2.36 | 20.11 | 58.41 | 0.656 | 0.36 | 0.64 | 0.03 | 0.01 | 0.64 | 0.048 | 16.06 | 27.80 | <5 | <30 | 3.53 | 35.60 | 50 | 394.00 |
| 09-1207/1 | Manganiferous pisolitic duricrust | LT203 | 669735 | 7166385 | 4.29 | 4.44 | 44.87 | 29.733 | 0.10 | 0.22 | 0.10 | 0.73 | 0.08 | 0.028 | 12.42 | 14.00 | <5 | 12785 | <2 | 565.00 | <20 | 1190.00 |
| 09-1207/2 | Manganiferous vermiform duricrust | LT231 | 669735 | 7166385 | 5.92 | 5.23 | 25.39 | 50.059 | 0.15 | 0.24 | 0.22 | 2.33 | 0.07 | 0.011 | 13.98 | 12.10 | <5 | 7939 | <2 | 434.00 | <20 | 1400.00 |
| 09-1221 | Colluvial gravelly clay | CV104 | 662355 | 7160895 | 34.76 | 7.51 | 47.08 | 0.506 | 0.11 | 0.00 | 0.01 | 0.23 | 0.73 | 0.145 | 8.12 | 42.40 | <5 | 977 | <2 | 47.70 | <20 | 15.90 |
| 09-1222 | Colluvial silty clay | CV102 | 662355 | 7160895 | 54.47 | 17.23 | 17.82 | 0.151 | 0.29 | 0.06 | 0.05 | 0.65 | 1.21 | 0.057 | 7.42 | 15.60 | <5 | 307 | <2 | 41.90 | <20 | 9.53 |
| 09-1223 | Colluvial gravelly clay | CV104 | 662355 | 7160895 | 52.65 | 10.10 | 27.36 | 0.604 | 0.26 | 0.07 | 0.05 | 0.43 | 0.88 | 0.077 | 6.43 | 24.40 | 10.0 | 1070 | <2 | 64.70 | <20 | 18.70 |
| 09-1232 | Ferruginous saprolite | SP000 | 669735 | 7166385 | 35.14 | 24.19 | 24.83 | 0.514 | 0.21 | 0.19 | 0.03 | 0.10 | 0.89 | 0.015 | 12.74 | 11.40 | <5 | 497 | <2 | 83.80 | <20 | 41.50 |

| | | INAA | INAA | XRF | INAA | XRF | INAA | INAA | INAA | INAA | XRF | XRF | XRF | XRF | XRF | INAA | INAA | INAA | XRF | INAA | INAA | INAA | XRF | 1NAA | XRF | INAA | XRF | XRF |
|---|---|---|---|---|---|---|---|---|---|---|---|---|---|---|---|---|---|---|---|---|---|---|---|---|---|---|---|---|
| | Sample No | Cr | Cs | Cu | Eu | Ga | Hf | La | Lu | Mo | Nb | Ni | Pb | Rb | S | Sb | Sc | Sm | Sr | Ta | Th | U | V | W | Y | Yb | Zn | Zr |
| | | 5 | 1 | 10 | 0.5 | 3 | 0.5 | 0.5 | 0.2 | 5 | 4 | 10 | 5 | 5 | 10 | 0.2 | 0.1 | 0.2 | 5 | 1 | 0.5 | 2 | 5 | 2 | 0.5 | 0.5 | 5 | 5 |
| Sample No | | ppm | ppm | ppm | ppm | ppm | ppm | ppm | ppm | ppm | ppm | ppm | ppm | ppm | ppm | ppm | ppm | ppm | ppm | ppm | ppm | ppm | ppm | ppm | ppm | ppm | ppm | ppm |
| 09-1157 | 09-1157 | 15.2 | 1.30 | 73 | 1.24 | 10 | 1.78 | 7.03 | 0.21 | 6.3 | 5 | 28 | <5 | 0 | 1500 | <0.2 | 24.80 | 4.24 | 19 | 1.78 | 2.05 | <2 | 229 | 2.71 | 9 | 1.82 | 94 | 83 |
| 09-1162 | 09-1162 | 196.0 | <1 | 144 | 0.98 | 21 | 2.81 | 4.47 | 0.22 | <5 | 0 | 123 | <5 | 2 | 548 | 0.49 | 56.80 | 3.02 | 0 | <1 | 3.13 | <2 | 616 | <2 | 6 | 1.87 | 25 | 129 |
| 09-1168 | 09-1168 | 932.0 | 1.46 | 15 | <0.5 | 34 | 5.97 | 7.25 | <0.2 | <5 | <4 | 16 | 42 | 19 | 840 | 1.14 | 24.10 | 1.18 | 9 | <1 | 39.70 | 2.29 | 622 | <2 | 11 | 1.21 | 27 | 244 |
| 09-1177 | 09-1177 | 678.0 | <1 | <10 | 0.74 | 50 | 5.67 | 14.50 | 0.24 | <5 | <4 | 51 | 30 | 11 | 2070 | 0.93 | 36.60 | 2.60 | 15 | 1.17 | 31.00 | <2 | 392 | <2 | 15 | 1.75 | 15 | 200 |
| 09-1199 | 09-1199 | 397.0 | <1 | 78 | <0.5 | 31 | 4.31 | 9.32 | <0.2 | <5 | 0 | 2 | 9 | 7 | 1260 | 0.32 | 49.40 | 1.50 | 7 | 1.19 | 20.80 | <2 | 388 | <2 | 7 | 0.95 | 34 | 173 |
| 09-1200/1 | 09-1200/1 | 562.0 | <1 | 13 | <0.5 | 44 | 5.12 | 4.12 | <0.2 | <5 | 5 | <10 | 8 | 4 | 1170 | 0.78 | 40.40 | 1.03 | <1 | 1.13 | 37.00 | <2 | 738 | 4.96 | 6 | 1.07 | 22 | 201 |
| 09-1200/2 | 09-1200/2 | 501.0 | <1 | <10 | <0.5 | 47 | 7.04 | 1.81 | <0.2 | <5 | 18 | 19 | 22 | 2 | 1230 | 0.60 | 15.20 | 0.93 | 6 | 3.00 | 15.30 | <2 | 404 | 8.10 | 10 | 1.72 | 16 | 267 |
| 09-1202 | 09-1202 | 108.0 | <1 | 66 | 2.68 | 17 | 2.47 | 57.30 | 0.51 | <5 | <4 | 127 | 53 | 64 | 440 | <0.2 | 36.20 | 10.50 | 243 | <1 | 10.60 | <2 | 231 | <2 | 33 | 3.89 | 101 | 81 |
| 09-1204 | 09-1204 | 384.0 | <1 | 26 | <0.5 | 14 | 6.05 | 2.59 | <0.2 | <5 | <4 | <10 | 37 | <5 | 930 | <0.2 | 104.00 | 1.33 | 10 | <1 | 32.50 | <2 | 148 | <2 | 3 | 0.88 | 16 | 203 |
| 09-1207/1 | 09-1207/1 | 37.3 | <1 | 155 | 6.90 | <3 | 0.95 | 100.00 | 1.37 | <5 | <4 | 126 | 17 | 14 | 210 | <0.2 | 31.20 | 30.00 | 280 | <1 | 2.62 | <2 | 65 | <2 | 35 | 11.30 | 214 | 6 |
| 09-1207/2 | 09-1207/2 | 59.2 | <1 | 122 | 10.80 | 7 | 1.33 | 176.00 | 2.49 | <5 | <4 | 180 | 48 | 31 | 200 | <0.2 | 15.70 | 45.10 | 668 | <1 | 3.63 | <2 | 54 | <2 | 125 | 17.50 | 163 | 25 |
| 09-1221 | 09-1221 | 1020.0 | 1.72 | 36 | 0.86 | 18 | 4.01 | 16.80 | <0.2 | <5 | <4 | 39 | 17 | 22 | 380 | 0.80 | 20.50 | 3.31 | 19 | 1.02 | 17.20 | <2 | 487 | <2 | 11 | 1.69 | 75 | 153 |
| 09-1222 | 09-1222 | 663.0 | 2.94 | 2 | 0.51 | 26 | 6.41 | 24.60 | 0.28 | <5 | 4 | 64 | 40 | 42 | 180 | 0.92 | 26.20 | 3.19 | 25 | 1.38 | 19.20 | <2 | 287 | <2 | 18 | 2.11 | 51 | 224 |
| 09-1223 | 09-1223 | 785.0 | 1.92 | 21 | 0.73 | 19 | 5.62 | 21.30 | 0.22 | <5 | <4 | 60 | 38 | 28 | 250 | 0.81 | 19.10 | 3.31 | 19 | <1 | 17.50 | <2 | 332 | <2 | 10 | 1.84 | 59 | 209 |
| 09-1232 | 09-1232 | 361.0 | <1 | 65 | 0.83 | 20 | 3.28 | 17.10 | 0.24 | <5 | <4 | 350 | 81 | 1 | 200 | 0.34 | 18.00 | 2.71 | 20 | 1.97 | 9.44 | <2 | 91 | <2 | 16 | 2.21 | 36 | 112 |

Colluvial fans and footslopes occur on the lower flanks of low hills of the Robinson and Horseshoe Ranges. These are commonly characterised by coarse to blocky clasts (>200 mm), a lag of ferruginous, lithic fragments, lithic clasts, and quartz (map unit D4). Similar materials characterise drainage depressions in areas underlain by the Narracoota Formation and Peak Hill Formation. Over metavolcanic rocks of the Narracoota Formation, they comprise a medium to coarse polymictic lag, dominated by lateritic nodules, pisoliths, mottles and ferruginous saprolite, with lesser amounts of quartz and ferruginous, lithic clasts (map unit D5; Figure 6H). These clasts are set in a red, silty-clay soil, commonly overlying ferruginous saprolite, on pediments adjacent to low rises. Colluvial materials, developed over the Narracoota Formation, generally appear as red-magenta on the Landsat image. Quartz and ferruginous lithic clasts are dominant in colluvium derived from the Peak Hill Formation (map unit D6).

Unit D7, a claypan, is found southwest of the Harmony deposit. This appears as a distinctive, pale yellow area on the Landsat image. Active alluvial channels, including those marked by lines of vegetation on the sheetflood fans around Harmony, are designated unit D8.

### *3.1.2 In-situ regolith*

A significant proportion of the area covered by the mapping is *in situ* regolith. The dominant units include residual soils developed over saprolite, ferruginous saprolite and saprock (map units E1 to E7). In the Robinson and Harmony ranges, to the southwest and northeast of the Harmony deposit respectively, areas of prominent outcrop or extensive subcrop commonly occur (map unit E6). These areas are generally characterised by very coarse lag, including boulders and cobbles of partly weathered bedrock. Small areas of lateritic duricrust (map units R1 to R4) also occur, although most are too small to be represented at 1:25 000.

Immediately to the south of the Harmony deposit, colluvium mantles a long, gentle, concave slope which rises to a gently bevelled crest (breakaway) which faces south. This is shown as an orange lineation trending approximately east on the enhanced Landsat TM image (Figure 5). Near the crest of this breakaway, a pisolitic duricrust is developed (map unit R1). The bedrock comprises metasediments of the Ravelstone Formation and the duricrust developed on them is clay rich and consists mainly of quartz, kaolinite, goethite and barite (Sample 09-1177; Tables 1 and 2). The pisoliths (Figure 7A) consist of a conglomerate of tiny, subangular, hematitic granules and kaolinite balls, indicating a complex process of formation. Late barite occurs in very fine solution channels in the pisoliths.

Towards the base of the breakaway, circular structures of varying sizes are present in the weathered metasediments (Figure 6I). They contain nodules and pisoliths which may have originated from a previously overlying duricrust or colluvium. Their development may be linked to biological activity. An erosional plain has developed to the south of the breakaway where the regolith comprises a ferruginous saprolite, mantled by a coarse, blocky, quartz-rich, polymictic lag, including ferruginous lithic fragments (map unit E1; Figure 6J). These areas are dull brown-magenta and green on the Landsat image (Figure 5). The plain is punctuated by sporadic quartz blows, leaving scattered subangular, blocky, quartz cobbles. Green patches on the satellite image are generally associated with abundant quartz in the lag. This is particularly evident over the schists of the Peak Hill Formation (see the area south of the Peak Hill Mine on the Landsat image of Figure 5). Here a coarse, quartz-rich lag is developed on a gently sloping pediplain. The coarse lag on these erosional plains is interspersed with sporadic outcrops of ferruginous-saprolite and saprock (Figures 6H and O).

Low rises occur to the east and southeast of the Harmony deposit (*e.g.*, Figure 6L). Here, the regolith is commonly developed over mafic and ultramafic metavolcanics of the Narracoota Formation and consists of Fe-rich, lateritic duricrust, lateritic gravels and ferruginous saprolites (map unit E4; appearing as oranges and reds on the Landsat image; Figure 5). The composition of ferruginous saprolite is shown in Tables 1 and 2 (Sample 09-1162). Fe-rich duricrusts are developed over mafic volcanics of the Narracoota Formation (map unit R3; Figure 6M), tend to be black, massive and silicified and are dominated by hematite and goethite (sample 09-1157; Tables 1 and 2).

Sediments of the Ravelstone and Horseshoe formations and the Padbury Group have weathered to a range of duricrusts in addition to those described above. Their composition commonly reflects the original composition of the underlying sediments. Iron-rich (map unit R2; see Figure 6K) and manganiferous (map unit R4; see Figure 6P) duricrusts occur and examples of these are illustrated in Figure 7; their compositions are provided in Tables 1 and 2. The Fe-rich varieties exhibit different fabrics (Figures 7B and E). An Fe-rich, pisolitic-nodular duricrust, shown in Figure 7B is developed on sediments of the Ravelstone Formation. It consists of closely packed haematitic pisoliths, set in goethite-rich clay containing gibbsite with a minor amount of quartz filling the interstices. This pisolitic-nodular duricrust grades downward into nodular duricrust.

A dark, brownish red, vermiform duricrust (Figure 7C), is related to interstratified, calcareous, manganiferous shale and subgreywacke of the Horseshoe formation. It consists dominantly of goethite and some kaolinite, gibbsite and calcite. The vesicles in this vermiform duricrust seem to have developed by dissolution of carbonates in the clay-rich matrix (Figure 7D). A fragmental duricrust, probably derived from banded iron formation of the Horseshoe Formation (Figure 7E), consists of angular, ferruginous fragments and pisoliths. It is blocky and the blocks are coated with black Mn oxides. The ferruginous fragments and pisoliths contain magnetite grains pseudomorphed by hematite (martite) with a characteristic trellis fabric (Figure 7F). It consists dominantly of hematite and goethite with some quartz and kaolinite.

To the northeast of the Harmony deposit, in low hills developed on mixed sediments of the Horseshoe Formation, thick, massive to vermiform, manganiferous, lateritic duricrusts have developed in places (Figure 6P; map unit R4). These were mined for manganese in 1948-69 (Subramanya *et al.*, 1995). Several origins have been proposed for these materials. MacLeod (1970) and Blockley (1975) considered them to represent deposits infilling drainage lines, or fossil lakes and swamps formed on a dissected Tertiary plateau. They were classified as bog manganese ores. More recently, Gee (1987) considered these to have resulted from a lateritic enrichment from primary manganese in underlying shales and siltstones of the Horseshoe Formation. Although field relationships with other regolith materials supports the latter hypothesis, there is evidence for lateral migration and accumulation of manganese. In some of the old mine pits, manganiferous duricrusts lie directly over Fe-rich, massive to vermiform duricrusts and ferruginous saprolite. The contact is generally angular.

Different types of manganiferous duricrusts indicate various degrees of Mn mobilisation. Generally, cauliflower-pisolitic manganiferous duricrust are developed over nodular or vermiform duricrust (Figure 7G) which is underlain by massive, manganiferous duricrust. The manganiferous vermiform duricrust contains cryptomelane, goethite and hematite (sample 09-1202 of Tables 1 and 2). Colloform growth rings within pisoliths are shown in Figure 7H. Compositions of other manganiferous duricrusts are also shown (09-1207/1 and 09-1207/2 in Tables 1 and 2) which unconformably overlie ferruginous saprolite (09-1232 in Tables 1 and 2). The spatial extent of all duricrusts found in the study area is generally very limited and their occurrence very patchy.

## 3.2 Local regolith geology

In the immediate vicinity of the Harmony deposit, the regolith consists of a surface-hardpanised, red-brown colluvium of variable thickness, overlain by a polymictic lag that has been sorted into different size fractions by sheetwash. Beneath this, the degree of complexity varies considerably and drillhole logging was required to reveal the details. In places, particularly close to the

Harmony deposit, the colluvium directly overlies a regolith of ferruginous saprolite, saprolite and saprock developed on Proterozoic rocks. Elsewhere, notably to the north and south of the Harmony deposit, the colluvium is underlain by various mottled clay sediments that infill palaeovalleys cut into the Proterozoic basement. Parts of the basement saprolites are mantled by buried lateritic residuum, having nodules and pisoliths coated with pale brown, clay-rich cutans. Horizons containing lateritic nodules and some pisoliths, with cutans, also occur within and above the valley-fill sediments.

Because of the complexity of the sub-surface regolith and the very extensive drilling around the Harmony deposit, an overview of the regolith was undertaken to develop a 3D regolith stratigraphic model for the site. A total of 708 drillholes were logged, noting the major regolith units (colluvium, valley-fill sediment, lateritic duricrust) and the top and nature of the residual profile. A detailed lithological log was not attempted as this had already been completed by AFMECO Pty Ltd. Each regolith log was corrected for hole inclination and collar elevation and a database assembled. Details of the logging method are given in Appendix 9.

### *3.2.1 Palaeotopography*

Contour maps of the various buried interfaces and isopach maps of each of the regolith units provided a palaeotopographic model to indicate the spatial disposition of regolith materials (Figures 8A-E). The outline of the Harmony pit and the most recent interpretation of the bedrock geology obtained from drilling (see Figure 4A) were added to aid interpretation.

The 'palaeotopography' provided by these contour maps has some limitations. The 'surfaces' that they represent may be used to approximate the form of the topography of a basement prior to a particular sedimentary event. Only those parts of the surfaces that were subsequently blanketed and not eroded later are accurately preserved. The exposed parts would have suffered some erosion since and so must be regarded as 'minimum' surfaces. These 3D relationships provide an improved understanding of landscape development, may be used to guide sampling of the most appropriate medium, assist in understanding dispersion processes and may be used to predict dispersion directions and to interpret geochemical data. A schematic representation of the regolith about the deposit is shown in Figure 9 as a cut-away 3D model.

The palaeosurface (Figure 8A) of the residual profile on the basement (including the top of the saprolite and their associated mottled clays and lateritic residuum on metasediments and metavolcanics) shows that the deposit is on a north-northwest trending palaeohigh. The highest part of this palaeohigh is occupied by ultramafic rocks of the Narracoota Formation and its resistance may be related to slight surface silicification prior to erosion. The basement palaeosurface had a palaeorelief of about 40 m within the study area.

The palaeotopography contains two palaeovalleys. A major, deep palaeovalley, referred to here as the Waste Dump palaeovalley, parallels the trend of the palaeohigh and lies to the south of the Harmony deposit. A west-northwest flow direction from the volcanics into the metasediments is implied from trends in the topography of the valley floor and a greater valley width to the west (Figure 8A). Another, apparently shallower and sub-parallel, palaeovalley lies north of the deposit. A small branch of this, the Harmony palaeovalley, drains the Harmony deposit to the north-northeast, locally incising the palaeohigh. The alignment of the palaeovalleys are most probably related to underlying structures and lithological differences in the basement.

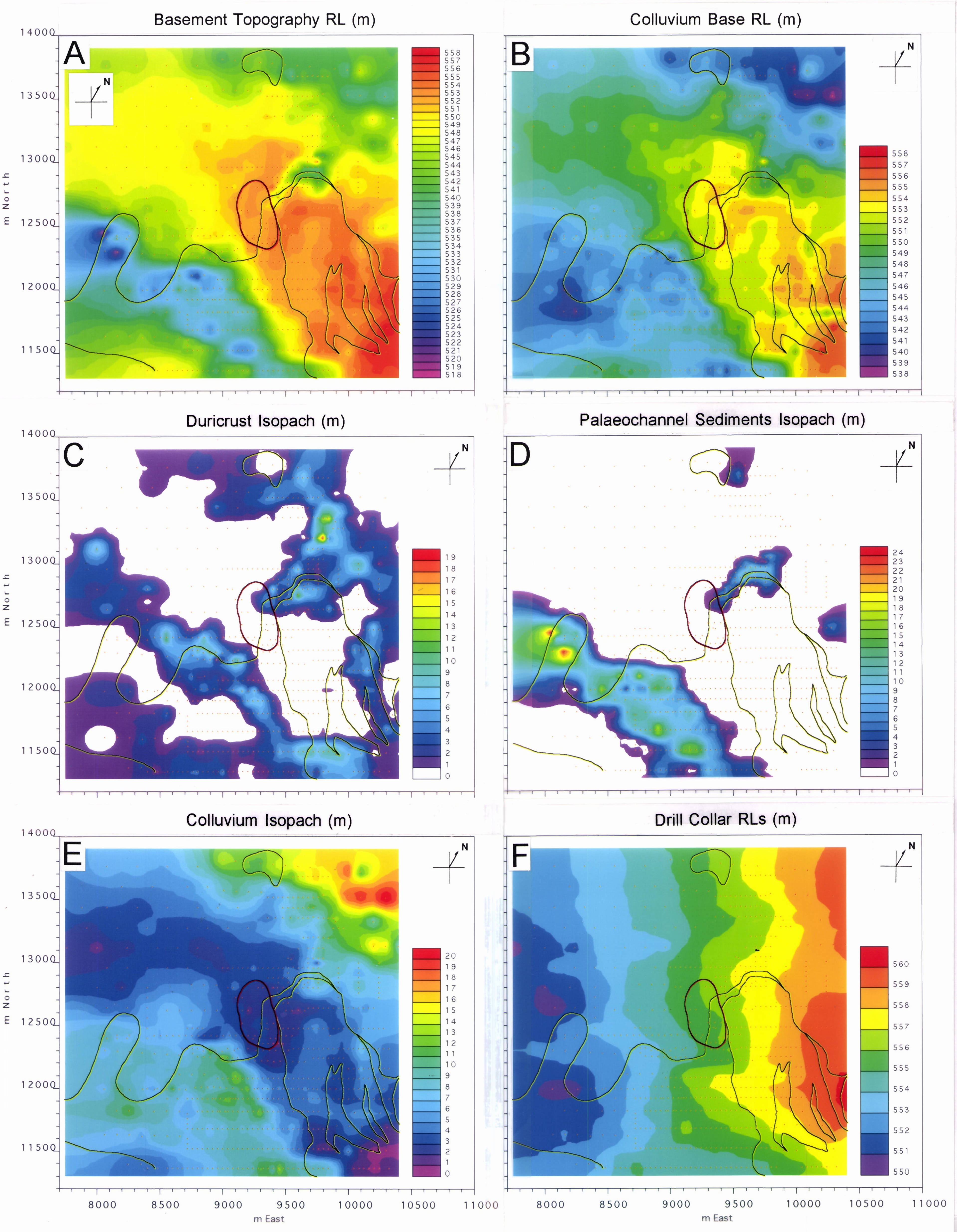


Figure 8. Colour contour maps of the palaeotopography and isopach maps of some regolith units around the Harmony deposit showing the palaeotopography of the residual profile (A), the palaeotopography prior to deposition of the colluvium (B), the distributions and thicknesses of lateritic duricrust (C), valley-fill sediments (D) and colluvium (E) and the present surface (F). The bedrock geology (Figure 4A), pit outline and data points have been added.

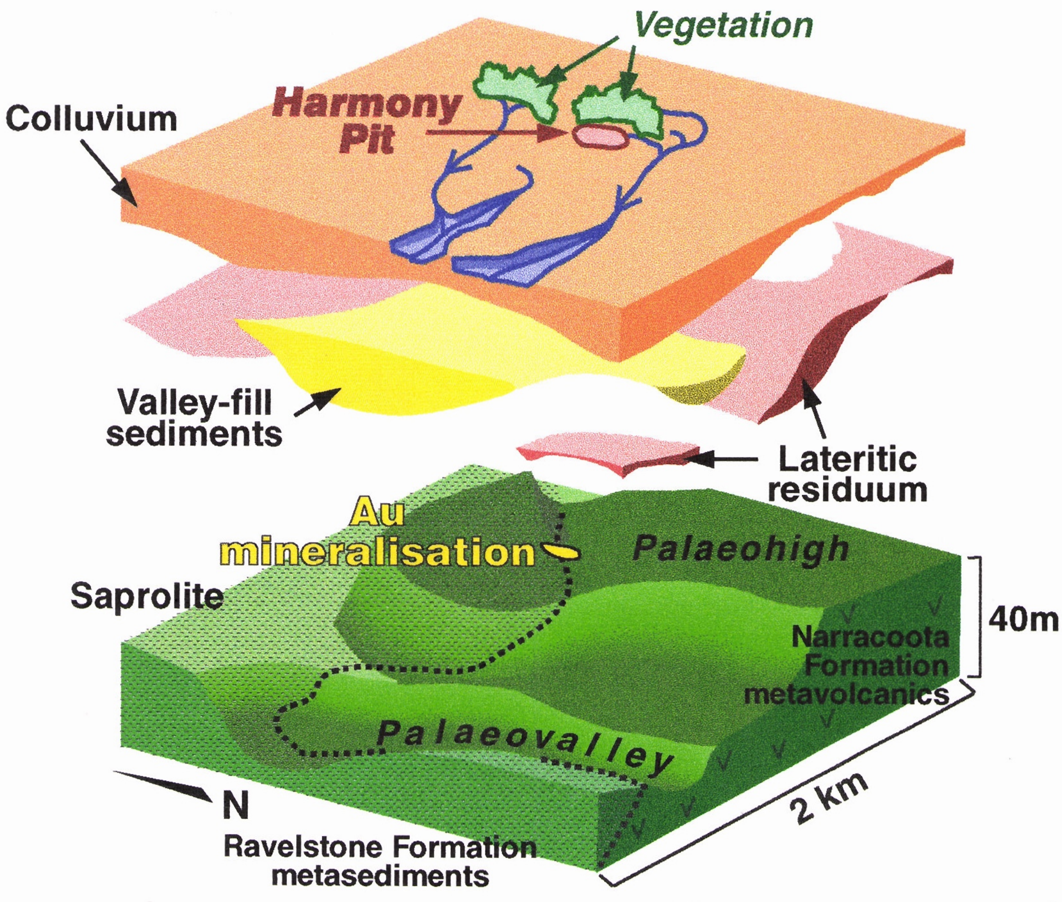


Figure 9. Block model of regolith relationships around the Harmony Au deposit. Proterozoic metavolcanics and metasediments, with Au mineralisation located at their contact, have been eroded and lateritised. Palaeovalleys have been partly filled with clay-rich valley-fill sediments, which have also been lateritised. Finally, the palaeotopography has been filled in and blanketed by colluvium-alluvium to leave a very flat plain, completely concealing the Au mineralisation and the complex regolith.

## FIGURE 10

## RAB DRILLSPOIL HEAPS - WASHED BY RAIN

**A.** Colluvium. Dark brown chips, pisoliths and lithorelics derived from lateritic residuum from which the cutans have been abraded. This is set in a slightly lighter brown pulp of quartz, goethite and fine mica. Drillhole 263H440 1-2 m depth down hole: co-ordinates 8855 mE 12421 mN.

**B.** Interface. Gravelly base of the colluvium and top of the duricrust which is rich in pisoliths and nodules. A few have retained parts of their cutans but considerable wear is evident in others. Drillhole 263H837 3-4 m depth down hole: co-ordinates 10160 mE 12159 mN.

**C.** Mottled clays of the Waste Dump palaeovalley. Fine chips of yellow-brown and white, puggy clay in a clay pulp. Some of the clay is mottled with a light-brown stain of goethite. Drillhole 263H1033 12-13 m depth down hole: co-ordinates 8920 mE 11680 mN.

**D.** Lateritic residuum. Broken, deep red-brown pisoliths and nodules with thin, yellow-brown cutans in a light-brown clay. Some of the clay was probably washed down from above. Drillhole 263H440 14-15 m depth down hole: co-ordinates 8855 mE 12421 mN.

**E.** Mottled zone. Deep red-brown, hematite-rich, mottles and elongate nodules with a thin, yellow cutan of goethite-rich clay as fragments and chips in powdery, white kaolinite. Drillhole 263H440 at 23-24 m depth down hole: co-ordinates 8855 mE 12421 mN.

**F.** Saprolite. Chips of kaolinite-rich saprolite, slightly stained with goethite, clearly showing the schistose fabric of the metavolcanics (Narracoota Formation) in powdered material of a similar composition. Drillhole 263H829 at 7-8 m depth down hole: co-ordinates 9640 mE 12080 mN.

## SOIL AND MOTTLED MATERIALS

**G.** Washed and unwashed mottled zone material. Washing has served to disaggregate the clays and remove them, leaving a highly ferruginous, ferruginous concentrate. Such treatment has left a material which is geochemically similar to the duricrust.

**H.** Soil. Cleaned fractions, from left to right 710-2000, 500-710, 250-500, 75-250 µm showing a concentration of ferruginous materials in the coarser fractions and increased silty and, in part, wind-blown, quartz in the finer fractions. Specimen RBX-445.

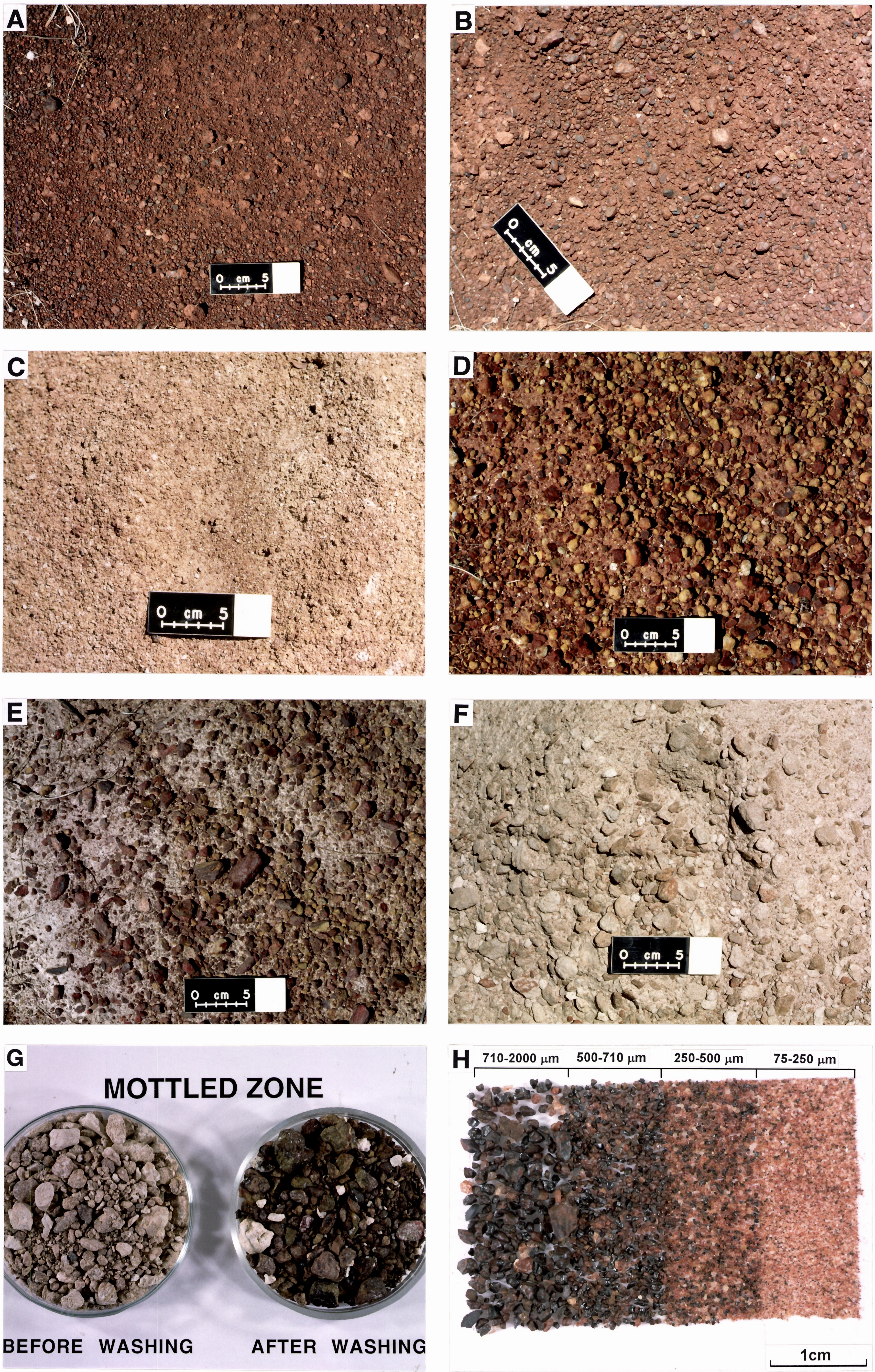
A
0 cm 5
B
0 cm 5
C
0 cm 5
D
0 cm 5
E
0 cm 5
F
0 cm 5
G
MOTTLED ZONE
BEFORE WASHING
AFTER WASHING
H
710-2000 µm
500-710 µm
250-500 µm
75-250 µm
1cm

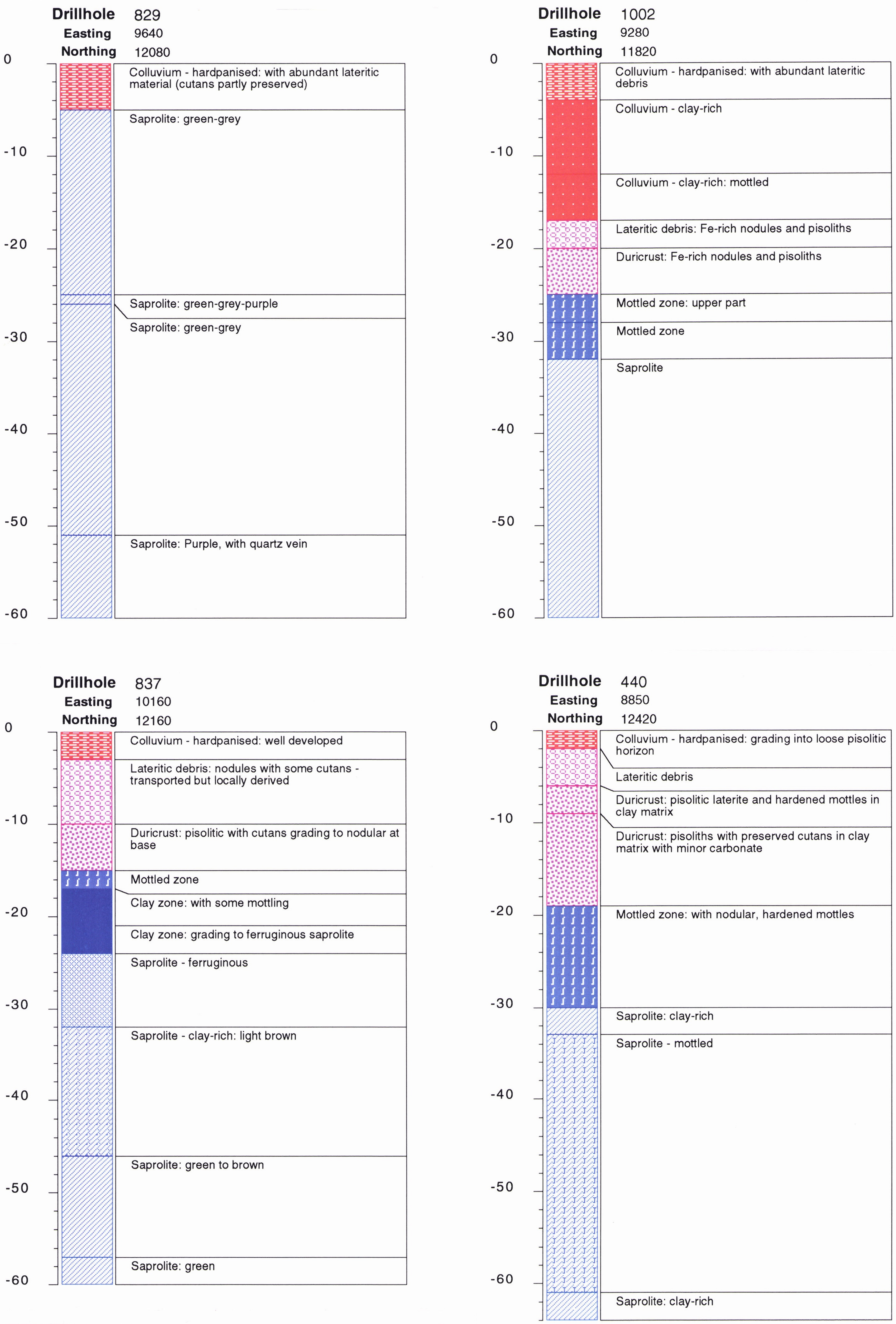


Figure 11. Typical regolith sections developed on mafic and ultramafic rocks of the Narracoota Formation and metasediments of the Ravelstone Formation from logging of drillspoil.

### *3.2.2 Weathered Profiles on the Basement*

The palaeohigh consists largely of weakly indurated, ferruginous saprolite. The saprolite and ferruginous saprolite are grey and light yellow-brown respectively; the shapes of the chips in the drillspoil are controlled by the fabric of the saprolite (Figure 10F). An example of the regolith stratigraphy developed over an ultramafic rock on the palaeohigh is illustrated in Figure 11A which has a thin veneer of colluvium over saprolite.

The floors of the palaeovalleys are particularly deeply weathered and have been eroded to mottled zones and clay-rich saprolites. In drillspoil, the mottled material consists of a mixture, in varying proportions, of dark red or yellowish brown nodules and powdery, white kaolinite (Figure 10E).

Lateritic duricrust and lateritic gravels are preserved largely on the flanks of the palaeohigh. Combined, they vary in thickness, generally being about 8 m thick but, in places, reaching 19 m (Figure 8C). Some of the thicker parts are likely to have an upper, slumped or transported component. The duricrust occurs neither in the axes of the palaeovalleys, nor on the palaeohigh. Its nodules are generally dark red in drillspoil and have distinctive, yellow-brown cutans (Figure 10D).

Typical regolith sections illustrating stratigraphic relationships as described above are shown in Figure 11B, C and D which all contain lateritic duricrust. Figure 11B is typical of the stratigraphy on the northern flank of the Waste Dump palaeovalley on mafic metavolcanic rocks of the Narracoota Formation where the residual regolith is covered by thick colluvium. This may be contrasted with Figure 11C where the colluvium is thin and the bedrock is similar. Figure 11D illustrated a profile from very close to the Harmony deposit, where a thick layer of lateritic duricrust and lateritic debris (partly transported) is developed on metasediments of the Ravelstone Formation. Here the colluvium is very thin.

### *3.2.3 Valley-fill sediment*

The palaeovalleys have been partly filled with clay-rich sediments, generally about 10 m thick but reaching 24 m locally (Figure 8D). Mostly, these consist of soft, puggy, grey, green or light-brown clays (Figure 10C) which are slightly mottled and have a tendency to crack on drying. A very thin layer of sand occurs at the base in a very few places. These valley-fill sediments are extensive in the Waste Dump palaeovalley but are developed only patchily in the northern palaeovalley (probably partly removed by erosion). The residual regolith beneath the valley-fill sediments consists largely of mottled clays, clay-rich saprolite and some lateritic duricrust, with very little ferruginous saprolite (Figure 4B).

### *3.2.4 Colluvium*

After deposition of the valley-fill clays and some subsequent erosion (Figures 8B and D), there has been extensive deposition of a dark brown, gravelly to silty colluvium that has infilled the remaining palaeolows. The thickest colluvium (Figure 8E) has been deposited over the palaeovalleys, where it generally reaches a thickness of 7-12 m and, locally, 20 m but it is only 0.5-3.0 m thick over the palaeohigh and the Harmony deposit. The relief, prior to deposition of the colluvium, is shown in Figure 8B. The palaeohigh, below the colluvium, is dominated by weakly silicified ferruginous saprolites on mafic and ultramafic rocks, although the relief was more muted (15 m) compared to 40 m on the basement.

The upper part of the colluvium has been silicified to a red-brown hardpan. It consists of sand- and gravel-sized, matrix-supported, subangular to subrounded granules and lateritic clasts, with some minor quartz, in a silty matrix of quartz, kaolinite, mica and Fe oxides. In drillspoil, the colluvium is rich in brown, worn, polymictic granules and fragments of ferruginous lithorelics (lacking cutans) in a small amount of brown clay-rich pulp (Figure 10A). The unconformity at the base of the colluvium contains a mixture of colluvium and the underlying regolith (lateritic duricrust, ferruginous saprolite or mottled zone). Here, some granules have thin, partly worn cutans (Figure 10B).

### *3.2.5 Present surface*

The present surface, with a total relief of 10 m across the study area (2.8 km), is gently inclined to the west-southwest and is incised by west-southwest flowing drainages (Figures 8F and 9). This surface is mantled by a patchily-developed, polymictic lag of ferruginous lithorelics, BIF fragments, lateritic residuum and quartz that has been partly sorted by sheetwash and aeolian action.

# 4 REGOLITH STRATIGRAPHY AND CHARACTERISTICS

## 4.1 Introduction

Initially, the regolith stratigraphy was known only from RAB drill cuttings. However, following the discovery of the Harmony deposit, the regolith and bedrock were investigated by diamond drilling, some of which was cored from surface. Most of the diamond drilling was concentrated on the palaeohigh, proximal to the Harmony deposit, giving several sections through the thin colluvial cover and ferruginous saprolite. Here, there are some complex relationships between the colluvium and the basement, where they are separated by a mixed zone of 0.2-0.7 m thickness, comprising blocks of saprolite in a matrix of earthy colluvium, which could represent a palaeosol. However, there were no cored stratigraphic sections through the thicker colluvium and the valley-fill sediments, marginal to this palaeohigh and distant from Harmony, until a special-purpose triple-tube diamond hole (DDH PHD-006) was drilled in the Waste Dump palaeovalley at the end of 1995. Despite intersecting smectite-rich clays, the core recovery was good, with minor loss confined to poorly consolidated sand and the interfaces between soft and relatively hard materials. Some unusual drilling artefacts, resembling conglomerate layers, were produced by the forced emplacement by drilling of hard, particulate material, which had caved from above, into soft, plastic clay at the top of a drilling interval. Numbers in parenthesis in the following description refer to the stratigraphic core segments of Figure 12. Detailed petrographic information is given in Appendix 5. Locations of specimens are given in Appendix 5 and Figure 12.

## 4.2 Waste Dump palaeovalley

### *4.2.1 Basement*

DDH PHD-006 penetrated the top 6 m of a clay-rich saprolite of the slightly schistose mafic metavolcanics of the Narracoota Formation (Figures 12 and 13) before it was terminated. The lower part of the saprolite is coarsely cleaved, reddish brown (Figure 14P), hematite-bearing, and mottled with grey (15). The upper part is highly bleached to white or very pale grey (14) and contains a few disaggregated quartz veins (Figure 14O), notably at 38.7 m. The saprolite has a consistent mineralogy, being rich in muscovite, quartz and kaolinite, the colour differences being due to minor variations in hematite content. The bleaching may be related to leaching of Fe oxides by groundwater just below the permeable, sandy base of the valley-fill sediment.

### *4.2.2 Valley-fill sediment*

At the base of the valley-fill sediment is a very thin (1.20 m) unbedded, grey, fine-grained sand (13). It is relatively clean, well sorted and closely packed, consisting of a small size range (0.1-3.0 mm) of quartz, minor quartzite grains (Figure 14N) and a trace of rounded tourmaline. The larger grains are well rounded; the smaller grains are angular and vary from equant to shard-like. The intergranular space is occupied by very fine-grained kaolinite. The upper part of the sand is particularly fine grained and stained with goethite, presumably from the overlying ferruginous material.

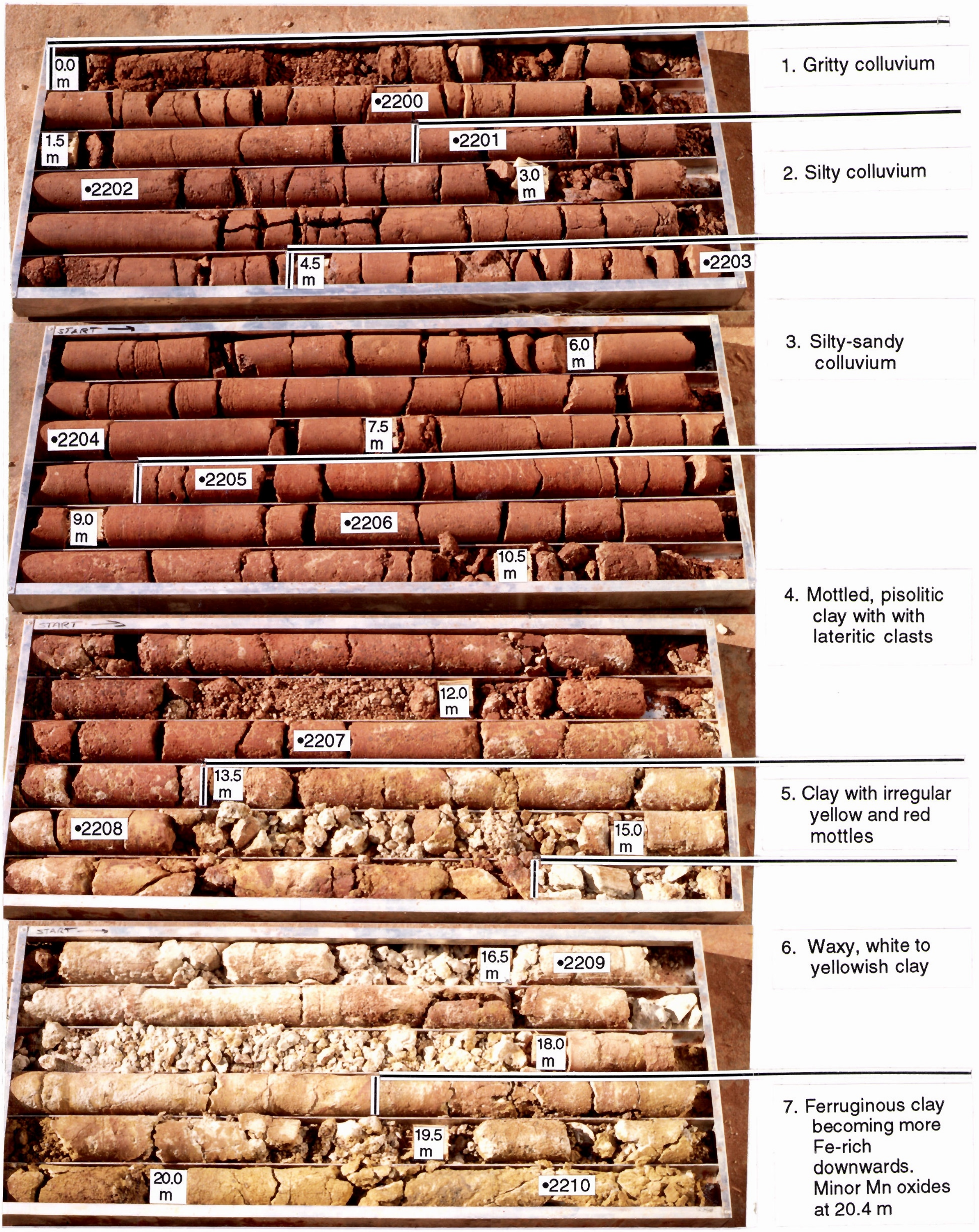


Figure 12. Composite photographic record of the drillcore of DDH PHD-006 from the Waste Dump palaeovalley, prior to sampling. Major stratigraphic units are numbered (see text), down-hole depths are shown and specimen locations are numbered. Collar location 8790 mE 12090 mN.


Figure 12. (cont'd). Composite photographic record of the drillcore of DDH PHD-006 from the Waste Dump palaeovalley, prior to sampling. Major stratigraphic units are numbered (see text), down-hole depths are shown and specimen locations are numbered. Collar location 8790 mE 12090 mN.

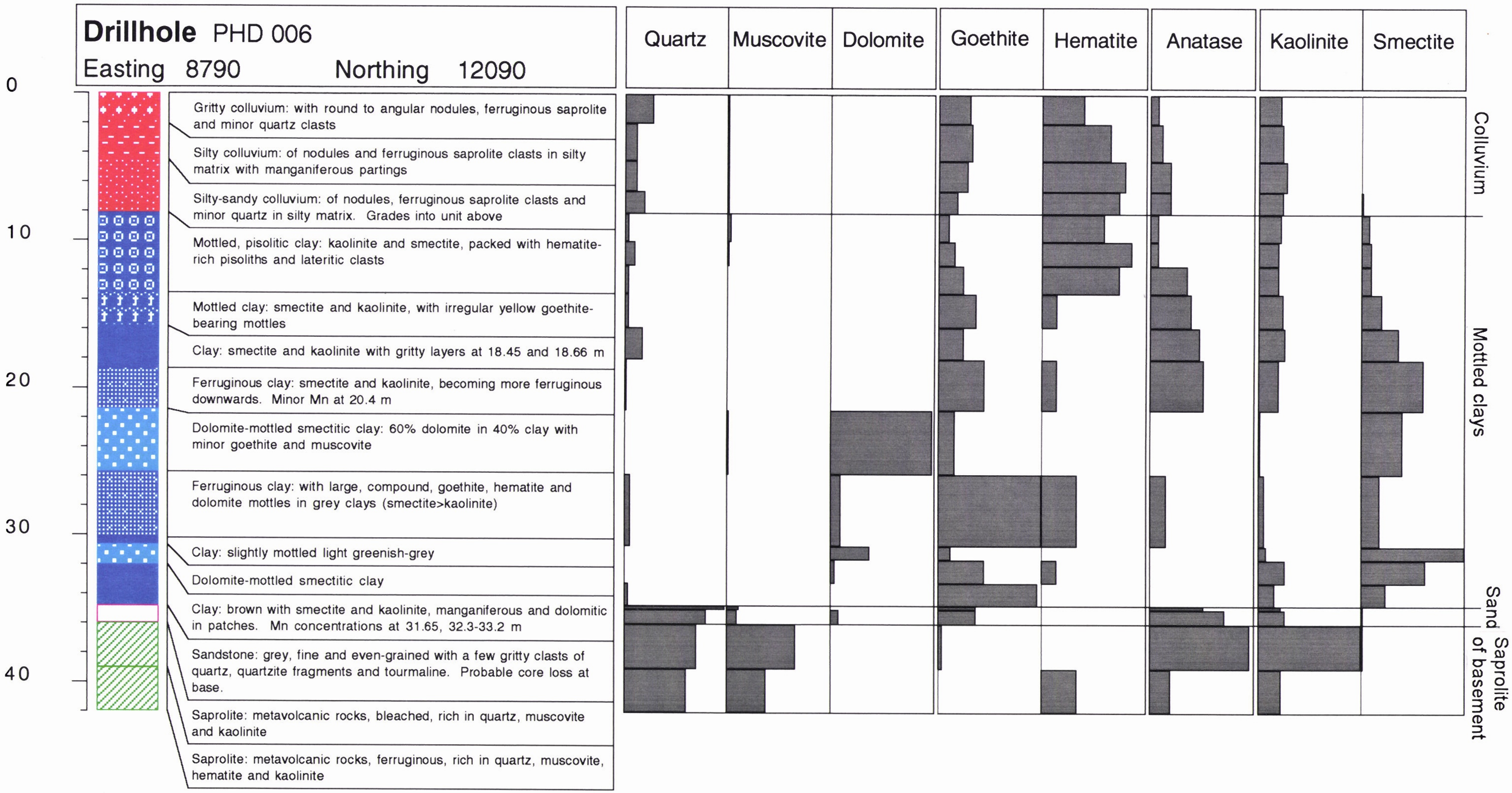


Figure 13. Detailed drill log of DDH PHD-006 with semiquantitative mineralogy. Note that each mineral maximum has been normalised to unity so comparisons should not be made *between* minerals. Collar location 8790 mE 12090 mN.

## FIGURE 14

## FABRICS OF TRANSPORTED MATERIALS FROM THE WASTE DUMP PALAEOVALLEY - DDH PHD-006

**A.** Gritty-sandy colluvium. A mass of polymictic, angular to subrounded, yellow, clay nodules (CN), goethite-rich clasts (GO) and minor quartz (QZ) are set in a matrix (MX) of smaller fragments, quartz grains, clay and mica. Specimen RBX-2200 from 1.35 m depth. Close-up photo of polished surface in oblique reflected light.

**B.** Silty-sandy colluvium. A few subangular to subrounded goethite-rich clasts (GO) and quartz (QZ) set in a fine-grained matrix (MX) of quartz, clay and mica. This is similar to A, in clasts and matrix, but the proportion of large clasts is less. Specimen RBX-2203 from 5.30 m depth. Close-up photo of polished surface in oblique reflected light.

**C.** Silty-sandy colluvium. Angular to subangular, goethite-rich lateritic clasts (GO) in a fine-grained, light-brown matrix (MX) of quartz, clay and mica. Voids (VO) have developed in the matrix and these have been largely infilled with laminated clay (LC). Specimen RBX-2204 from 7.15 m depth. Close-up photo of polished surface in oblique reflected light.

**D.** Mottled clay. Small subrounded goethite fragments and larger pisolitic nodules (PN) of hematitic clay, with included quartz grains (QZ) and coated with pale-brown, laminated clay, are set in a matrix similar to the colluvium (compare A-C) but contain a few clay spherules (SP). Specimen RBX-2205 from 8.18 m depth. Close-up photo of polished surface in oblique reflected light.

**E.** Ferruginous nodules in spherulitic smectitic clay. Goethite-rich nodules (GO) lie in a matrix of smectitic clay spherules (SP). Despite being outwardly varied, the goethite-rich nodules, which contain included mica, are mineralogically and texturally quite similar internally. Voids have been infilled with finely laminated clays. Specimen RBX-2206 from 9.35 m depth. Close-up photo of polished surface in oblique reflected light.

**F.** Smectitic clay with hematitic clay nodules. Hematitic clay nodules (PN) are set in churned matrix of smectitic clay spherules (SP). Older voids are filled with laminated clay (LC) but these and the matrix have given way to a younger generation of voids (VO). Cracking in the rock (CR) reflects an increased smectite content. Specimen RBX-2207 from 12.75 m depth. Close-up photo of polished surface in oblique reflected light.

**G.** Mottled, nodular clay. Hematitic clay nodules (PN) are set in a matrix of yellow and white smectitic clay (CL). Parts of the clay are goethite stained (GT). Specimen RBX-2208 from 14.35 m depth. Close-up photo of polished surface in oblique reflected light.

**H.** Valley-fill clay from within mottled zone. Waxy, pale-green clay set with small quartz grains. Cracking of this material indicates a high smectite content. Specimen RBX-2213 from 27.2 m depth. Close-up photo of polished surface in oblique reflected light.

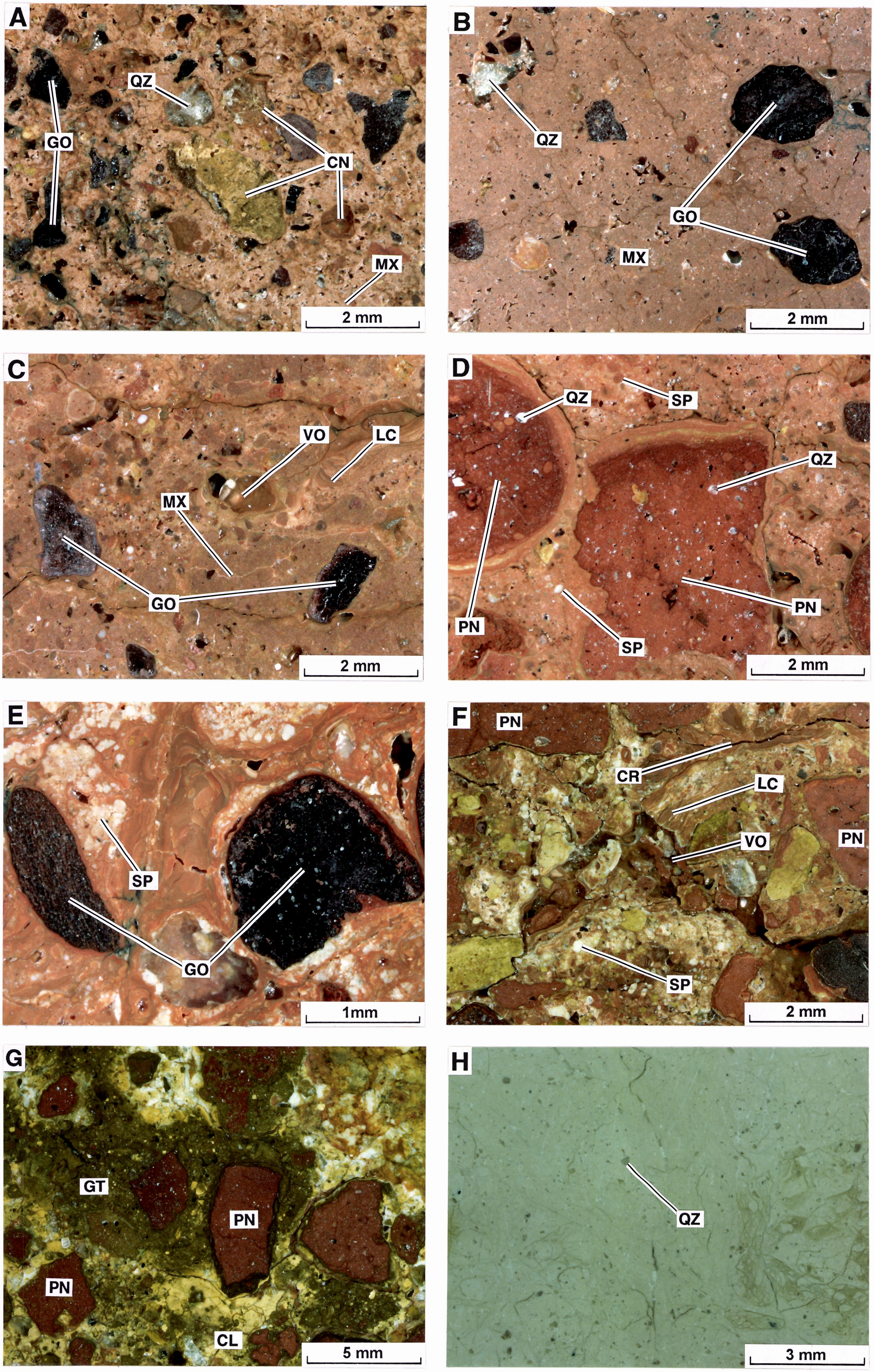
A
QZ
GO
CN
MX
2 mm
B
QZ
GO
MX
2 mm
C
VO
LC
MX
GO
2 mm
D
QZ
SP
QZ
PN
PN
SP
2 mm
E
SP
GO
1mm
F
PN
CR
LC
VO
PN
SP
2 mm
G
GT
PN
PN
CL
5 mm
H
QZ
3 mm

**FIGURE 14 (Contd)**

**FABRICS OF TRANSPORTED MATERIALS FROM THE WASTE DUMP PALAEOVALLEY - DDH PHD-006**

**I.** Complex mottles in clay. Brown, complex nodules (ND), containing fossil wood, are encased in hematitic mottles (HM) which, in turn, are set in smectitic clay (SM) from 27.1 m depth. Photograph of wet drillcore.

**J.** Clay with hematitic mottles and fossil wood. Details of compound nodules containing both fossil wood (FS) and attached goethite-stained sediment (GS) set in hematitic clay mottles which are encased in cracked and slightly Fe-stained clay. Specimen RBX-2212 from 27.05 m depth. Close-up photo of polished surface in oblique reflected light.

**K.** Fossil wood cross section. Large, round, central tracheid vessels (TR) surrounded by numerous, small, round parenchyma packing cells (PA) separated by chains of elongated ray cells (RA). The cell walls have been delicately replaced by goethite. Specimen RBX-2212 from 27.05 m depth. Photomicrograph in normally reflected light.

**L.** Fossil wood in nearly longitudinal section. Lensoid tracheid vessels (TR) surrounded by small, round parenchyma packing cells (PA) and a group of ray cells (RA). Obliteration of the fossil structure by secondary goethite has begun along narrow cracks (CR). Specimen RBX-2212 from 27.05 m depth. Photomicrograph in normally reflected light

**M.** Large dolomite mottles in smectitic clay. Large compound nodules or mottles of dolomite (DO) in cracked, light-grey, waxy smectitic clay from the depth range 23-26 m. Photograph of drillcore.

**N.** Sand with subrounded gritty clasts. A fine-grained, white sandstone (SS) containing a few subrounded, gritty quartz clasts (GQ) at the base of the palaeovalley at 35.3 m depth. Photograph of drillcore.

**O.** Partly disaggregated quartz vein in bleached saprolite. The previously compound quartz grains of a quartz vein (QZ), cutting bleached quartz-kaolinite-muscovite saprolite (SP), have been partly separated by recrystallised kaolinite (KA) from the floor of the palaeovalley at 38.7 m depth. Photograph of drillcore.

**P.** Schistose fabric in saprolite. A brown quartz, muscovite, kaolinite and hematite saprolite of metavolcanics of the Narracoota Formation (SP) from 40 m depth showing a coarse cleavage (CL). Photograph of drillcore.

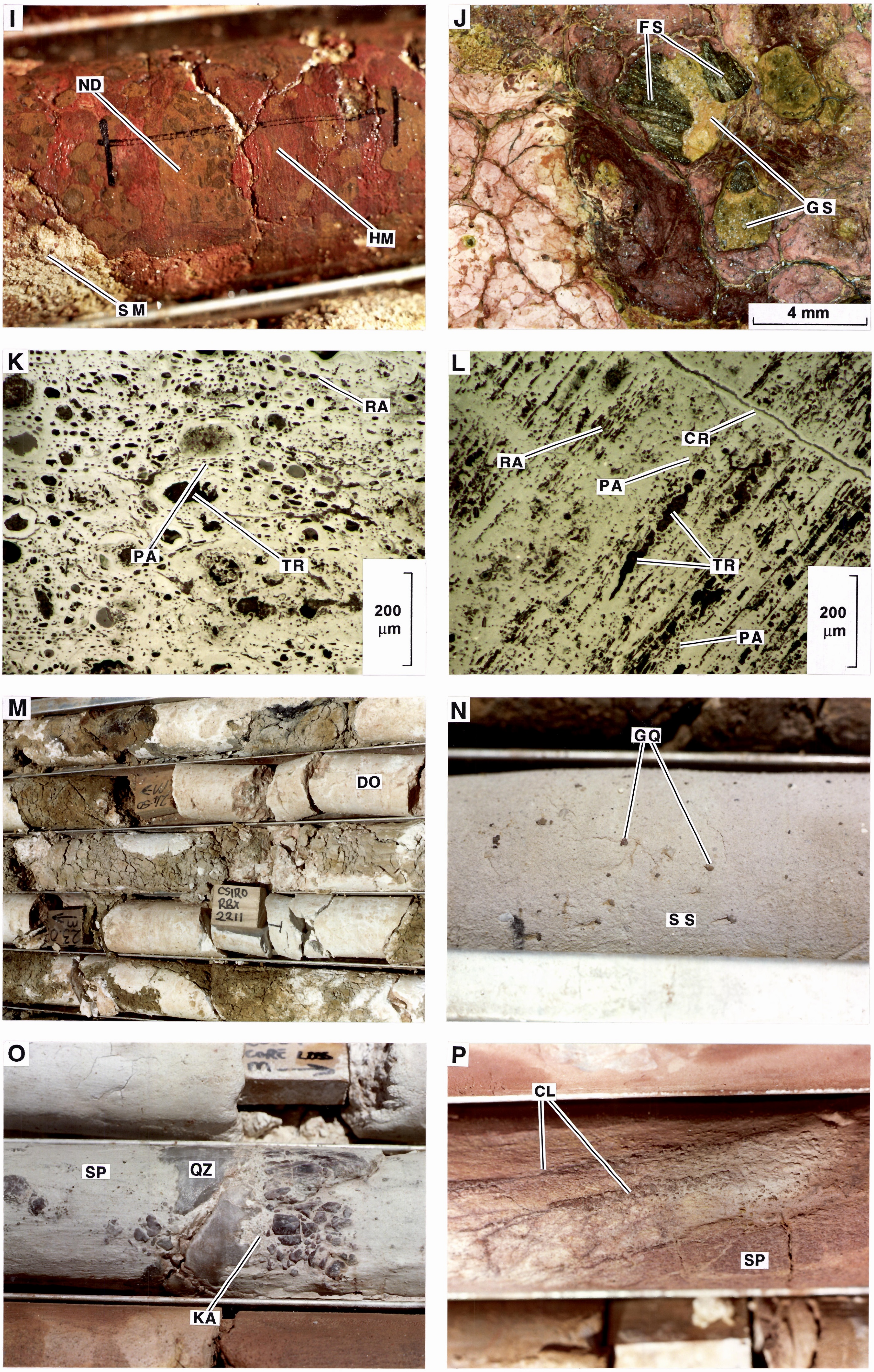
I
ND
HM
S M
J
F S
G S
4 mm
K
RA
PA
TR
200 µm
L
RA
CR
PA
TR
PA
200 µm
M
DO
CSIRO RBX 2211
N
GQ
S S
O
SP
QZ
KA
P
CL
SP

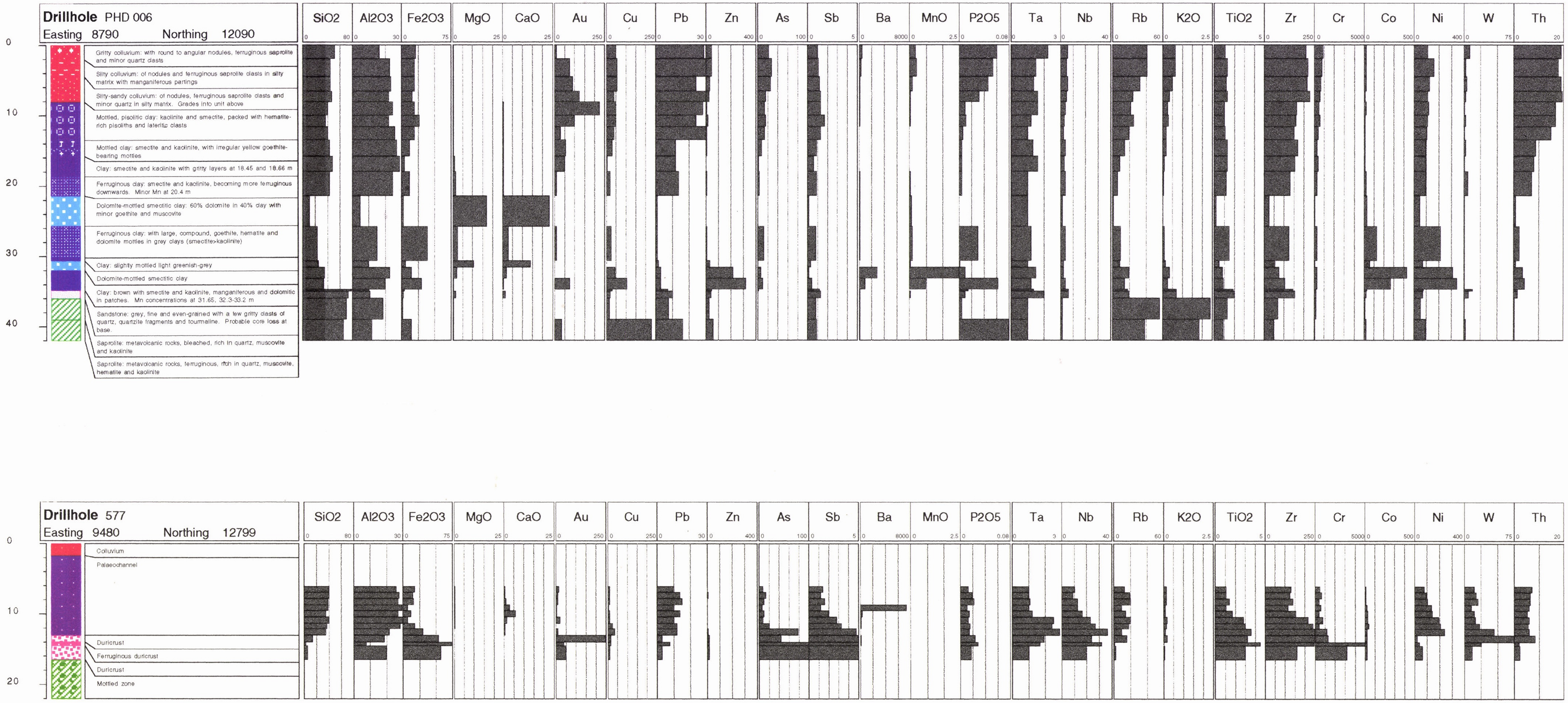


Figure 15. Detailed logs and geochemistry of DDH PHD-006, from the Waste Dump palaeovalley and RAB drillhole 263H577 from the Harmony palaeovalley.

The sand is overlain by 2.8 m of brown smectite and kaolinite clay which is goethitic, manganiferous and dolomitic in places (12). This is followed by a thin band (1.3 m) of dolomite-mottled smectitic clay (11) and by 0.5 m of a slightly mottled light greenish-grey clay (10) and 4.5 m of waxy, pale-grey to slightly greenish smectitic clay (Figure 14H) with large, compound 'mega-mottles' (Figure 14I) of goethite, hematite and dolomite (9). This mottled zone could represent an old watertable where Fe was precipitated from groundwater at an oxidation front.

Above is a substantial zone of dolomite-mottled smectitic clay (Figure 14M), consisting of about 60% of fused nodules of very fine-grained dolomite forming masses about 0.3 m in size (Figure 12; Unit 8), internally cemented with similar but slightly coarser-grained dolomite. This is followed by friable goethite- and hematite-stained clay (smectite and minor kaolinite) with a few remaining streaks of unstained, waxy clay (7). Set in the clay are a few goethite-rich granules (1-2 mm), glassy quartz (<0.5 mm) and a trace of tourmaline. Minor Mn oxides occur at 20.4 m. This is followed by more clay (smectite and kaolinite) (6) slightly stained with Fe oxides. Above this, the clay (5) becomes progressively more mottled with hematitic nodules (1-20 mm) and yellowish goethite granules and is less smectitic.

The mottled clays (4) become progressively more Fe rich. The contact between the mottled and pisolitic top of the valley-fill clays and the colluvium is sharp and is marked by a distinctive fabric change but this could be missed in drill cuttings, as materials on either side of the contact are quite similar. The valley-fill clays become strongly mottled and nodular (Figures 14E, F and G) within a matrix of greenish-white clay ooliths. The nodules of hematitic goethite contain varying amounts of very small mica flakes. The matrix has been extensively dissolved and the voids infilled with a brown, laminated kaolinite with a slight sheen (Figure 14F). At the top, the pisoliths have thin, partly worn cutans of light brown clay (Figure 14D), indicating minor transport. Although the matrix contains ooliths of ferruginous or white clay, it has some similarities to the matrix of the colluvium above and forms a zone transitional with it.

The nodular and pisolitic fabric at the top indicates weathering of the upper part of the valley-fill clay sediments, with development of a mottled zone and pisolitic structures. This appears to have been an event more recent than the weathering of the bedrock. This weathering was followed by some leaching, subsequent collapse and very minor transport of the lateritic material, leading to broken cutans. Deposition of the colluvium followed, with further matrix dissolution and eluviation of clay from the matrix of the colluvium into the upper part of the valley-fill sediment. This is reflected in the chemical composition (see below).

There is a small proportion of quartz grains in the valley-fill clays which are rounded and water-worn; these are generally about 1 mm in size. Most of the smaller grains (0.5-0.2 mm) are subrounded to angular and appear to have resulted from breakdown of composite metamorphic quartz grains. This quartz occurs throughout the smectitic clays, its abundance decreases down the profile and it is similar in size and shape to the quartz sand at the base of the sequence and to quartz in the saprolites of the basement. It seems likely that the basal sand was largely concentrated from the saprolite and that the valley-fill clays were formed from locally derived saprolite detritus.

### *4.2.3 Colluvium*

The upper eight metres consist of brown colluvium which may be divided into an upper, gritty-sandy part (1) and lower silty-sandy parts (2 and 3). The gritty-sandy colluvium contains matrix-supported, polymictic, subangular to subrounded goethitic and ferruginous clay fragments (1-3 mm) with some quartz in a vesicular, brown clay matrix (Figure 14A). The clasts contain remnant mica, some pseudomorphs of fibrous silicates, some pseudomorphs of secondary accordion and coarse, clay fabrics. The matrix is a pale, pinkish, yellow-brown, clay-rich silt, consisting of quartz, kaolinite and Fe oxides. Some vesicles are lined with brown, goethitic clay.

In the silty-sandy colluvium, the clasts and matrix are very similar to those of the gritty-sandy colluvium but the proportion of coarse, clastic material is much less (Figure 14B). These are set in a dull-brown matrix of kaolinite, quartz, Fe oxides and anatase. Some voids in the matrix are lined with a light-brown, laminated clay (Figure 14C).

#### *4.2.4 Chemical composition*

The chemical composition of PHD-006 is tabulated in Appendix 3 and a selection of the data are plotted in Figure 15. Compared to the transported materials, the saprolites of the metavolcanics of the Narracoota Formation are enriched in Rb, K, where not leached, Cu and P and have a much greater K/Rb ratio.

The colluvium is slightly richer in Zr (>170 ppm) than the valley-fill sediments. Enrichments in other elements, namely Pb, P, K, Rb, Th and the REE (La, Ce) also distinguish the colluvial sediments from the valley-fill sediments. Leaching and clay illuviation have imprinted some of the geochemical characteristics of the colluvium onto the mottled and pisolitic upper parts of the valley-fill sediments. This is particularly clearly shown by K, Rb, Pb, P, La, Th and Ce which decrease progressively downwards from the contact.

The two dolomitic layers within the valley-fill sediments are distinguished by greatly increased Ca (10-17% CaO) and Mg (14-23% MgO) contents, which have diluted all other elements. The upper and thickest dolomitic horizon seems to have acted as a chemical barrier to downward leaching of Pb, P, La, Rb, K and Th.

Drillhole PHD-006 is located down the palaeo-slope from the Harmony Au deposit and the Coe anomalies (Figure 4A). Gold is preferentially enriched in the upper, pisolitic part of the valley-fill sediment (max 224 ppb) and in the lower part of the colluvium (max 125 ppb). The Au contents of the remainder of the valley-fill sediments (mean 25, maximum 74 ppb Au) and the basement saprolite (max 33 ppb) are relatively low. There has been ample opportunity for mechanical dispersion down slope of Au-rich detritus into the sediments and lower colluvium. In addition, later hydromorphic dispersion may have introduced Au from primary sources into neo-formed ferruginous materials during weathering of the upper part of the valley-fill sediments and along the contact with the colluvium. Thus, lateral, largely mechanical but possibly partly chemical dispersive origins for this Au are likely. The highly manganiferous (0.8-2.5% MnO) clays are hydromorphically enriched in Cu, Zn, REE, Co and Ni.

#### *4.2.5 Palaeontology and age*

Yellow-brown granules of fossil wood, now replaced entirely by goethite, were found among pink, clay-bearing ferruginous mottles at 27.05 m (Figure 14J) within the valley-fill clays. Some contained attached, goethitic, exogenous, quartz-rich sediment. The cell patterns and their scale are typical of woody tissue. Cross sections (Figure 14K) show patterns that may be interpreted as larger, water-carrying, tracheid vessels surrounded by smaller parenchyma or packing cells and some evidence for ray cells. That the larger vessels are tracheid vessels rather than xylem is indicated by their lensoid form in near longitudinal sections (Figure 14L). This material probably formed stem or root material and the presence of tracheid vessels rather than xylem implies a relatively primitive vegetation, cycad, fern or conifer, with no evidence of the higher, flowering plants (J.K. Marshall, pers comm; 1996).

It is difficult to tell whether this woody tissue was incorporated into the sediments as (i) already fossilised detritus (ii) woody detritus that was fossilised in place or (iii) plant material that was growing in the clays at some time after their deposition and was fossilised later. The first hypothesis seems the more likely in view of (i) the attached exogenous sedimentary material, (ii) the marked contrast between the goethite replaced fossils and the hematite-clay mottles that surround them, (iii) the sharp contact between the two materials and (iv) the fragmentary nature of the fossil material.

An attempt was made to palaeomagnetically date some of the ferruginous, mottled material from 27 m ±0.5 m (Dr, B. Pillans pers. comm; 1996). Although friable, three ferruginous specimens were treated with stepwise alternating field demagnetisation. There was no agreement between the three specimens. Only one specimen had stable, positive (reversed) magnetic declination, indicating an age of >0.78 ma. The others did not have stable magnetisations.

### 4.3 Harmony palaeovalley

A small palaeovalley drains north-northeast from the Harmony deposit and is exposed in the north-east pit wall (Figures 16A and B). It has a floor of lateritic duricrust and has been filled with the mottled, puggy clays characteristic of the palaeovalleys which are directly overlain by 2-3 m of colluvium. The white, pale yellow or pale pink, puggy clays are similar to those of the Waste Dump palaeovalley, and contain hematitic and goethitic mottles and a few dark red-brown hematitic granules. The clays contain small, subangular grains of glassy quartz and are very similar to those of PHD-006. They consist of quartz, smectite, kaolinite, goethite and hematite with minor anatase. A little calcite (calcrete) occurs from 8.5-11.5 m but there are no dolomite nodules. As there are no ferruginous, pisolitic materials in the upper parts of the valley-fill clays, these sediments may have been partly eroded prior to deposition of the colluvium.

A ferruginous cementation of the lateritic duricrust is also exposed in the pit, a few metres below the base of the valley-fill sediment (Figure 16B). The extent of this layer closely matches that of the palaeovalley and it probably marks a redox front where Fe was precipitated and indurated the surrounding lateritic duricrust. Similar ferruginous cementations have been described at Lawlers (Anand *et al.,* 1991). The residual lateritic duricrust consists of goethite, hematite, gibbsite, minor quartz and kaolinite; there is no smectite.

Samples of the lateritic duricrust were collected from the pit. Valley-fill sediment samples were collected from drillhole 263H577, about 120 m outside the pit, along the axis of the Harmony palaeovalley, to investigate the mineralogy and chemistry of the valley-fill sediments and any mechanical or hydromorphic dispersion from the Harmony deposit. The results are tabulated in Appendix 4; the lateritic duricrust data have been included with them and plotted in Figure 15.

Most of the Au is concentrated in the upper part of the lateritic duricrust (823 ppb), the ferricrete and lower lateritic duricrust containing little Au (41 and 51 ppb respectively). The Au concentration of the upper part of the lateritic duricrust of drillhole 263H577 is 137 ppb and forms part of the 'lateritic' geochemical halo around the Harmony deposit. In contrast, the Au concentrations in the clays of the Harmony palaeovalley are low (mean 10 ppb). Arsenic and Sb are concentrated in the ferricrete and in the lower part of the lateritic duricrust (mean 711 and 8 ppm respectively); the valley-fill clays are As- and Sb-poor (mean 19 and 2.3 ppm respectively).

Although W is weakly enriched in the sand at the base of the Waste Dump palaeovalley (13.3 ppm), as a placer concentration, the mean content in the clays above is only 2 ppm. There is no sand in the axis of the Harmony palaeovalley but W concentrations in the clay are nearly an order of magnitude greater (mean 18.4 ppm). Thus, the clays of the Harmony palaeovalley contain significant mineralised detritus from the Harmony deposit. The low Au content here suggests that either the clay-rich detritus was poor in Au or, more likely, that Au has been leached after deposition. It is unlikely that mechanical sorting of Au from W occurred as the clay-rich sediments indicate a very low-energy environment. The voids, filled with eluviated clays, in the top part of the Waste Dump valley-fill sediments indicate that leaching was operative here.

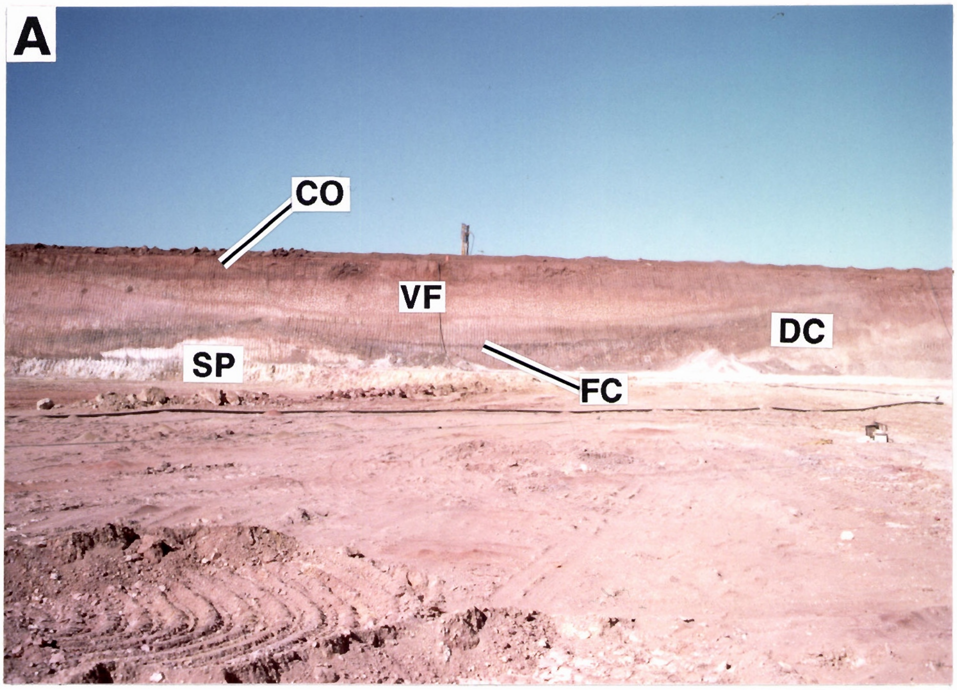


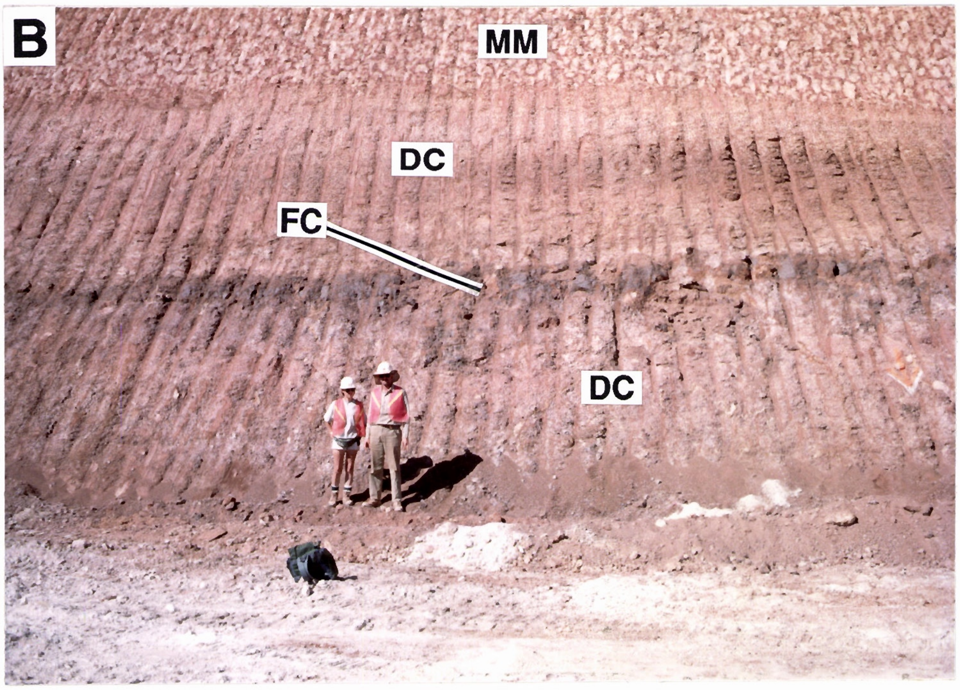


Figure 16. (A) A section across the Harmony valley-fill sediments (VF) as they appear in the northeast wall of the Harmony pit. This is underlain by duricrust (DC), ferricrete (FC) and saprolite (SP) and overlain by colluvium (CO).

(B) Detail of the 'mega-mottled' smectitic clays (MM) filling the Harmony palaeovalley and the thin ferricrete layer (FC) in the duricrust (DC) beneath the valley-fill clays.

Slight increases in Cr, Ni, Cs, Rb, Nb and Ta in the Harmony palaeovalley, relative to the Waste Dump palaeovalley, indicate the greater proportion of ultramafic, mineralised and phyllic halo rocks in the Harmony palaeovalley catchment. Concentrations of Cu, Zn, Sr and Ba (except for one S-rich sample) are low in the Harmony palaeovalley. Although Au may not be a good indicator for Au mineralisation in a palaeovalley catchment, W seems to be effective.

## 5 FRESH ROCK GEOCHEMISTRY

Nine spot samples of 200 mm of half or quarter core were taken in mineralised zones from HDH1, 3, 7 and 39. Four similar samples of basaltic and ultramafic metavolcanic rocks distant from mineralisation were collected, to establish local background abundances (see drill logs in Appendix 6). Such a small data set could not be used to estimate the extent of fresh rock halos but only to determine which elements are pathfinders for mineralisation. The statistical base is small so care is necessary in interpretation.

### TABLE 3

### STATISTICS OF MINERALISED AND UNMINERALISED FRESH ROCK

| | | Background (n=4) | | | Mineralised (n=9) | | |
|---|---|---|---|---|---|---|---|
| | Units | Minimum | Geom. Mean | Maximum | Minimum | Geom. Mean | Maximum |
| SiO2 | % | 42.01 | 44.67 | 46.85 | 32.14 | 42.13 | 48.18 |
| Al2O3 | % | 8.85 | 10.81 | 12.28 | 10.54 | 14.36 | 20.24 |
| Fe2O3 | % | 8.36 | 8.96 | 9.69 | 6.36 | 11.30 | 27.52 |
| MnO | % | 0.156 | 0.17 | 0.197 | 0.091 | 0.18 | 0.489 |
| MgO | % | 7.33 | 10.47 | 20.09 | 3.5 | 5.80 | 9.74 |
| CaO | % | 6.85 | 9.44 | 11.57 | 0.14 | 3.63 | 14.27 |
| Na2O | % | 0 | 0.55 | 2.92 | 0.11 | 1.72 | 5.49 |
| K2O | % | 0.01 | 0.03 | 0.2 | 0.01 | 0.22 | 2.91 |
| TiO2 | % | 0.16 | 0.33 | 0.48 | 0.17 | 0.30 | 0.72 |
| P2O5 | % | 0.022 | 0.04 | 0.045 | 0.004 | 0.03 | 0.095 |
| As | ppm | 1 | 1.55 | 2.46 | 1 | 3.94 | 34.8 |
| Au | ppb | 5 | 6.69 | 9.3 | 5 | 52.33 | 1720 |
| Ba | ppm | 4 | 13.37 | 35 | 0 | 62.65 | 897 |
| Ce | ppm | 2 | 3.39 | 4.23 | 2 | 4.28 | 8.93 |
| Cl | ppm | 40 | 51.80 | 60 | 0 | 46.21 | 320 |
| Co | ppm | 36.2 | 52.40 | 97.2 | 13.5 | 37.86 | 89.4 |
| Cr | ppm | 86.4 | 522.91 | 3180 | 72 | 180.57 | 336 |
| Cs | ppm | 1 | 1.23 | 2.3 | 1 | 1.09 | 2.2 |
| Cu | ppm | 67 | 104.09 | 234 | 0 | 29.30 | 121 |
| Eu | ppm | 0.5 | 0.54 | 0.67 | 0.5 | 0.58 | 0.96 |
| Ga | ppm | 7 | 9.33 | 12 | 7 | 10.34 | 14 |
| Hf | ppm | 0.5 | 0.70 | 1.17 | 0.5 | 0.62 | 1.26 |
| La | ppm | 0.63 | 1.39 | 2.14 | 0.73 | 1.76 | 3.32 |
| Lu | ppm | 0.2 | 0.22 | 0.26 | 0.2 | 0.31 | 0.64 |
| Nb | ppm | 0 | 3.72 | 6 | 2 | 3.94 | 7 |
| Ni | ppm | 56 | 255.87 | 1311 | 48 | 82.78 | 160 |
| Pb | ppm | 5 | 7.67 | 11 | 2 | 7.34 | 15 |
| Rb | ppm | 0 | 2.05 | 6 | 1 | 9.97 | 61 |
| S | ppm | 70 | 315.82 | 3760 | 60 | 621.23 | 3640 |
| Sb | ppm | 0.2 | 0.26 | 0.37 | 0.2 | 0.46 | 0.71 |
| Sc | ppm | 28.3 | 36.33 | 41 | 36.3 | 47.75 | 62.9 |
| Sm | ppm | 0.47 | 0.98 | 1.38 | 0.47 | 1.02 | 2.36 |
| Sr | ppm | 48 | 76.08 | 95 | 13 | 64.80 | 135 |
| Ta | ppm | 1 | 1.00 | 1 | 1 | 1.14 | 1.89 |
| Th | ppm | 0.5 | 0.53 | 0.64 | 0.5 | 0.53 | 0.83 |
| V | ppm | 126 | 176.34 | 221 | 159 | 200.63 | 257 |
| W | ppm | 2 | 2.00 | 2 | 2 | 9.20 | 66.9 |
| Y | ppm | 9 | 12.00 | 16 | 12 | 17.56 | 30 |
| Yb | ppm | 1.09 | 1.44 | 1.69 | 1.49 | 2.22 | 3.77 |
| Zn | ppm | 32 | 49.73 | 61 | 16 | 61.35 | 150 |
| Zr | ppm | 8 | 18.96 | 27 | 9 | 19.45 | 44 |

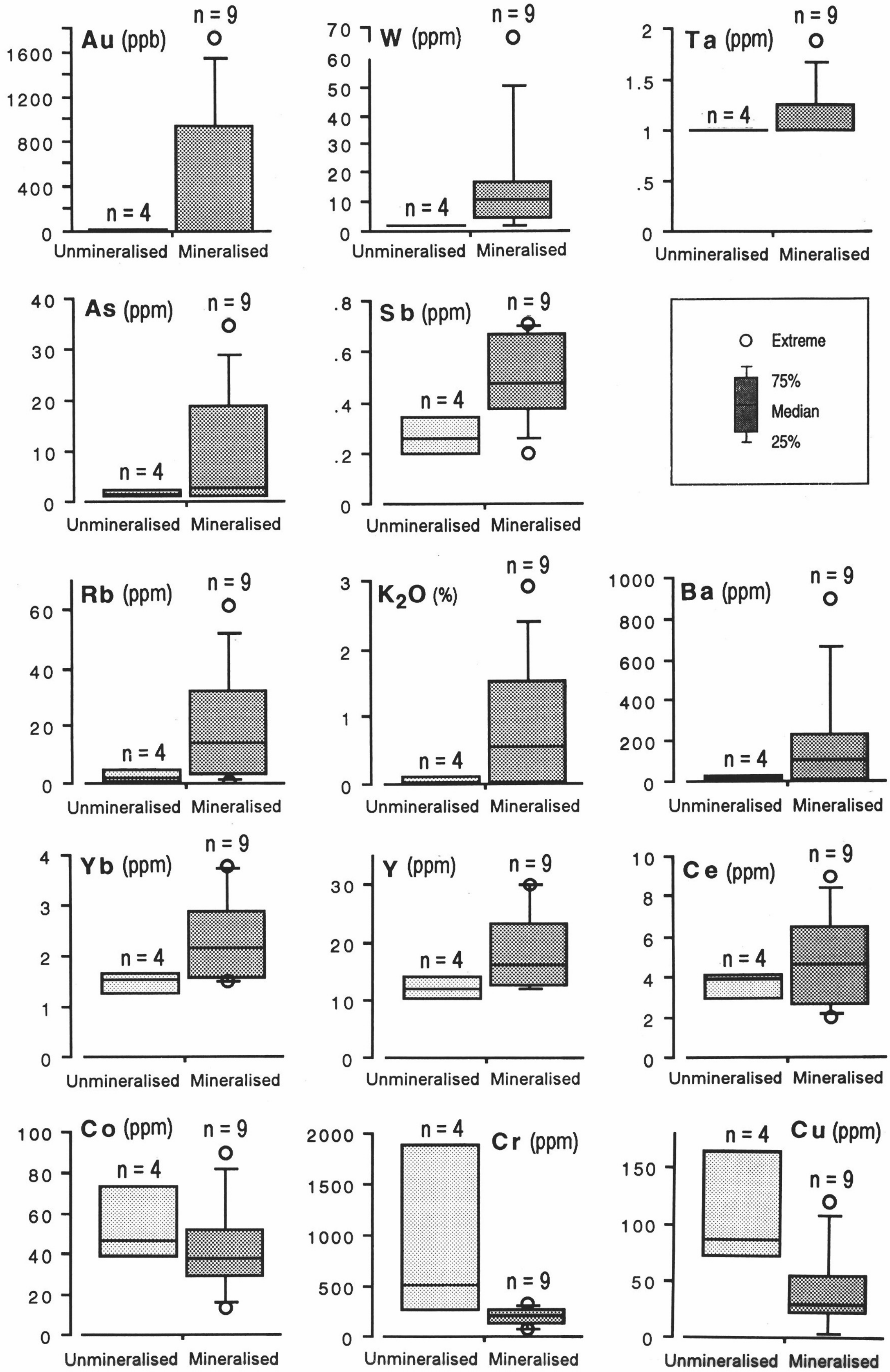


Figure 17. Box and whisker plots comparing local background for fresh rocks with primary mineralisation from Harmony for the indicator elements (Au, W, Ta), metalloids (As, Sb), phyllic halo elements (Rb, K, Ba), REE (Yb, Y, Ce) and lithology related elements (Co, Cr, Cu). Circles represent outliers.

The analytical results (XRF and INAA) are tabulated in Appendix 6. The ranges and geometric means of the mineralised and background data are given in Table 3 and the elements compared as box-plots in Figure 17.

Mineralisation has not greatly influenced the proportions of the major elements, apart from minor increases in the Fe (sulphide) and Al (mica) contents and slightly decreased Si, Mg and Ca. However, mineralisation has greatly increased the ranges and abundances of Au and W. Increases in K, Rb and Ba imply phyllic alteration; Na is only slightly increased. Some REE, in particular Eu, La, Lu, Sc, Y and Yb also increase in abundance and range, in the mineralised parts. The concentrations of metalloids, As and Sb, are weakly enriched but their abundances are low compared to some mineralisation styles.

It is concluded that useful indicator elements for Harmony-style Au mineralisation are primarily Au and W; Rb, K and Ba may indicate phyllic alteration where micas might survive weathering. Although chalcophile As and Sb occur at low concentrations at Harmony, there may be variations in mineralisation styles so there could be places where As and Sb may assume greater importance. The reasons for concentration of REE with the Harmony mineralisation are, as yet, not clear.

Gray (1995) noted elevated abundances of Sc, Mo, W and Rb in groundwaters near the Harmony mineralisation. The Peak Hill Mine was also anomalous in W (G. Chessell, pers communication, Nov 1993).

# 6 COMPOSITION OF THE UPPER RESIDUAL REGOLITH

## 6.1 Introduction

The upper horizons of the residual regolith were sampled on an approximately triangular grid from existing RAB drilling to determine the extent and strength of geochemical dispersion below the cover. This, in turn, represents the source for subsequent geochemical dispersion into the valley-fill sediments and colluvium. The sample materials consisted of lateritic duricrust (LT200; Anand *et al.*, 1989) or, where these were unavailable, mottled zone (MZ100) or ferruginous saprolite (SP200). These samples were washed to remove clays (Appendix 9). Washing of the lateritic duricrust removed small amounts of clay, some of which may have been derived from the cover materials. Washing the mottled zone material (Figure 10G) concentrated the hematite- and goethite-rich mottles. Washing ferruginous saprolite made little substantial difference.

The duricrust, mottles and ferruginous saprolite samples were analysed and their geochemical data are tabulated in Appendix 1 and contoured in Appendix 2 and in Figures 19-21. Details of the sampling, sample preparation and analytical methods are given in Appendix 9.

## 6.2 Elements associated with mineralisation (Au, W)

Gold has been plotted logarithmically (Figure 19B) because of its range over three orders of magnitude. Gold appears unaffected by regolith differences; the two greatest Au concentrations occur separately in lateritic duricrust and ferruginous saprolite. A very strong, single point Au anomaly of 977 ppb occurs proximal to the southwest of the Harmony pit in ferruginous saprolite, possibly related to veining; the two samples of ferruginous saprolite from within the pit were not particularly Au enriched (15 and 72 ppb), indicating limited Au dispersion in this material. However, the nearby Au anomaly is reinforced by a wide zone of anomalous Au (>70 ppb) that extends from Coe, through the Harmony deposit to COB (Figure 4A). The strongest three-point Au anomaly reaches 1439 ppb in lateritic duricrust and marks the Contact North anomaly. A belt of Au anomalies marks Enigma North and Ovett (see Figure 4A).

Tungsten tends to be independent of Au and is little dispersed in the regolith. Because of this, W may occur where Au has been leached. The second greatest W concentration of 31 ppm (Figure 19A) occurs in the southern part of the Harmony pit (co-incident with 15 ppb Au) and is part of a two-point W anomaly between the Harmony deposit and Coe. The greatest W concentration (39 ppm) depicts Enigma North and Ovett. Logarithmic treatment of the W data emphasises this but also draws attention to weak anomalies at Contact North (>5 ppm) and Enigma (>12 ppm). These also carry anomalous Ta (5 ppm) and Nb (60-70 ppm) in backgrounds of 2 and 25 ppm respectively (Figures 19E and F). As expected, Ta and Nb are well correlated.

### 6.3 Major elements

Silicon, Al, Fe, some minor lattice water and, in a very few, Ca and $CO_2$ are the major constituents. The relationships of the major oxides are shown in Figure 18. The clay-free lateritic duricrust and mottles have quite similar compositions but the ferruginous saprolite remains more Si- and Al-rich due to kaolinite and quartz. Some of the lateritic duricrust also contains gibbsite.

The distributions of the major elements (Appendix 2) demonstrates the close relationship of Si with ferruginous saprolite and Fe with lateritic duricrust. Although Ga and Al have similar distributions and there is a relatively consistent Ga-Al ratio, Ga is enriched in some lateritic duricrust. There is no relationship between this enrichment and the Harmony mineralisation.

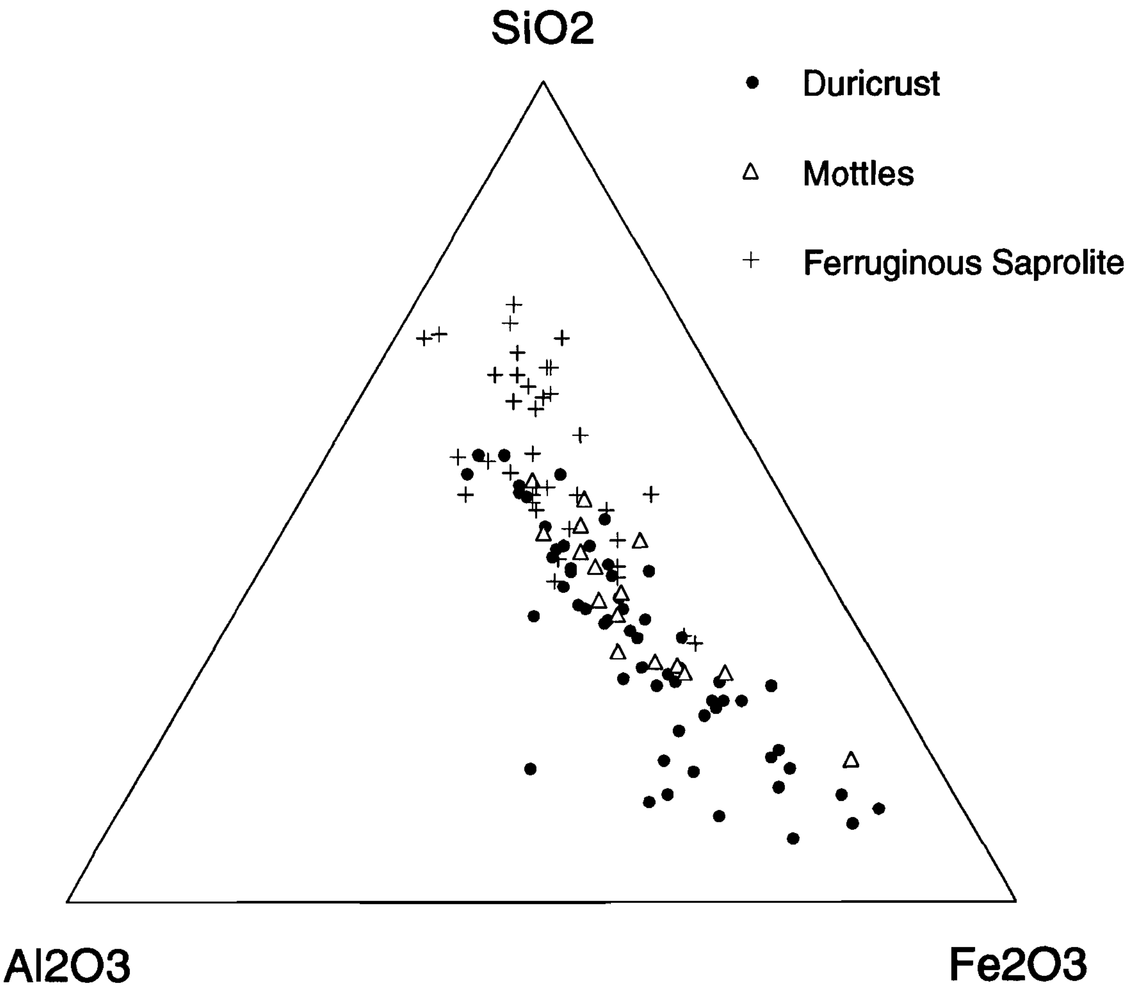


Figure 18. Si-Al-Fe ternary plot of basement samples demonstrating the siliceous nature of the ferruginous saprolite, the similarity between the duricrust and mottles and the gibbsitic nature of parts of the duricrust.

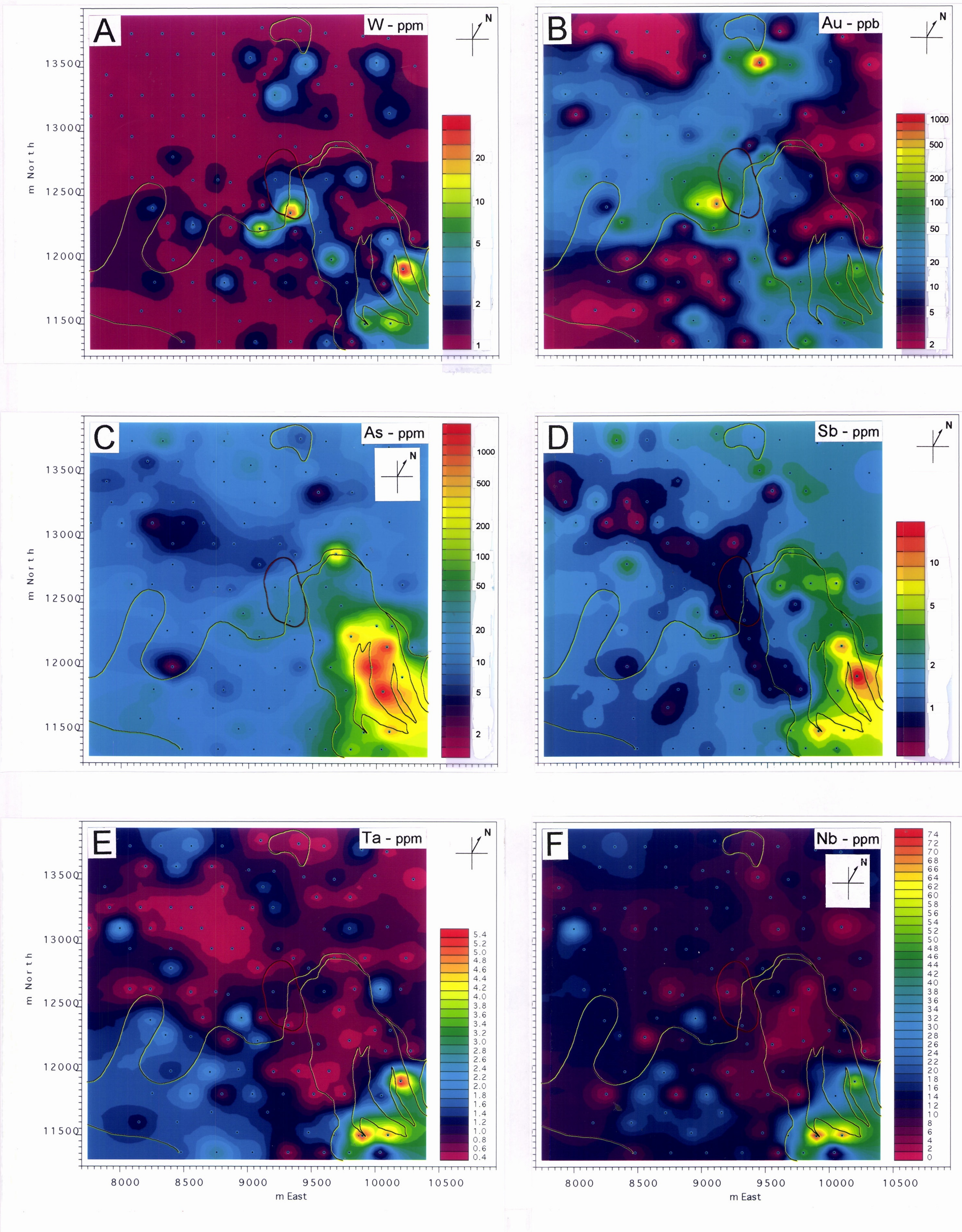


Figure 19. Distributions of W, Au, As, Sb, Ta and Nb in the uppermost residual regolith. Pit outlines and geology have been added (Figure 4A). Compare Figure 4B for distribution of regolith materials.

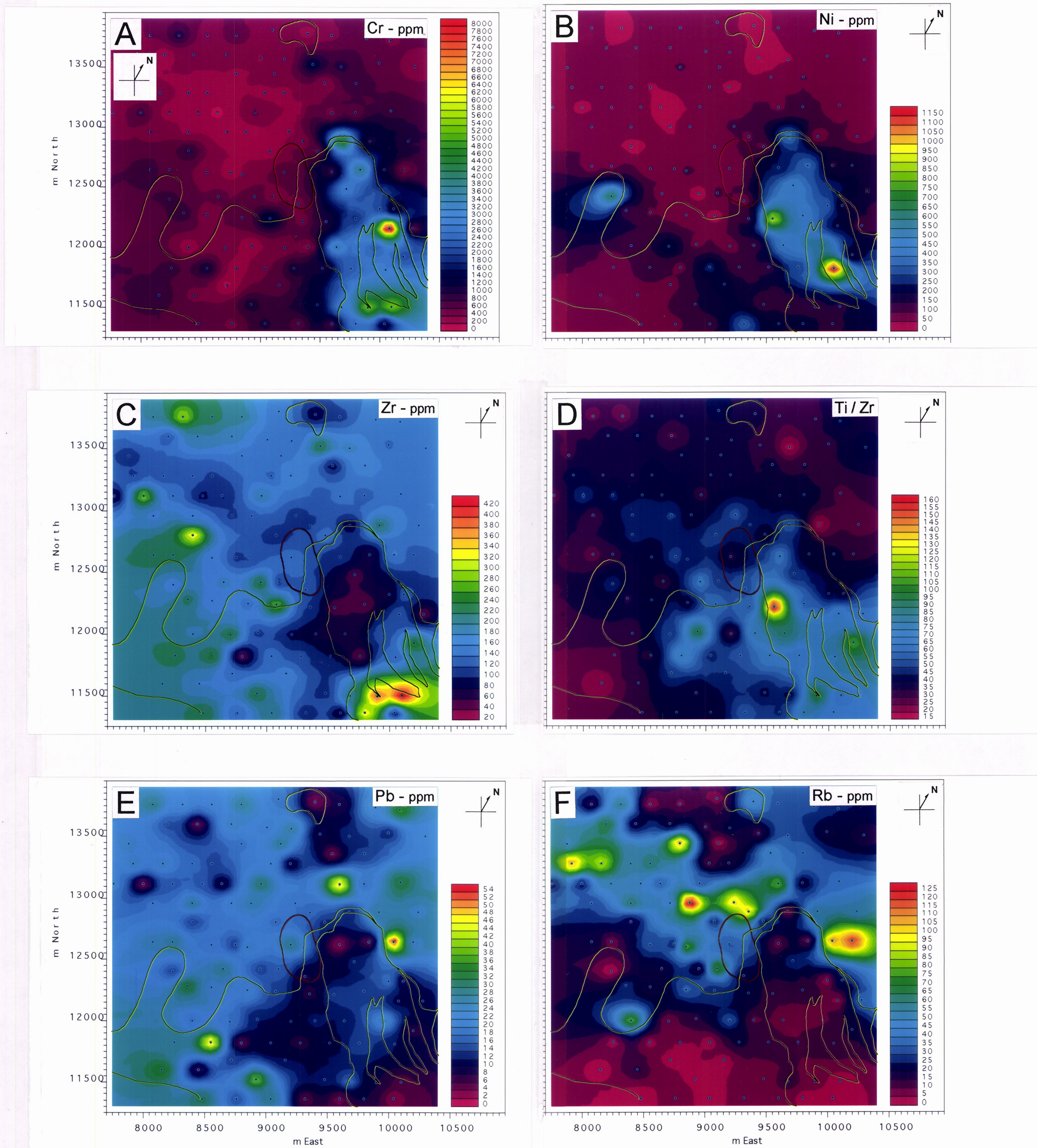


Figure 20. Distributions of Cr, Ni, Zr, Ti/Zr, Pb and Rb in the uppermost residual regolith. Compare Figure 4B for distribution of regolith materials.

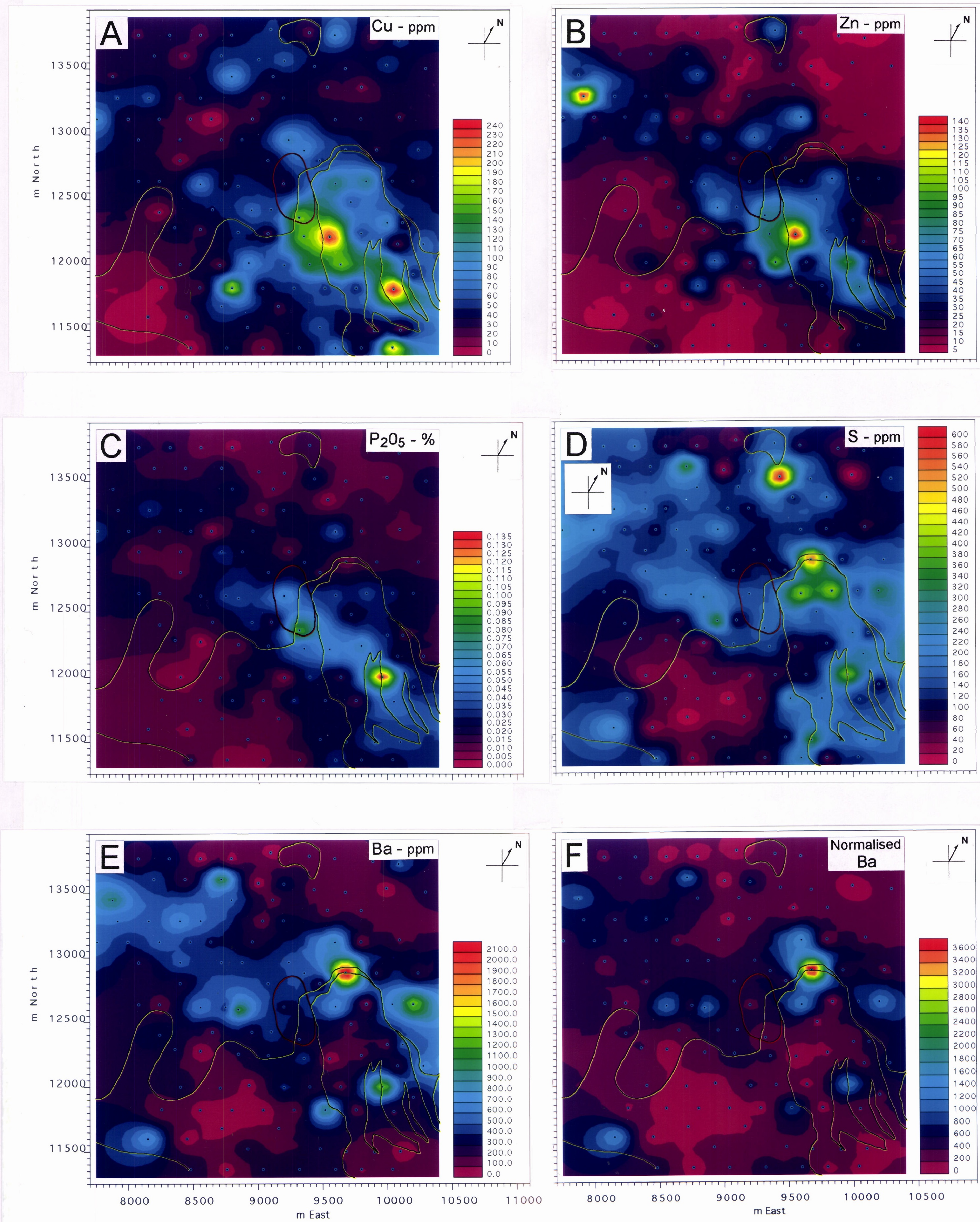


Figure 21. Distributions of Cu, Zn, P, S and Ba in the uppermost residual regolith. Compare Figure 4B for distribution of regolith materials.

### 6.4 Halogens

Local increases in the halogens, Cl and Br, are related to subcropping lateritic duricrust and mottled zone rocks but not to one another (Appendix 2). There is no relationship between halogen concentrations and mineralisation.

### 6.5 Alkaline earths

The abundances of the light alkaline earths are generally low (<1% CaO, <0.4% MgO and <40 ppm Sr), but a few localised concentrations (19% CaO, 6.8% MgO and 140 ppm Sr) occur in the ferruginous saprolite over all lithologies, corresponding to secondary carbonate (calcrete).

### 6.6 Lithology-related elements

The ultramafic rocks of the Narracoota Formation are clearly delineated by Cr and Ni (>2000 and >300 ppm respectively) in the upper regolith. The remaining lithologies (basaltic metavolcanics of the Narracoota Formation and metasediments of the Ravelstone Formation) are Cr and Ni poor (Figures 20A and B), although Cr is concentrated in lateritic duricrust relative to ferruginous saprolite. The metasediments are weakly enriched in Pb (>20 ppm), Rb (>20 ppm) and in Th (>10 ppm) relative to the metavolcanics (Figures 20E and F).

Relatively immobile elements are related to zircon (Zr and Hf) and to ilmenite, rutile and anatase (Ti and V). Zirconium (Figure 20C) and Hf show almost identical patterns with greater concentrations (>320 and >9 ppm respectively) in the east-southeast and lesser concentrations over most of the ultramafic rocks of the Narracoota Formation. Trends of lesser Zr and Hf follow the axis of the basement palaeohigh, corresponding to subcropping ferruginous saprolite; conversely, there are slightly greater concentrations of Zr and Hf corresponding to subcropping lateritic duricrust and mottled zone in the palaeovalley. Both Ti and V appear to be concentrated more in the lateritic duricrust and mottled zone than in the ferruginous saprolite and appear to be largely independent of the underlying geology. The Ti-Zr ratio (Hallberg, 1984) reliably delineates the basaltic and ultramafic rocks (>50) of the Narracoota Formation (Figure 20D). However, the lateritic duricrust and mottled zone in the palaeovalley have lesser Ti-Zr ratios than elsewhere, which may either imply a more felsic volcanic composition or, more probably, preferential leaching of Ti by deep weathering. Similar changed Ti-Zr ratios occurred at Beasley Creek in the mottled zone and lateritic duricrust relative to the saprolite (Robertson, 1991).

The ultramafic rocks of the Narracoota Formation are enriched in Cu (>80 ppm) relative to their basaltic equivalents (Figure 21A). However, the trend to further enrichment in Cu (>160 ppm) and Zn (>55 ppm; Figure 21B) from Harmony to Enigma North may be related to mineralisation. A similar trend is shown by P (Figure 21C). No useful information can be gathered from Mo, U and Co.

### 6.7 Mica-related elements (K, Rb, Cs, Ba)

The heavier alkalis and alkaline earths form an easterly trend, probably mica-related, that passes just north of the Harmony deposit. It is most clearly shown by the more abundant elements (K, Rb; Figure 20F) and imperfectly by Cs and Ba. Although this trend lies within the metasediments of the Ravelstone Formation and not over the metavolcanics of the Narracoota Formation, it seems to be linear and not to be linked directly to any specific lithology. It closely follows a similar trend in silica and the axis of the subcrop of ferruginous saprolite, hence delineating a zone of less weathered micaceous rocks. The ferruginous saprolite consistently has a slightly greater K-Rb ratio than the lateritic duricrust and mottles. There is a strong correlation between Sr and Rb but little between Sr and Ca. The Sr-Rb relationship is not radiogenic because the amount of Sr that would be produced radiogenically from Rb since the Proterozoic would be minute (~0.1% of the Rb concentration).

### 6.8 Metalloids

The regolith on metasediments of the Ravelstone Formation and the basaltic units of the Narracoota Formation are poor in As (<30 ppm) and Sb (<3 ppm), but some of the ferruginous saprolite and lateritic duricrust on the ultramafic lithologies, over Enigma North are very anomalous (up to 1500 ppm As, 20 ppm Sb; Figures 19C and D) suggesting more sulphidic mineralisation with a broader suite of indicator elements.

A logarithmic plot of the data shows reduced Sb contents (<1 ppm) in ferruginous saprolite on axis of the palaeohigh, whereas lateritic duricrust is relatively enriched in Sb (2 ppm). Arsenic shows a similar distribution where the regolith is developed from metasediments (<40 ppm) but the regolith developed on ultramafic rocks is As enriched (>50 ppm).

All the Se data lie below detection (10 ppm). The S distribution (Figure 21D) is similar, in part, to As and Sb, in part to Ba (Figure 21E) and in part to the occurrence of ferruginous lateritic duricrust (enriched in As and Sb). Although the mineralisation of the Harmony deposit is S poor, most of the other known anomalous areas are S enriched (>200 ppm; Contact North, COB, Coe, Enigma North, Ovett).

### 6.9 Data normalisation

The distributions described above imply an assumption that the ferruginous saprolite, lateritic duricrust and mottles are comparable. This is not necessarily true because they represent different parts of a weathering profile and, hence, have different matrices, backgrounds and degrees of dispersion. Wet sieving has helped to equate the ferruginous segregations of the mottled zone with the lateritic duricrust, but the composition of the ferruginous saprolite has not changed significantly. It is clear from the discussion above that the distributions of numerous elements (Si, Fe, Cr, Zr, Hf, Ti, V, K, Rb, Ba, Sb, As) are influenced, to some extent, by regolith distribution. Thus, some form of data normalisation is needed to remove, as far as possible, the effect of regolith variation and leave, or accentuate, any influence of mineralisation.

Two possible methods were considered; normalisation to range and normalisation to background. The former would have been effective if indications of major mineralisation had been encountered in all three media. However, most mineralisation (*e.g.*, the Harmony deposit) is in areas of ferruginous saprolite, with minor lateritic duricrust. Thus, normalisation to background was used. The mode of the background population for each potential indicator element for each medium was estimated from normal probability plots and tabulated. The data were rescaled to the medium with the greatest background and the data set re-gridded and re-plotted (Figures 21F and 22A-F).

Normalisation of Ba (Figure 21E and F) has served to accentuate the Ba anomaly in the lateritic duricrust that underlies the palaeovalley at COB. The trend of the palaeohigh has been removed from the K and Rb data (compare Figure 20F with 22F), accentuating an area north of COB. This trend has also been removed from the As and Sb data (Figures 22C and D) but, otherwise, the locations of the anomalies are unchanged. The Au, Ta and W distributions are unchanged (Figures 22B, E and A).

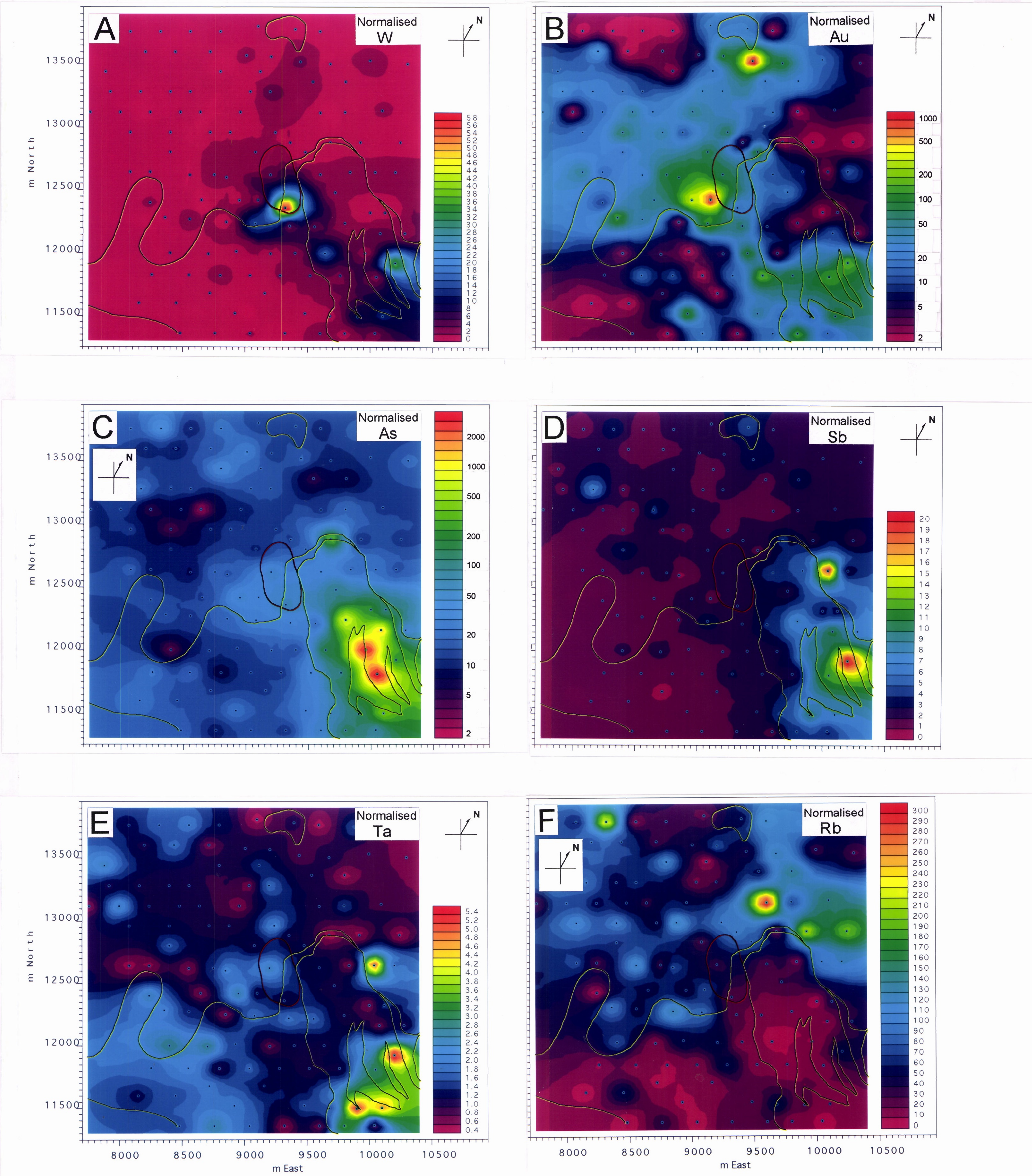


Figure 22. Distributions of normalised W, Au, As, Sb, Ta and Rb in the uppermost residual regolith. Compare Figure 4B for distribution of regolith materials.

# 7 DISPERSION AT THE BASE OF THE COLLUVIUM

## 7.1 Introduction

The weathered Proterozoic basement is considered to have been eroded prior to deposition of the colluvium with only partial preservation of buried lateritic residuum. The Harmony deposit is in an area dominated by ferruginous saprolite on which lateritic residuum was either only partly developed or has been stripped from the upper parts of the landscape. In consequence, geochemical anomalies tend to present very small targets. It is essential to capitalise on any dispersion halos that may have developed on the basement or any that developed since burial. The following may be present:-

i) Lateritic halos may be preserved in very small remnant pockets of mottled zone and lateritic duricrust, although it is unlikely that many of these would be intersected by broad-spaced drilling. However, their derived gravels could be more widely spread, by mechanical processes, into the base of the colluvium.
ii) Halos formed in palaeosols on the partly eroded profile, now also incorporated into the base of the colluvium.
iii) Halos formed during or after deposition of the colluvium, chemically dispersed into the sediments or along the unconformity. Such a dispersion mechanism could still be active.

Dispersion in basal colluvium has been recorded from Mt McClure (Anand *et al.,* 1993), Mt Gibson (Anand *et al.,* 1989), Lawlers (Anand *et al.,* 1993), Mt Magnet (Robertson *et al.,* 1994) and Bronzewing (Varga *et al.,* 1996), indicating that the unconformity would be a useful geochemical medium. At Mt Magnet, sampling of the unconformity has proved to yield broader but less intense anomalies than sampling the top of the basement on stripped, residual regoliths overlain by colluvial sediments (Robertson *et al.*; 1994), allowing broader-spaced sampling and a higher probability for exploration success. Sampling this interface requires particularly accurate logging and careful selection to ensure the unconformity is included. A metre too high and the sample would be of transported overburden; a metre too low and locally barren basement may be encountered. This interface material would be classified as a mixture of CV305 and SP200 (Anand *et al.,* 1989).

In these stripped but obscured areas, the unconformity generally could be identified in drilling as a mixed material, containing both colluvium and chips of ferruginous saprolite or duricrust. Where the interface could not be identified and neighbouring drillspoil were of basement and cover, similar proportions of each were combined to ensure that material from the unconformity was included.

Forty three interface samples were collected from existing RAB drilling on a triangular grid at about 150 m spacing within 850 m of the centre of the Harmony pit. The results are tabulated in Appendix 8 and the more important elements are plotted in Figures 23A-F. Details of the sample preparation and analytical methods are given in Appendix 9.

## 7.2 Results

*Gold and Tungsten.* Much of the unconformity material in the southern part of the Harmony pit is anomalous in Au (Figure 23B) and there appears to be a dispersion train extending to the southwest down the palaeoslope towards the Waste Dump palaeovalley and the environs of PHD-006. A weaker dispersion train extends down slope to the north, along the trend of the Harmony palaeovalley. Tungsten shows similar results (Figure 23A) but dispersion is less. The pit area is generally anomalous, with short dispersion trains to the north and south.

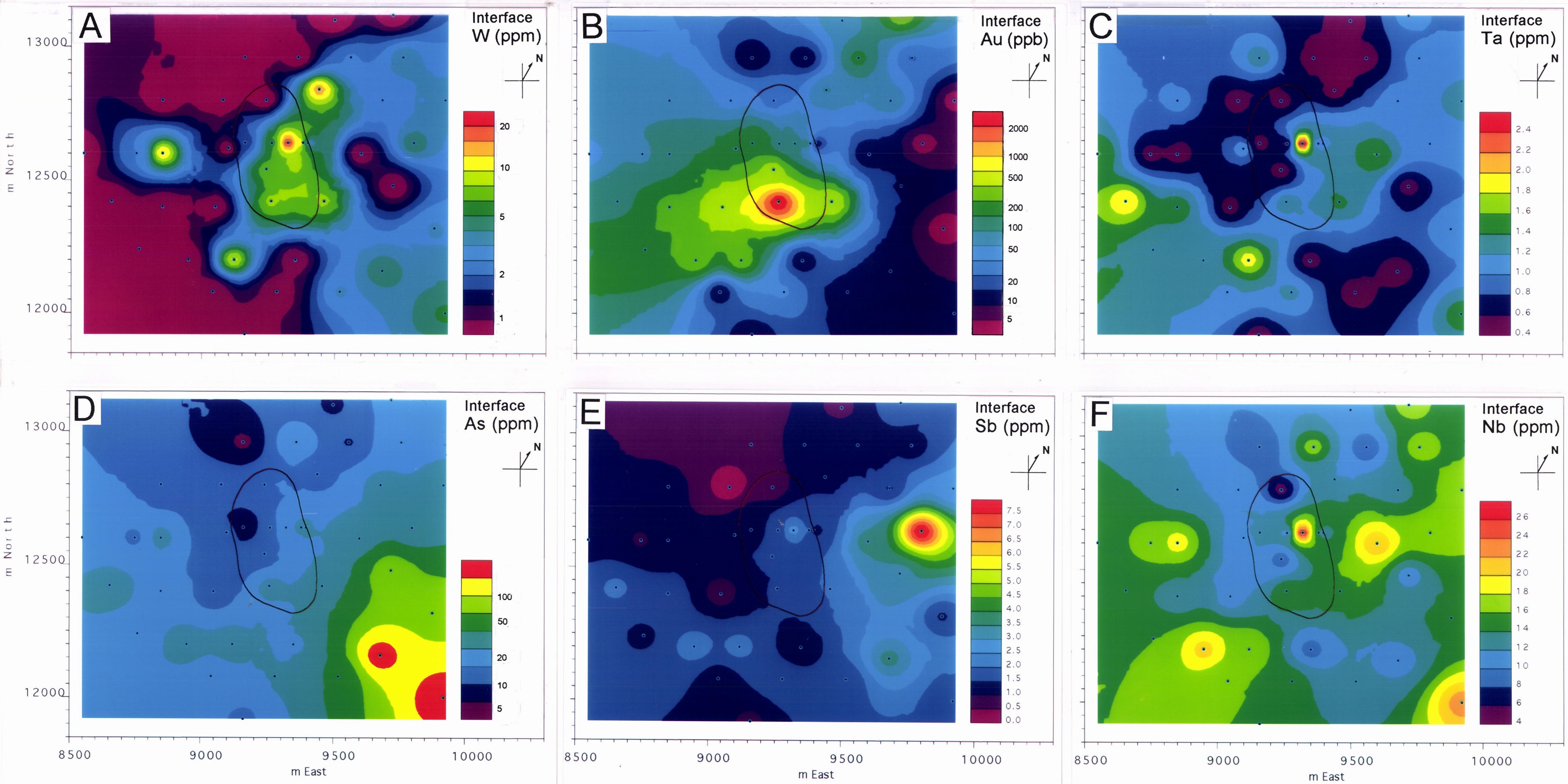


Figure 23. Distributions of W, Au, Ta, As Sb and Nb at the colluvium-basement unconformity. The area covered by this figure in only part of that covered by Figures 6 and 16-19.

*Tantalum and Niobium.* The eastern portion of the pit is marked by anomalies in Ta and Nb (2.4 and 26 ppm respectively; Figures 23C and F). There is some indication of weak north and south dispersion trains down the palaeoslopes. Tantalum and Nb may be useful indicator elements, even though they did not appear useful in the very limited fresh rock study, but they occur at low abundances.

*Arsenic and Antimony.* Arsenic and Sb anomalies occur at the interface to the southeast and east of the Harmony deposit respectively (Figures 23D and E). These are equivalent, in position and in intensity, to anomalies in the basement and are part of larger patterns that extend beyond the present confines of the interface sampling. It is difficult to determine if these represent better targets than those of the upper residuum.

*Others.* Although K, Rb, Ba, Pb and Cu do not indicate the location of the Harmony mineralisation in the basement or in the interface sampling, the underlying geochemical structures and abundances are similar in both media.

# 8 SOIL

## 8.1 Introduction and pilot study

Five selected soil samples were wet sieved into their >2000, 710-2000, 500-710, 250-500, 75-250 and <75 µm fractions (see Appendix 9) and the fractions examined petrographically. The soil has a bimodal size distribution (Figure 24). The coarse fraction (>2000 µm) dominates three out of the five pilot samples and an important fine fraction (<250 µm) dominates the others. The coarse fraction consists largely of ferruginous nodules and angular fragments of ferruginous saprolite; detrital material derived from breakdown of the upper layers of the colluvium. The intermediate fraction (75-500 µm) consists of a mixture of ferruginous saprolite, lateritic granules and quartz; the quartz content increases (Figure 10H) in the finer, silty fraction (75-250 µm). Some quartz grains are slightly frosted and rounded, indicating that a proportion of the quartz was derived from distant sources by fluvial and aeolian action, although most was probably brought in by sheetwash. The silty fraction consists largely of quartz. Quartz, kaolinite, hematite, with minor feldspar and mica, make up the <75 µm fraction. This soil would be classified as SU203 (Anand *et al.,* 1989).

The ferruginous, coarse fraction represents the source of the colluvium, which may or may not be mineralised (see Robertson *et al.*; 1994), but this is unlikely to be relevant to the underlying basement. There may have been some mechanical dispersion from deeper within the colluvium, by bioturbation but, where the colluvium is thick, dilution is likely to be considerable.

Mechanical dispersion within the fine fraction has similar limitations, although it is more readily churned. However, the high content of clay and Fe oxides and hence, the high surface area is favourable for retention of hydromorphically dispersed elements. Thus, the clay-rich (<75 µm) fraction of the soil was selected for geochemical analysis. Fifty eight soil samples were collected on a triangular grid of approximately 250 m spacing within 850 m of the centre of Harmony pit. Close to the pit, the sample spacing was reduced to about 125 m to provide additional resolution. The sampling method is described in Appendix 9, the results are tabulated in Appendix 7 and some elements have been contoured in Figures 25A-F.

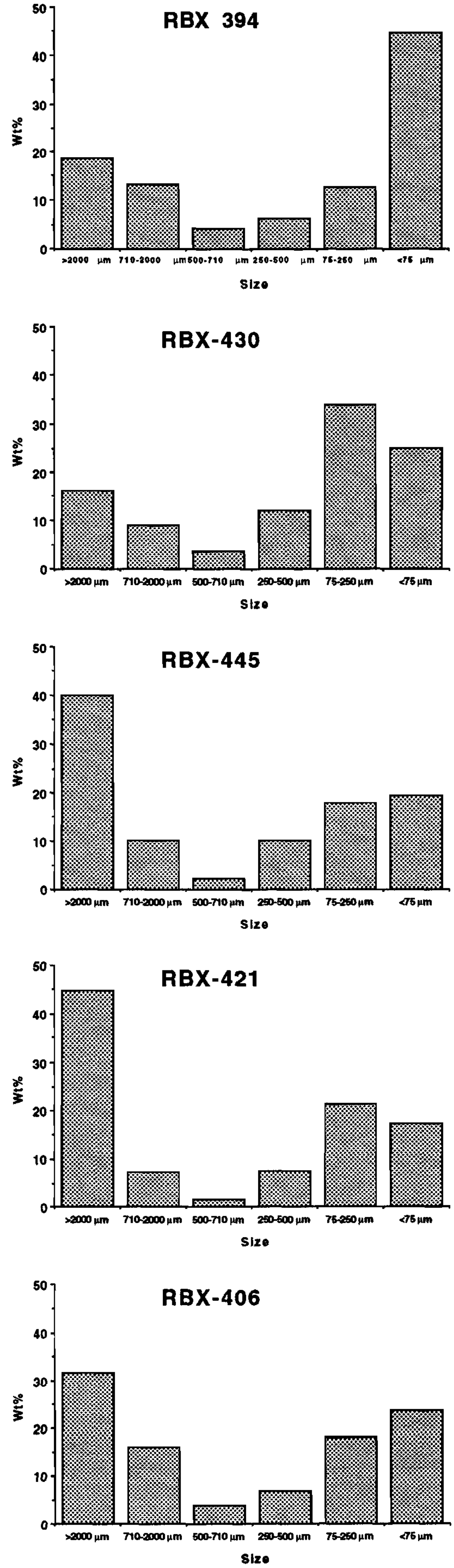


Figure 24. Soil size fraction analysis demonstrating the preponderance of coarse and fine fractions. The area covered by this figure in only part of that covered by Figures 6 and 16-19.

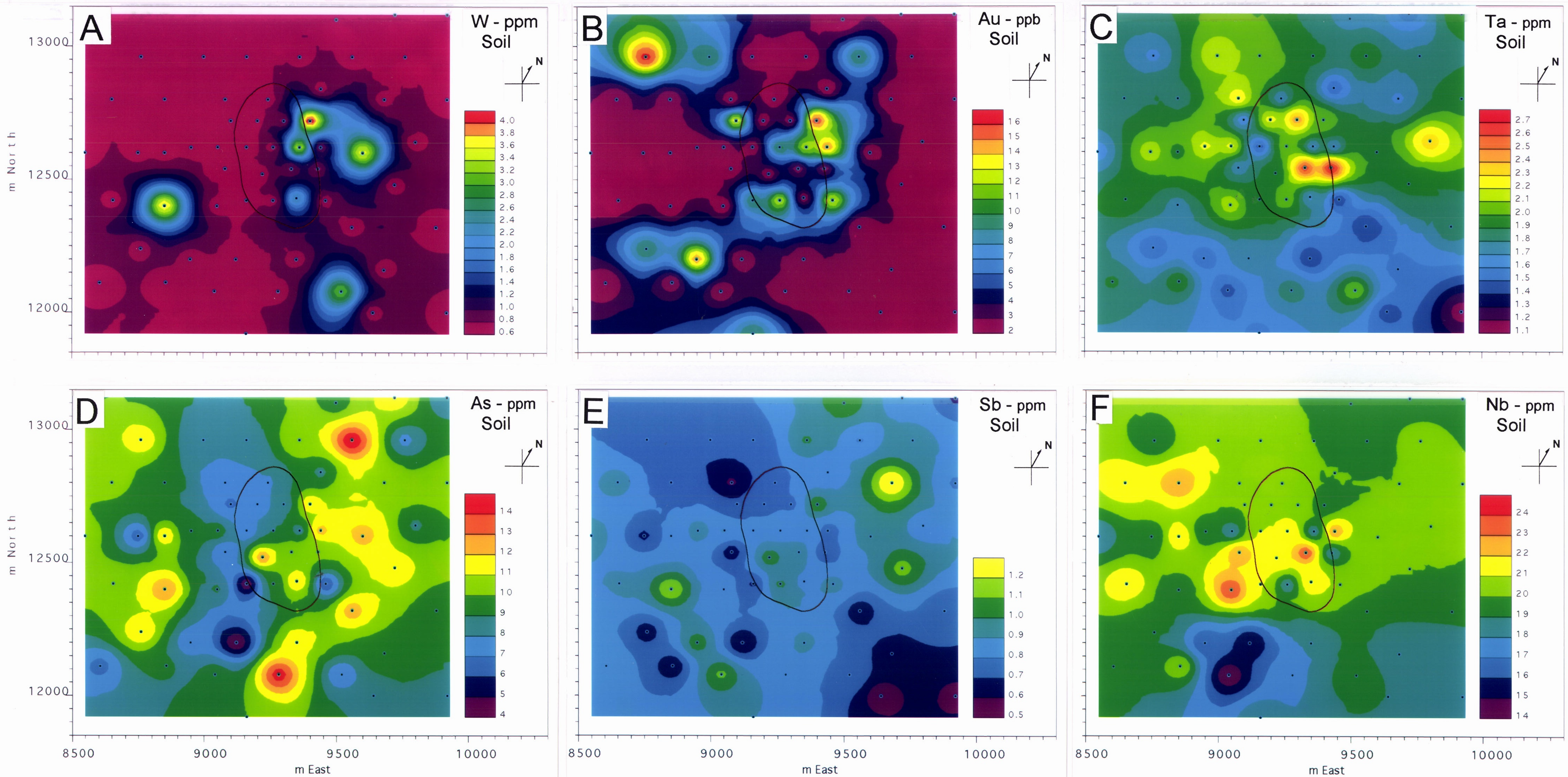


Figure 25. Distributions of W, Au, Ta, As, Sb and Nb in the soil <75 μm fraction .

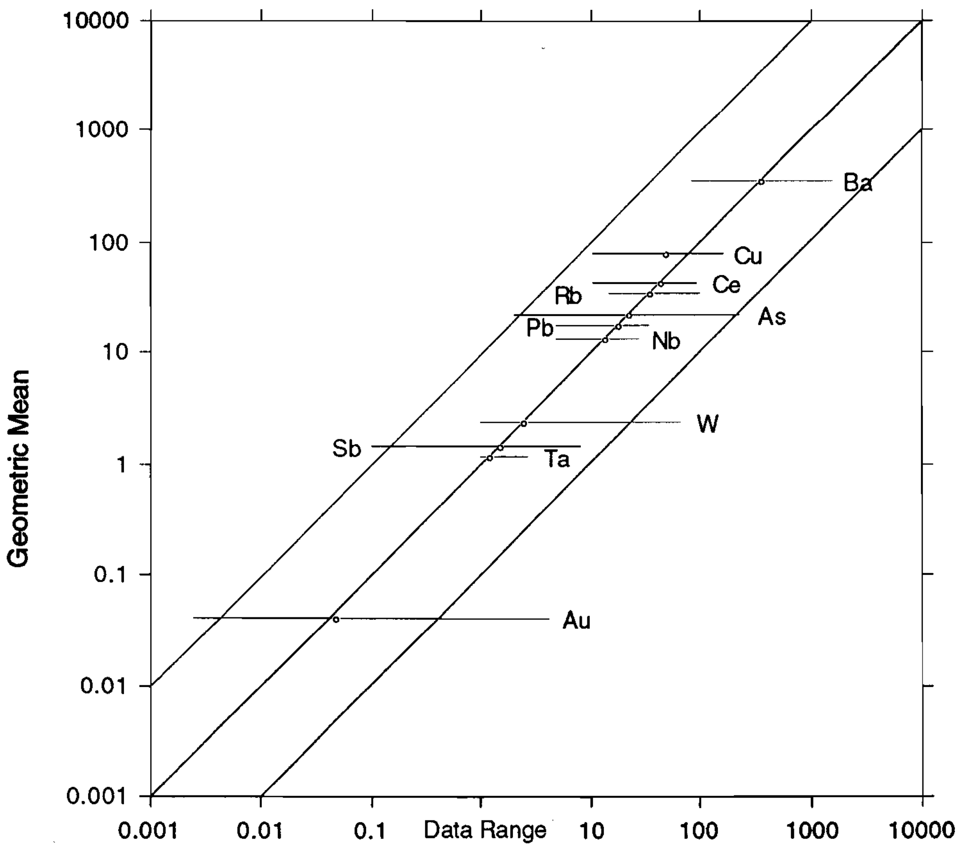


**Figure 26A.** **Interface sampling. Log-log plot of the geometric mean of the data against the data range showing a much greater data range than in Figure 23B. Circles indicate geometric mean.**

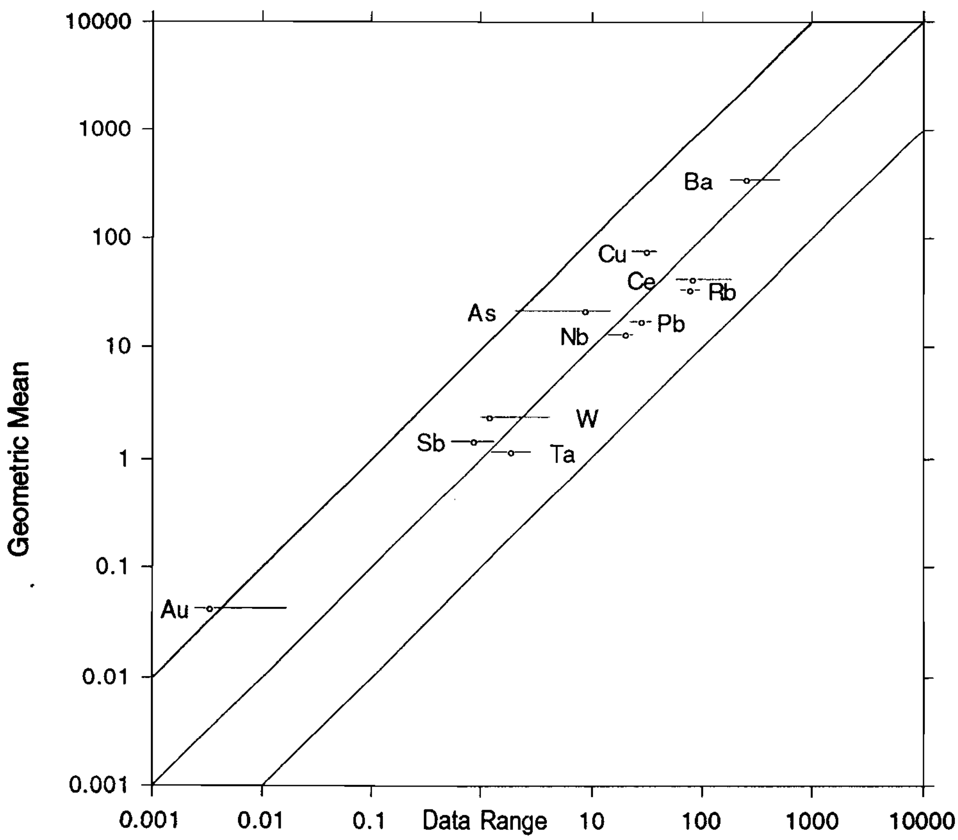


**Figure 26B.** **Soil sampling. Log-log plot of the geometric mean of the data against the data range showing a very small data range (compare Figure 23A). Circles indicate geometric mean.**

## 8.2 Results

*Gold and Tungsten.* There are weak Au and W anomalies (15 ppb and 4 ppm in backgrounds of 4 ppb and 1 ppm respectively; Figures 25A and B) over and near the Harmony pit. They occur only where the colluvium is particularly thin (0.5-1.0 m; see Figure 8E) and bioturbation has brought mineralised material to the surface without excessive dilution.

*Tantalum and Niobium.* The Ta and Nb distributions revealed by interface sampling (Figures 23C and F) and soil sampling (Figures 25C and F) are quite dissimilar, so it is unlikely that there is any link between the two. However, there are some small Ta and Nb anomalies in the soil in the area of the pit (Figures 25C and F) where the colluvium is particularly thin (Figure 8E).

*Arsenic and Antimony.* In comparison to the interface sampling, the highest As and Sb abundances in the soil are little above background concentrations (Figures 25D and E). Peaks in the soil As and Sb soil concentrations bear no relationship to the underlying interface or basement sampling. Thus, they probably represent geochemical noise.

*Other elements.* Although the maximum abundances of K, Rb, Ba, Pb and Cu of the soil and interface are similar, the geochemical ranges of the soil are smaller and there is no spatial relationship between distributions in soil, interface or upper residuum. There is no association with mineralisation and the data reflect the upper layers of the colluvium. Variations from the mean are random.

A comparison between log-log plots of the soil (Figure 26B) and the interface (Figure 26A), shows abundance ranges of indicator elements are much less in the former (0.5-1 orders of magnitude) than in the latter (2-3 orders of magnitude), implying that the variance in the soil is random rather than related to mineralisation. This is supported by the low averages for common indicator elements such as Au, W, Ba, Cu, As and Sb; averages are marginally increased for Ce, Rb, Pb, Nb and Ta.

# 9 SUMMARY AND CONCLUSIONS

## 9.1 Regolith-landforms and sampling media

The present, relatively flat surface around the Harmony pit indicates little of the complex regolith beneath (see Figure 9). However, the polymictic lag implies a depositional area where further investigation must be by drilling and costeaning. There is a considerable basement relief (40 m), with the Harmony deposit lying beneath a palaeohigh of ferruginous saprolite. Deep palaeovalleys, to the north and south of the deposit, dissect this landscape and are underlain by saprolite and mottled zone. Lateritic duricrusts are preserved on the flanks of the palaeovalleys. There are, thus, at least three major residual regolith geochemical sampling media available immediately underlying the transported overburden which would be expected to be disparate in their geochemical backgrounds and dispersion characteristics. Combining them may inadvertently present a significant exploration problem. Mapping regolith relationships and distributions, using exploration drilling, has revealed details of this sub-surface landscape and the sampling materials that would be expected, so governing the sampling strategy.

Cover materials include smectitic and kaolinite clays, partly filling palaeovalleys and a variable thickness of colluvium covering all, including the palaeohigh. This is mantled by a thin veneer of soil. Recognition of these cover units is fundamental to an exploration strategy that aims to use shallow regolith sampling.

## 9.2 Transported overburden

### *9.2.1 Valley-fill sediments*

The valley-fill sediments appear to have been deposited in a very low-energy environment. Very restricted, thin sand layers were found at the base of a very few palaeovalleys. Although these sands were probably deposited in narrow, clearly-defined channels, do not show any current bedding (seen elsewhere), such structures may have been obliterated by subsequent weathering. The remainder of the sediments consist largely of waxy clays (kaolinite and smectite) and contain small quantities of minute (0.5 mm) quartz grains. There were no signs of the coarse bedding and discrete kaolinite layers that would be expected in a debris flow (Robertson, 1990).

Although most of the quartz grains in the clays are angular to shard-like (small, detrital grains are readily cushioned in an aqueous environment), a few larger grains show some rounding. There is a remarkable similarity between the abundance, size and appearance of the quartz of the basement saprolites and that of the valley-fill sediments. Such a comparison may be extended to the total mineralogy. The basement saprolites consist of kaolinite, muscovite and quartz; the valley-fill sediments of kaolinite, smectite and quartz. It is suggested that the palaeovalleys were filled with locally-derived, finely comminuted saprolite detritus under conditions of sluggish stream flow. Muscovite, in the original sediment, could have reacted with dissolved bases and silica, under conditions of restricted drainage, to produce smectite (reaction 1, below). However, it is probable that most smectite was formed from kaolinite (reaction 2).

The above reactions imply variations in pH, from acidic to alkaline, depending on the availability and the quantities of weathering muscovite. Temporary alkaline conditions, brought about by reaction 1, and excess dissolved Ca, Mg and $HCO_3^-$ in the groundwater would favour deposition of dolomite in the clays.

1) $$\underset{\text{Muscovite}}{K_2Al_6Si_6O_{20}(OH)_4} + \underset{\text{silicic acid}}{0.8Si(OH)_4} + \underset{\text{dissolved bases}}{Mg^{2+}_{0.8}} + \underset{\text{water}}{(n-1)H_2O} \rightarrow \underset{\text{smectite}}{Mg_{0.8}Al_4(Si_{6.4}Al_{1.6})O_{20}(OH)_4.nH_2O} + \underset{\text{kaolinite}}{0.2Al_2Si_2O_5(OH)_4} + \underset{\text{alkalinity}}{0.4OH^-}$$

2) $$\underset{\text{kaolinite}}{2.8Al_2Si_2O_5(OH)_4} + \underset{\text{silicic acid}}{0.8Si(OH)_4} + \underset{\text{dissolved bases}}{0.8Mg^{2+}} + \underset{\text{water}}{(n-4.4)H_2O} \rightarrow \underset{\text{smectite}}{Mg_{0.8}Al_4(Si_{6.4}Al_{1.6})O_{20}(OH)_4.nH_2O} + \underset{\text{acidity}}{1.6H^+}$$

The valley-fill sediments have had a complex weathering history and show internal signs of oxidation fronts, including development of manganiferous layers, mottling with goethite and hematite and even lateritic duricrust in their upper parts, all of which could be confused easily with similar phenomena in the residual regolith.

In the north, the upper layers of the valley-fill sediments were eroded, whereas they are largely preserved in the south. Here, the lateritic materials, formed on the valley-fill sediments, are complex, with a mixture of *in situ* clay-rich pisoliths and some apparently exogenous nodular material. The latter may have been released by dissolution of the matrix of an existing *in situ* lateritic duricrust, followed by collapse and minor transport or, alternatively, deposited following local erosion of residual lateritic material from the adjacent slopes of the palaeovalley. This may have carried with it any associated mechanical Au dispersion. These mechanisms may have formed a continuum. The matrix of the ferruginous parts of the upper valley-fill sediments contains both physical and geochemical evidence of illuviation of fine-grained pedogenic materials from the colluvial-alluvial cover.

Mega mottles are characteristic of clay-rich valley-fill sediments (Anand *et al.,* 1993). Iron-rich fragments of fossil wood, with attached exogenous sedimentary material, occur as detritus within mottled material in the Waste Dump valley-fill clays. The clay-rich valley-fill sediments probably lay in shallow depressions in the landscape. Development of smectites indicates impeded drainage and moist conditions ideal for dense vegetation. Despite a strong W geochemical anomaly in the Harmony valley-fill sediments, the Au abundance is low. This may be due to post-depositional leaching of Au or by its initial absence.

#### *9.2.2 Colluvium*

The layer of colluvium varies considerably in thickness, from 0.5 m over parts of the Harmony deposit to 12 and locally 20 m over the palaeovalleys. Thick sediments in places implies that some was alluvial but exposure was not available to determine this. The valley-fill sediment had been eroded partly, prior to deposition of the colluvium. The colluvium layer provides a significant hindrance to exploration, effectively blocking physical transfer of geochemically anomalous material to the surface except where it is extremely thin (0.5 m). Structures seen in pit faces and in drilling indicate shallow but broad lenses of gravelly material, typical of sheet flow.

The base of the colluvium varies from a simple, sharp, erosive unconformity to a complex mixture of saprolite and colluvium, nearly a metre thick, probably constituting saprolite blocks included in a palaeosol, which was later buried. This latter interface, where it occurs, provides a particularly promising geochemical medium in which greater dispersion than in the underlying saprolite may be expected.

#### *9.2.3 Soil*

Soil developed on the colluvium is closely related to its substrate, being rich in coarse, ferruginous lithic fragments and granules. This material has been moved about considerably by sheetwash and its composition reflects that of its remote source. The fine, silty portion (75-250 μm) is largely quartz-rich, with some small ferruginous granules; it is probably aeolian in part. Aeolian input may have occurred during colluvial action, during soil formation or both. The clay-rich fraction consist of quartz, mica, kaolinite and Fe oxides.

### 9.3 Geochemistry

#### *9.3.1 Fresh rock*

Limited spot sampling of diamond drillcore suggests that only Au, W, possibly Ta and Nb have potential as primary indicator elements at the Contact deposit. The alteration halo is defined by K, Rb and Ba. Some REE (Eu, Lu and Yb) increase in both abundance and range in fresh mineralised materials. Although the concentrations of As and Sb increase near mineralisation, their abundances are low compared to many other deposits.

#### *9.3.2 Weathered residuum*

The uppermost horizon of the residual regolith was sampled; materials included lateritic duricrust or, where unavailable, mottles or ferruginous saprolite. Both Au and W are anomalous close to the Harmony deposit (>100 ppb and >6 ppm). The very weak Au and W enrichments of some of the ferruginous saprolite from within the remainder of the Harmony pit indicates very restricted dispersions in this sampling medium. This would necessitate closer-spaced sampling (50 m) than that used for this study (250 m). Wide-spaced sampling is generally adequate for sampling areas of buried lateritic residuum. The strongest anomalies for Au (1.4 ppm) and W (39 ppm) occur distant from the pit in other areas of economic interest.

Although most of the lateritic duricrust is siliceous and kaolinitic, some is gibbsitic. Some parts of the ferruginous saprolite were cemented with calcrete, resulting in local concentrations of Ca, Mg and Sr. Nickel and Cr concentrations delineate ultramafic portions of the Narracoota Formation;

increased Pb (>20 ppm) and Rb (>20 ppm, mica-related) indicate the metasediments of the Ravelstone Formation.

As expected, anomalies in As and Sb do not depict the Harmony mineralisation but they are anomalous (1500 and 20 ppm respectively) in ultramafic rocks over the Enigma North Anomaly, suggesting a more sulphidic mineralisation style.

Some lithology-related elements, notably Si, Fe, Cr, Zr, Hf, V, Rb, Ba, As and Sb, are influenced, to some extent, by the nature of the regolith. Data normalisation, using the modes of the background populations, was able to remove most of this dependency and accentuate some distribution trends but the Au, Ta and W anomalies were unaltered.

### *9.3.3 Colluvium-basement interface*

Interface sampling on a 150 m triangular grid yielded anomalies in W and Au over much of the southern part of the Harmony pit and dispersion trains are apparent in both directions down the palaeoslopes. The eastern portion of the pit is also anomalous in Ta and Nb. Interface As and Sb anomalies to the southeast support the basement anomalies at Enigma North.

This sampling method may be used in stripped and subsequently buried regimes, where lateritic duricrust is absent, in preference to sampling ferruginous saprolite. The data should be treated separately from other media as anomalies in interface sampling are generally more subtle because of dilution. If a combined display is required, data normalisation would be needed.

### *9.3.4 Valley-fill sediments*

The geochemistry of the valley-fill sediments is complex, being, in part, governed by provenance, by internal barriers related to ferruginous, dolomitic and manganiferous layers and in part by vertical leaching and physical and chemical transfer from the colluvium to the upper layers of the valley-fill sediments. Gold, in particular, is largely at low abundances. However, where a palaeovalley cuts across the Harmony deposit, the valley-fill sediments are anomalous in W, by about an order of magnitude, relative to background. However, Au remains at very low abundances. There is also a very weak, probably placer concentration of W in the sands at the base of the Waste Dump palaeovalley.

Analysis of valley-fill clays for mechanical dispersions of W could be used to detect buried mineralisation in a palaeovalley catchment. However, the extent of such a dispersion train needs to be determined. Gold analysis is likely to be ineffective, but could be directed at the interface at the base of the valley-fill sediment.

### *9.3.5 Soil*

The soil covering the Harmony deposit has a bimodal size distribution, dominated by coarse and fine fractions. The exogenous, coarse, gravelly material (derived from the colluvium) and the quartz-rich and probably aeolian, intermediate fractions are unlikely to be suitable sample media. The clay- and Fe oxide-rich <75 μm fraction was analysed from soil collected on a triangular grid (125-250 m spacing), because there was a slight possibility that the fine soil fraction may contain trace elements adsorbed from the hydrological environment.

There are very weak soil Au and W enrichments (15 ppb and 4 ppm respectively) in backgrounds of 3 ppb and 1 ppm respectively over and in the vicinity of the Harmony pit. These only occur where the colluvium is particularly thin (<1 m) and mineralised material has been brought to the surface without excessive dilution.

It is concluded that soil sampling will be unsuccessful on colluvium-covered areas. However, there can be sporadic windows where the colluvial cover is extremely thin and the soil effectively lies directly on basement.

## 9.4 Gold mobility and palaeoclimate

Gold is unlikely to be mobile in the present groundwater (Gray, 1995) due to the neutral pH and the low $Cl^-$ content. However, it is unlikely that present conditions have been maintained since inception of weathering. Substantial Au enrichment within the duricrust at the Harmony pit, in places reaching several tens of ppm, implies substantial residual accumulation. This presumably occurred with formation of the duricrust during an early, seasonally humid period and Au mobility could have been achieved by mechanical processes, residual accumulation and some chemical mobility assisted by organic ligands possibly related to the primitive vegetation suggested by the palaeontology.

Minor erosion of the palaeovalleys followed development of duricrust. This may have occurred during the decline of the humid phase or during a temporary humid phase within the shift to aridity. A few relatively low energy streams developed within confined channels but sedimentation changed to very low energy conditions and the palaeovalleys became choked with clays, resulting in impeded drainage and development of smectites. These valley-fill sediments are similar to those developed on the Yilgarn Craton and reported elsewhere as part of the P409 Project (*e.g.*, at Mt Magnet, Robertson *et al.,* 1994; at Kanowna, Dell and Anand, 1996; at Greenback, Viner, 1996; and at Bronzewing, Varga *et al.,* 1996). Conditions must have remained sufficiently wet to allow weathering of the upper parts of the valley-fill sediments and there must have been fluctuating watertables with still-stands to produce the complex mottled zones within the sedimentary profile.

Selective leaching of Au, but not W, from the valley-fill clays of the Harmony palaeovalley would imply Au mobility during or just after clay sedimentation. The palaeovalleys may have supported a denser vegetation than their surroundings. Unfortunately dating of the valley-fill sediments by nodule palaeomagnetism or manganese mineral geochronology, although attempted, has been unsuccessful so far. Clay sedimentation and leaching were followed by minor erosion and colluvial-alluvial sedimentation marking arid conditions.

## 9.5 Implications for exploration

i) Where transported overburden dominates the landscape, sub-surface regolith mapping and determination of regolith stratigraphy by drilling is an essential precursor to sampling.
ii) Basement sampling of buried residual materials (lateritic duricrust, mottled zone material and ferruginous saprolite) is a valid method but background geochemical abundances and dispersion sizes are likely to differ between sample media. Thus, normalisation may be required if the data are to be pooled and sample spacing will need to be varied according to the medium used.
iii) A sample interval of 250-500 m is recommended for sampling lateritic duricrust but this would have to be substantially decreased to 50 m for sampling ferruginous saprolite.
iv) Where the buried regolith has been stripped to saprolite, interface sampling is preferred over saprolite sampling; a sampling interval of 100-200 m is recommended.
v) Soil sampling on colluvial material is not recommended; it will only be successful where the colluvium is extremely thin (<1 m).
vi) Sampling valley-fill sediments for W has potential for detecting Harmony-style mineralisation in the palaeovalley catchment but the extent of the dispersion train has to be determined. Gold analysis is unlikely to be successful in this environment, probably due to leaching of Au.

## 10 ACKNOWLEDGMENTS

Assistance from AFMECO was from R. Grivas, D. Boyer and S. Mann in the early days. Later, M.G. Hills, M. Moroney, G. Chessell, M. Harper and D. Lenartowics of Plutonic Resources assisted at Peak Hill. Thin and polished sections were prepared by R.J. Bilz. Geochemical analyses were by M.K.W. Hart and S. Derriman (XRF) at CSIRO and Becquerel Laboratories (INAA) at Lucas Heights. Field sampling was assisted by W.L. Maxwell. Sample preparation was by E.G. Hudson, J.F. Crabb, S. Derriman and D.J. Winchester. X-ray diffraction analysis was by M.K.W. Hart and S.L. Derriman; Debye-Scherrer diffractograms were by E.H. Nickel. Interpretation of XRD traces and Debye Scherrer films was by E.H. Nickel and R.R. Anand. Assistance with the petrography of Fe-rich minerals was provided by R.C. Morris and with weathering reactions by D.J. Gray. Artwork was prepared by A.D. Vartesi. J.K. Marshall of Marcam Environmental advised on cell structures in fossil wood, B. Pillans palaeomagnetically examined hematite nodules, P. Vasconcelos examined Mn minerals of mottled materials and M.F. Killick gave advice on sedimentology. P.J.D. Phillips and J. Porter assisted with layout and document formatting. R.R. Anand, R.E. Smith and C.R.M. Butt provided critical review of the manuscript. All this assistance is acknowledged with appreciation.

## 11 REFERENCES


Anand, R.R., Churchward, H.M., Smith, R.E. and Grunsky, E.C. 1991. Regolith-landform development and consequences on the characteristics of regolith units, Lawlers District, Western Australia. CSIRO Division of Exploration Geoscience Restricted Report 166R.

Anand, R.R., Smith, R.E., Innes, J. and Churchward, H.M. 1989. Exploration geochemistry about the Mt Gibson Gold Deposits, Western Australia. CSIRO Division of Exploration Geoscience Restricted Report 20R.

Anand, R.R., Smith, R.E., Innes, J., Churchward, H.M., Perdrix, J.L. and Grunsky, E.C. 1989. Laterite types and associated ferruginous materials, Yilgarn Block, WA. Terminology, classification and atlas. CSIRO Division of Exploration Geoscience Restricted Report 60R.

Anand, R.R., Smith, R.E., Phang, C., Wildman, J.E., Robertson, I.D.M. and Munday, T.J. 1993. Geochemical exploration in complex lateritic environments of the Yilgarn Craton, Western Australia. CSIRO Division of Exploration Geoscience Restricted Report 442R.

Blockley , J.G., 1975. Peak Hill manganese deposits, W.A., *in* Economic Geology of Australia and Papua New Guinea, Vol. 1 edited by C.L. Knight, AusIMM, Mon. 5, p1021.

Bradley, J., Sanders, A.. J., Varga, Z.S., and Storey, J.M., 1995. Geochemical mapping of the Leonora 1:250,000 sheet: Western Australia Geological Survey, Geochemical Series Explanatory Notes, 35p.

Dell, M. and Anand, R.R. 1996. Kanowna district. in Eastern Goldfields Field Excursion Field Guide, CRC LEME Restricted Report 4R.

Gee, R.D. 1987. Peak Hill, WA (2nd edition) Western Australia Geological Survey 1:250 000 Geological Series Explanatory Notes. 24 p.

Gozzard, J.R., Munday, T.J., Hunter, W.M., and Gabell, A.R., 1992. An evaluation of SPOT Panchromatic Imagery as an aid to regolith-landform mapping in the Ora-Banda area, Eastern Goldfields Province, W.A. CSIRO-IMEC Division of Exploration Geoscience Restricted Report 233R.

Gozzard, J.R., Sumramanya, A.G. and Sanders, A.J. 1995. 1:250 000 Peak Hill Regolith Materials Series. WA Department of Minerals and Energy.

Gray, D.J. 1995. Hydrogeochemical dispersion of gold and other elements at Baxter, Western Australia. CSIRO Division of Exploration and Mining Restricted Report 169R.

Hallberg, J.A. 1984. A geochemical aid to igneous rock type identification in deeply weathered terrain. Journal of Geochemical Exploration. 20. 1-8.

Mabbutt, J.A., 1963. Wanderrie banks: microrelief patterns in semi-arid Western Australia. Bull. Geol Soc Am. 74. p529-40.

MacLeod, W.N., 1970. Peak Hill, Western Australia: Western Australia Geological Survey 1;250,000 Geological SeriesExplanatory Notes. 21p.

Norrish, K. and Hutton, J.T. 1969. An accurate X-ray spectrographic method for the analysis of a wide range of geological samples. Geochimica et Cosmochimica Acta. 33. 431-435.

Ollier, C.D., Chan, R.A., Craig, M.A. and Gibson, D.L. Aspects of landscape history and regolith in the Kalgoorlie region, Western Australia. BMR Journal of Australian Geology and Geophysics, 10, 309-321.

Pirajno, F. and Occhipinti, S. 1995. Bryah, WA. (Preliminary edition). Western Australian Geological Survey 1:100 000 Geological Series.

Pirajno, F., Adamides, N.G., Occhipinti, S., Swager, C.P. and Bagas, L. 1995. Geology and tectonic evolution of the early Proterozoic Glengarry Basin, Western Australia. Western Australian Geological Survey Annual Review 1994-1995. 71-80.

Robertson, I.D.M. 1990. Weathering at the Trial Hill Tin Mine - Queensland. Centre for Australian Regolith Studies Occasional Publication No 1.

Robertson, I.D.M. 1991. Multi-element dispersion in the saprolite at the Beasley Creek Gold Mine, Laverton, Western Australia. CSIRO Division of Exploration Geoscience Restricted Report 152R.

Robertson, I.D.M., Dyson, M, Hudson, E.G., and Crabb, J.F. 1995. A case-hardened, low contamination ring mill for multi-element geochemistry. In K.S. Camuti (Ed) Extended abstracts, 17th IGES Conference, Townsville. James Cook University. 379 p.

Robertson, I.D.M., King, J.D., Anand, R.R. and Butt, C.R.M. 1994. Regolith geology and geochemistry - Mt Magnet Distict. Geochemical orientation studies, Stellar and Quasar deposits. CSIRO Division of Exploration and Mining Restricted Report 48C.

Robinson, P.F. 1992. Baxter Project. Geology and exploration activity. AFMECO Pty Ltd.

Subramanya, A.G., Faulkner, J.A,. Sanders, A.J. and Gozzard, J.R. 1995. Geochemical mapping of the Peak Hill 1:250 000 sheet. Explanatory notes. Geological Survey of Western Australia

Tapley, I.J. and Gozzard, J.R. 1992. Landform and regolith mapping in the Lawlers district: Landsat Thematic mapper image processing techniques for terrain mapping. CSIRO-IMEC Division of Exploration Geoscience Restricted Report 233R.

Varga, Z.S., Anand, R.R. and Wildman, J. 1996. Bronzwing gold deposit. In Eastern Goldfields Field Excursion Field Guide, CRC LEME Restricted Report 4R.

Viner, J. 1996. Greenback gold deposit. in Eastern Goldfields Field Excursion Field Guide, CRC LEME Restricted Report 4R.